

# The Ross seal and its underwater vocalizations

## Diplomarbeit

am Department Biologie II,  
der Ludwig-Maximilians-Universität München  
in Kooperation mit dem  
Alfred-Wegener-Institut für Polar- und Meeresforschung  
in der Helmholtz-Gemeinschaft, Bremerhaven



————— **LMU**  
Ludwig ———  
Maximilians —  
Universität —  
München ———

Vorgelegt von:  
**Anna-Maria Seibert**

**AWI**   
Alfred-Wegener-Institut  
für Polar- und Meeresforschung  
in der Helmholtz-Gemeinschaft

Betreuer am AWI: Prof. Dr. Peter Lemke  
Erstgutachter an der LMU: Dr. Lutz Wiegrebe  
Zweitgutachter an der LMU: Prof. Dr. Gerd Schuller

München, den 27. Dezember 2007

## Zusammenfassung

Seit ihrer Entdeckung im Jahre 1840 wurde die Rossrobbe (*Ommatophoca rossii*) nur selten beobachtet. Die vorliegende Arbeit gibt einen Überblick über die Biologie der Rossrobbe aus bisherigen Veröffentlichungen. Die artspezifischen Unterwasserlaute dieser Robbenart wurden jedoch noch nicht genauer beschrieben.

Da das Südpolarmeer weitgehend frei von menschlichen Einflüssen ist, stellt es einen idealen Standort für Langzeitaufnahmen der Unterwassergeräuschkulisse dar, was mit PALAOA (**P**erenni**AL** **A**coustic **O**bservatory in the **A**ntarctic Ocean) realisiert wurde. Diese Horchstation, die 2005 vom AWI installiert wurde, befindet sich in der Antarktis auf dem Ekström Eisschelf nahe der Atka Bucht und besteht aus einem Hydrophon-Array unter dem Eis. PALAOA wurde konzipiert, das ganze Jahr über autonom breitbandige Unterwasseraufnahmen (15 Hz – 96 kHz) mit hoher Auflösung (bis zu 24 Bit) zu liefern, mit gleichzeitiger Zugriffsmöglichkeit in Echtzeit. Für die Auswertung wurden diese Aufnahmen visuell und akustisch durchgesehen, um daraus 280 Rossrobberufe genau zu vermessen und weitere 17 000 Rufe für Saisonalität und Tagesgänge auszählen zu können.

Das Hauptergebnis dieser Arbeit ist die Differenzierung von vier klar voneinander unterscheidbaren Rufen: drei sirenenartige Rufe (High, Mid, Low) und der Whoosh. Diese Rufe können klar anhand ihrer Minimum- und Maximumfrequenzen determiniert werden. Die genaue Beschreibung der Unterwasserrufe von Rossrobben stellt die Grundlage für weitere Untersuchungen zur geographischen Variabilität der Vokalisation dar und ist wichtig zur Entwicklung automatisierter Mustererkennung. Rossrobben sind jährlich von Mitte Dezember bis Anfang Februar in der Atka Bucht zu hören. Die starke Zunahme der Rufe Mitte Januar passt zu den Ergebnissen aktueller Tagging-Experimente und zeigt wahrscheinlich die Ankunft zusätzlicher Robben an, die sich vorher im offenen Ozean aufgehalten haben. Die abrupte Abnahme der Rufe Ende Januar ist dementsprechend auf das Abwandern der Tiere zurückzuführen. Während ihrer Anwesenheit vor PALAOA folgt die Vokalisationsrate der Rossrobben eindeutig einem Tagesrhythmus, bei dem die höchste Aktivität gegen Mitternacht zu verzeichnen ist. Dieser Rhythmus korreliert eher mit dem Tageslicht als mit den Gezeiten. Auch andere antarktischen Robbenarten besitzen den hier beobachteten nächtlichen Höhepunkt der Vokalisationsrate.

## Summary

Since its discovery in 1840, the Ross seal (*Ommatophoca rossi*) has rarely been observed. The present thesis provides an overview of the biology of the Ross seal acquired from the literature available. However, the corresponding underwater vocalizations have not been described in detail before.

The Southern Ocean is largely unaffected by anthropogenic noise. Therefore, it provides the ideal location for long-term underwater recordings as implemented with PALAOA (**P**erenni**AL** **A**coustic **O**bservatory in the **A**ntarctic Ocean). This listening station, set up by the Alfred Wegener Institute for Polar and Marine Research (AWI) in 2005, is located on the Ekström Ice Shelf at Atka Bay, Antarctica, consisting of an array of hydrophones deployed through the ice shelf. PALAOA was designed to autonomously obtain year-round broadband (15 Hz - 96 kHz) and high resolution (up to 24bit) underwater recordings, while providing real-time data access. For analysis, these recordings were scanned visually and aurally to characterize 280 Ross seal calls in detail, and to count an additional 17 000 calls for seasonal and diurnal calling rates.

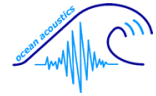
The main result of this thesis is the differentiation of four distinct call types: three siren calls (High, Mid, Low) and the Whoosh. These call types can easily be discerned by their maximum and minimum frequencies. This detailed characterization of underwater call types provides the basis for further investigations on geographic variation within Ross seal vocalizations, and for the development of automated pattern recognition algorithms. It has been found that the annual acoustic presence of Ross seals at Atka Bay is the period between December and February only. The increase in calling rate in mid January matches recent satellite tagging experiments and is probably caused by the arrival of seals that were pelagic before. The striking drop at the end of January corresponds with the migration of most Ross seals northwards. During their presence at PALAOA, Ross seals show a clear diurnal calling pattern with peak calling rates around midnight, which correlates rather with daylight conditions than with tidal currents. The nocturnal peaks in calling rates of Ross seals are consistent with other Antarctic seal species.

# Contents

<b>1. Introduction</b>	<b>6</b>
1.1 Pack ice ecosystem	6
1.2 Biology of the Ross seal	8
1.2.1 Appearance and classification	8
1.2.2 Distribution and conservation status	9
1.2.3 Food and foraging	10
1.2.4 Reproduction	11
1.2.5 Behaviour	12
1.3 Importance of acoustics in marine environments	14
1.3.1 Sounds of the Ross seal	14
1.3.2 Sound production in Ross seals	15
1.4 Importance of acoustics in science	16
1.5 Scientific questions	16
<b>2. Material and methods</b>	<b>17</b>
2.1 PALAOA – an underwater listening station	17
2.1.1 Location	17
2.1.2 Description and function	20
2.1.3 Data acquisition	22
2.2 Software and settings	23
2.3 Acoustic measurements	24
2.3.1 Differentiation of call types	24
2.3.2 Duration	25
2.3.3 Minimum frequency, maximum frequency, and frequency range	27
2.3.4 Elements, subtypes, and sweep rates	29
2.3.5 Inter-harmonic intervals	31
2.3.6 Peak frequency and bandwidth	32
2.3.7 Echoes	35
2.3.8 Special features	36

2.4 Seasonal call counts	39
2.5 Diurnal call counts	39
2.6 Localization of the sound source	40
2.6.1 Estimation of the number of calling seals	42
2.6.2 Individual calling patterns	43
2.7 Problems of visual measurements	44
2.8 Statistical analysis	44
<b>3. Results</b>	<b>46</b>
3.1 Description of call types	46
3.1.1 High siren call	47
Bowl attachment	49
3.1.2 Mid siren call	50
Mid attachment	52
3.1.3 Low siren call	52
3.1.4 Whoosh components	54
A) Whoosh broadband component	55
B) Whoosh tonal component	56
3.2 Differentiation of call types	57
3.3 Presence and acoustic environment of Ross seals at Atka Bay, Antarctica	67
3.4 Seasonal calling pattern	68
3.5 Diurnal calling pattern	70
3.6 Localization and individual calling patterns	74
Estimation of calling seals and individual calling patterns	75
<b>4. Discussion</b>	<b>80</b>
4.1 Purposes for different call types	80
4.2 Inter- and intra-call specific differences	81
4.3 Structures of Ross seal vocalization	82
4.4 Difficulties in analysing Ross seal vocalizations	85
4.5 Seasonal calling pattern	86

4.6 Zeitgeber for diurnal calling rhythms	88
4.7 Localization and distribution	91
4.8 The ambient soundscape	92
4.9 Limits and outlook on the use of PAM (Passive Acoustic Monitoring)	93
<b>5. References</b>	<b>95</b>
<b>6. Appendix</b>	<b>I</b>
Tables of measurements	I
Scatterplots	VIII
<b>7. Acknowledgements</b>	



## 1. Introduction

The Ross seal (*Ommatophoca rossii*) is known as “the rarest of the world’s seals” (Bechervaise, 1967) which was the last to be discovered and about which the least is known (Ray, 1981). This statement still holds true, even though new methods and technologies enable us to shed more light on the life history of the Ross seal.

One of the new methods is the recordings of ocean acoustics. They provide us with valuable information from inaccessible areas, such as the polar oceans, and do this independently from weather, sea ice conditions, or even human presence. Advanced technology also allows long-term studies, just as the listening station set up in the Antarctic to collect bioacoustic data on which this thesis is based on.

The present work is the first in-depth analysis of underwater vocalizations of Ross seals, including two different approaches. One part of this thesis focuses on the first detailed acoustic description of the Ross seals’ different call types, while the second part focuses on diurnal calling patterns and seasonal abundance derived from the acoustic analysis. These findings allow insights into seal ecology and behaviour, whereas a distinct call differentiation sets the basis for call comparisons among locations in the Antarctic, and for the development of automated pattern recognition algorithms.

### 1.1 Pack ice ecosystem

The Antarctic sea ice zone provides a major habitat for six pinniped species (Siniff, 1991): southern elephant seals (*Mirounga leonina*), Antarctic fur seals (*Arctocephalus gazella*), leopard seals (*Hydrurga leptonyx*), Weddell seals (*Leptonychotes weddellii*), crabeater seals (*Lobodon carcinophaga*), and Ross seals (*Ommatophoca rossii*). The latter four exclusively live south of the Antarctic Convergence (approx. 60°S) and are referred to as pack ice seals.

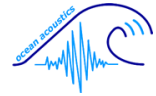


Three leading factors can be defined to influence the animals living in the Southern Ocean. First of all the changing sea ice conditions. During austral summer, the sea ice concentration is at its minimum, covering an area of 4 million km<sup>2</sup>. However, in the winter months June and July, it reaches a maximum coverage of 25 million km<sup>2</sup>. When the sea ice breaks up and retreats, it leaves the ocean scattered with ice floes of different sizes, which are referred to as pack ice. This pack ice region is the main habitat of crabeater, leopard, and Ross seals. The Weddell seal mainly occurs on coastal fast ice, which is adjacent to the continental ice shelf. This always-changing environment is quite challenging for living, because depending on the season, haul-out sites on sea ice and access to the water might be rare. Some smaller areas in the sea ice zone (polynias) remain unfrozen for most of the year due to katabatic (continental) winds, water currents and tidal movements. Polynias are frequented by crabeater and leopard seals, while Weddell seals in the fast ice have to actively keep their breathing holes open with their teeth.

The second factor would be the extreme seasonal light conditions with about three months' darkness in winter (June-August) and permanent daylight in summer (November-January). Depending on solar radiation and geographical location, the temperatures at the coast might rise up to 9°C at noon during December and January, but might drop down as low as -50°C during winter. The constantly blowing strong continental winds bring this region an average temperature of -17°C.

Yet a third factor should be considered: Antarctica is quite isolated in its location, being totally surrounded by the Southern Ocean with strong currents and heavy storms. The closest neighbouring coastlines of South America, Australia, and South Africa are at distances of 1000 km, 3000 km, and 4000 km respectively.

Along with a high biological abundance at its benthos, shelf ice areas and pack ice edges (Ackley et al., 2003), the Southern Ocean also holds the presumably largest biomass on earth. Nevertheless, it features quite a short food chain, which is typical for polar waters. The start of the food chain is set by phyto- and zooplankton, followed by large masses of Antarctic krill (*Euphausia superba*), which are the key food source for the largest animals – baleen whales – but also the food for a variety of fish and squid. The latter are preyed upon by the Antarctic top predators: penguins and seals, with Weddell seals having a higher trophic position than Ross seals (Zhao et al., 2004).



Exceptions are crabeater seals and leopard seals which also feed on krill. The carnivorous leopard seal additionally hunts other seals and penguins. Therefore, fluctuations in seal abundance may provide important information on the biotic environmental variability, especially on the abundance of krill as the main energy source in the Southern Ocean (Bester et al., 2002).

### 1.2 Biology of the Ross seal

#### 1.2.1 Appearance and classification

The Ross seal is named after the British commander Sir James Clark Ross who first discovered this species on his trip to the Ross Sea in 1840. Gray was the first to describe the species in 1844.

Kingdom: Animalia

Phylum: Chordata

Subphylum: Vertebrata

Class: Mammalia

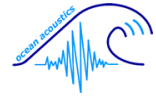
Order: Carnivora

Family: Phocidae

Genus: *Ommatophoca*

Species: *Ommatophoca rossii*

The Ross seal (*Ommatophoca rossii*) is the smallest Antarctic seal (Laws, 1984), not exceeding 2.4 m in body length and 200 kg in weight (Thomas, 2002). Its appearance is quite compact with a broad head, short snout with a rather small mouth, a barely visible neck, and short flippers. Just like all phocid seals, Ross seals have no external ears, as opposed to fur seals and other otariids. The Ross seal's most obvious feature is the forward pointing big eyes (approx. 7 cm in diameter; Stonehouse, 1972) giving their genus the Greek name 'omma' for 'eye', and an excellent optical sense both in water and on land (King, 1964). They also have a sack-like throat, which is enlarged during vocalization. Acoustics seem to play an important role in the Ross seal's life, however, since the auditory nerve has been described as large, whereas the optic nerve is quite small (King, 1964).



The adults' pelage is short and dark brown to black dorsally which gets lighter to the ventral side. Often dark stripes are reported on the sides, especially down the throat (Reeves et al., 2002). The pups' lanugo, though rarely seen, is also of a dark colour dorsally, turning into a yellow ventrally with a typical striped pattern on the throat (Thomas et al., 1980).

Although reports about the Ross seal's prey differ, their dentition proves them to be predators. Ross seal canine teeth are conical in shape and very sharp while their postcanines are rather small and blunt (Reeves et al., 2002).

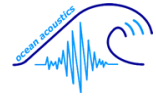
### 1.2.2 Distribution and conservation status

The Ross seals' distribution is circumpolar around the entire continent of Antarctica with increased abundance in the Ross Sea and the King Haakon VII Sea (King, 1964; Hall-Martin, 1974; Wilson, 1975; Condy, 1977; Siniff, 1991; Bester et al., 1995; Reeves et al., 2002). During austral summer, these animals can primarily be found in heavy pack ice as far south as 72°S. Formerly it was believed that they stay in dense pack ice all year round (King, 1990; Lucas, 1996), but Blix and Nordøy (2007) reported a more pelagic lifestyle, comparable with that of the harp seal *Phoca groenlandicus* or ribbon seal *Phoca fasciata* (Ray, 1981). Ross seals travel long distances north (up to 51°S) and stay offshore from March to October with few side trips returning south into the pack ice. During that time, the seals swim with a minimum surface speed of 1 ms<sup>-1</sup> and cover a distance of almost 2000 km in less than 3 weeks (Blix and Nordøy, 2007).

There have also been rare sightings of Ross seals in New Zealand, southern Australia (Reeves et al., 2002) and several subantarctic islands, such as Heard Island (Bechervaise, 1967), which suggests an even wider habitat range.

When sighted, Ross seals are usually solitary, except mother-pup pairs (Hall-Martin, 1974; Thomas et al., 1980; Splettstoesser et al., 2000; Southwell et al, 2003). Reported small groups, however, could be explained by a lack of ice to haul-out, since loose aggregations of seals have mostly been observed in areas of sparse ice (Bonner and Laws, 1964; Erickson et al., 1971; Splettstoesser et al., 2000).

To evaluate population sizes, seal censuses are being taken. However, as with whales and dolphins, such censuses are difficult since an unknown number of animals are



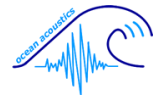
underwater and, therefore, out of range for counting. Only seals hauled-out on land or ice are taken into consideration. This is the reason why population estimates in this species vary by a factor of 10 from 20 000 to 220 000 Ross seals worldwide (King, 1964; Riedman, 1990; Thomas, 2002).

That large uncertainty in population estimates makes the Ross seal a specially protected species under Annex II of the Madrid Protocol to the Antarctic Treaty (since 1991) and it has the full protection status of the Convention for the Conservation of Antarctic Seals since 1978.

### 1.2.3 Food and foraging

A few studies indicate that the Ross seal preys mainly on midwater squid (e.g. *Psychroteuthis glacialis*, *Alluroteuthis antarcticus*, *Galiteuthis armata*, *Chiroteuthis sp.*), midwater fish (*Pleuragramma antarcticum*), and possibly krill (*Euphausia superba*) (Oritsland, 1977; Skinner and Klages 1994; Bengtson and Stewart, 1997). Riedman (1990) assumes that cephalopods make up 64% of the Ross seal diet, whereas it only consists of 22% fish, 9% krill and 5% other invertebrates (later confirmed by Zhao et al., 2004). Skinner and Klages (1994) challenged this and argued that fish may be just as important a prey as squid, with the latter being over-represented in seal stomach contents since their beaks remain there for a longer time. Presumably prey preference changes at different ages and even among the sexes, as it does in Weddell seals (Zhao et al., 2004).

Daily 12 kg of prey is hunted by Ross seals (Ray, 1981) on about 108 dives (Blix and Nordøy, 2007). During austral summer, when mating and moulting occurs in the pack ice, Ross seals stay under water for about ten minutes and dive to depths of 200-400 m. Their dives get deeper (up to 790 m) and longer (up to 30 min) when the seals live pelagic during winter time (Reeves et al., 2002; Blix and Nordøy, 2007). Apart from season, the Ross seal's diving activity shows a clear diurnal pattern with night-time dives being shallower than 200 m as opposed to day-time dives (Blix and Nordøy, 2007). The reason for this habitual behaviour could be the vertical migration of zooplankton. This predator-avoidance-behaviour of zooplankton (Bengtson and Stewart, 1997) is most likely the reason why Antarctic midwater fish can be found in deeper layers of the open



ocean (200-800 m) during the day, however, at night they move towards the surface to feed on zooplankton (Robison, 2003). Even though Ross seals do not prey on amphipods, they do prey on midwater fish and squid which follow these crustaceans on their vertical migration.

Ross seals share their habitat with three other seals and emperor penguins with somewhat similar prey. However, the extent of competition amongst them is not yet known (Skinner and Klages, 1994). It may not be of great importance due to geographical variance in prey species, hunting location within the water column, and temporal differences in foraging behaviour.

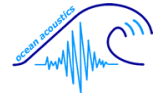
Evidence concerning the Ross seal's natural predators is still missing. It is most likely that at least one type of Antarctic killer whale (*Orcinus orca*) preys on Ross seals as it does with the other five seal species and baleen whales (Pitman and Ensor, 2003). Leopard seals (*Hydrurga leptonyx*) also have the potential to harm and kill animals the size of Ross seals, especially juveniles and the sick (Riedman, 1990). Though this is suspected, typical scars from leopard seals have not been found on Ross seals (Thomas, 2002). For humans this seldom encountered and protected species has never been worthwhile to hunt commercially. However, 58 individuals have been shot for scientific reasons during a Russian expedition in 1968 (Tikhomirov, 1975).

### 1.2.4 Reproduction

Blix and Nordøy (2007) showed that pupping and nursing takes place on drifting ice during November when females are continuously hauled-out. Since these dense pack ice areas are usually inaccessible for men, detailed information about the Ross seals' breeding behaviour is still missing. So far, no breeding concentrations have been observed (Thomas, 2002).

Since the Ross seals seem to be mostly solitary, the mating system may be of a serial monogamy rather than polygyny. There is no distinct sexual dimorphism in Ross seals (Reeves et al., 2002), except that females tend to be slightly larger (Riedman, 1990; Skinner and Klages, 1994; Thomas, 2002).

Scars on the males' chest, neck, and flippers suggest male fighting over access to females, but could also be hints for leopard seals preying upon Ross seals (King, 1969).



After mating, the females return to their feeding grounds farther north for another six weeks, before coming back to moult and to join the males, which stayed south in the pack ice (Blix and Nordøy, 2007).

The gestation period is estimated at approximately 9 months with a delayed implantation of the fertilized egg of 2-3 months (Tikhomirov, 1975; Ray, 1981; Skinner and Westlin-van Aarde, 1989; Thomas, 2002). Since mating takes place in November (Blix and Nordøy, 2007), birth would occur in the middle of winter without this delay. This way, Ross seal females avoid giving birth in an unsuitable environment, but in early austral summer instead.

A single pup is born weighing 16-27 kg and measuring 1-1.2 m in length (Oritsland, 1970; Thomas et al., 1980). The following nursing period may not exceed 2 weeks, whereupon mating occurs under water (Thomas, 2002; Blix and Nordøy, 2007). During this time, the pup may gain up to 4 kg per day from the mother's rich milk (up to 50% fat), reaching around 75 kg once they are weaned (Tikhomirov, 1975). Full length is reached at an age of about five years (Skinner and Klages, 1994).

The overall lifespan of Ross seals is believed to be 21 years for males and at least 20 years for females (King, 1990; Skinner and Klages, 1994; Thomas, 2002), reaching age sexual maturity at the age of 3-4 years for males and 2-7 years for females (Oritsland, 1970).

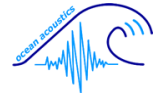
### 1.2.5 Behaviour

The Ross seal adapts to a typical head-up posture when approached (see Fig.1.2.5), bending back its neck and opening its mouth widely in a threatening manner but without emitting any sound (Reeves et al., 2002; Thomas, 2002). Attacks on humans have not been reported yet. However, Ross seals show no fear of humans at all (Ray, 1981; Thomas, 2002).



Figure 1.2.5: The Ross seal's typical head-up and mouth-open posture, witnessed by Joachim Plötz (AWI) at the Drescher Inlet, Antarctica, in 1989.

Annual moulting (the shedding of the fur layer) takes place from late January to early February, the exact date and duration depending on sex and age of the seal (Blix and Nordøy, 2007) and possibly even on the location, since several authors report different time spans which last from late December to early March (Skinner, 1984; Skinner and Westlin-van Aarde, 1989; Ackley et al., 2003; Southwell, 2005; Blix and Nordøy, 2007). The time of moulting is also the time when Ross seals haul-out most frequently, with the probability to see an animal on the ice being estimated over 60% during midday in the first week of February, compared to a 25% chance in the beginning of January, and almost no chance between March and October (Blix and Nordøy, 2007). This confirms earlier findings by Bengtson and Stewart (1997) in the Weddell Sea. After moulting the diving rate increases from 108 to 184 dives per day, suggesting that the animals have a need to refill their food reserves after the moult (Blix and Nordøy, 2007). Skinner and Klages (1994) even conclude that this seal fasts while moulting.



### 1.3 Importance of acoustics in marine environments

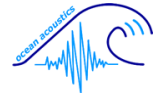
For most marine mammals hearing is far more essential than seeing. That is why some have even become almost blind (e.g. river dolphins) but with excellent hearing abilities. Toothed whales (*Odontoceti*) evolved a system for echolocation by emitting clicks in a frequency range of 20-20 000 Hz (Riedman, 1990) and “seeing” their environment by receiving the clicks’ echoes with distant-dependent time delay. Baleen whales (*Mysticeti*), on the other hand, are capable to produce high volume infrasonic sounds which can be heard over a distance of several hundred kilometres.

Marine mammals are specially adapted to underwater hearing. In land mammals perceiving directions in air is achieved by interaural intensity differences between the two ears. Underwater, however, this and the sensitivity for high frequencies are lost. Both pinnipeds and odontocetes have a well-developed underwater directional hearing, even though the sound waves do not enter the inner ear through the auditory canal only, but through the skull as well. Land mammals would perceive this as a sound coming from all directions at once. Seals are adapted to improve directional hearing and sensitivity. Their inner ear is located in a way that it does not touch most skull bones. Therefore it is not reached by non-directional sound waves. Additional structural modifications of the skull and the inner ear itself enhance sound reception and directionality. This is the reason why pinnipeds can hear a wide range of underwater frequencies up to 70 kHz (Riedman, 1990).

#### 1.3.1 Sounds of the Ross seal

Ross seals, also known as the ‘singing seals’ (Thomas, 2002) are quite vocal under water. They are comparable to Weddell seals, which even acoustically defend their underwater territory (Thomas and Kuechle, 1982, Evans et al., 2004) and own a variety of different calls for socializing, mating, pup finding etc. (Thomas and Kuechle, 1982; Pahl et al., 1997; Evans et al., 2004).

The Ross seals’ in-air vocalizations are comprised of an exhaling explosive sound produced while the mouth is still open along with a pulsed chug and a tonal siren call with closed mouth (Watkins and Ray, 1985; Thomas, 2002). The latter sounds like a



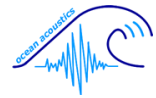
modified form of their underwater calls but with less variety and a narrower frequency range.

The Ross seals' typical underwater siren-like calls have only been described a few times in literature (Ray, 1981; Watkins and Ray, 1985). Their vocalization can be heard over a distance of several kilometres or more (Reeves et al., 2002).

Ray (1981) comments that the similarity of sounds that the Ross seal produces in-air as well as in water has helped to positively identify their underwater sounds. The meaning of the virtually continuous vocalizations is not yet clear since simultaneous behavioural observations are difficult to obtain. Some interpretations and ideas will be discussed in chapter 4.

### 1.3.2 Sound production in Ross seals

The exact location and process of sound production in Ross seals is still not understood. Ray (1981) was able to feel vibrations along the length of the seal's throat while it was vocalizing. King (1964) proposes that the distinctive explosive in-air sounds are produced by expanding the expansible posterior end of the long soft palate, much like the functioning of a bagpipe (King, 1968). Chugging noises, on the other hand, are generated with both the mouth and nostrils closed, which may indicate that air is transferred between different throat cavities. The sack-like throat, which can be enlarged as in bagpipes during in-air vocalization, is a quite obvious feature of Ross seals. This is taken as evidence that the inflation of laryngeal sacs might be the source of some odd in-air sounds when hauled-out seals are approached (Reeves et al., 2002). As in no other pinnipeds, the trachea is centrally expanded to a width of almost 9 cm with a very distensible tracheal membrane. This suggests that it plays an important role, together with the soft palate, as a resonating chamber in underwater sound production. This way no air is lost and underwater siren calls may be repeated over and over again. Only water depth with increasing pressure may limit to this way of vocalizing (Ray, 1981).



### 1.4 Importance of acoustics in science

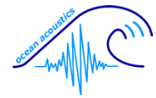
Scientists value acoustics in a variety of ways. Biologists use bioacoustics as a powerful tool to gather more information about a species or even an entire ecosystem. The inaccessibility of the Antarctic coast leaves researchers with only a small timeframe to observe animals throughout a year. However, underwater recordings provide access to an almost unknown habitat of marine mammals. By measuring underwater sounds at Atka Bay, Antarctica, the presence of certain seals and whales can be determined. The next step is to differentiate between and to look into vocalizations and their implications for further understanding of a species and its life history. However, there is also another reason for collecting underwater vocalizations in such remote parts of the world: the Southern Ocean is still largely unaffected by anthropogenic noise and therefore provides a perfect opportunity to study the effects men has on those ecosystems (especially exploration and tourism). Furthermore, noise-free recordings of marine mammal vocalizations are useful for the development of automated pattern recognition algorithms for further understanding and processing.

### 1.5 Scientific questions

Since the lack of knowledge about Ross seals and their life history by far exceeds what is known about them, there are numerous questions to be asked. Only a few can be answered by ocean acoustics, and even less in this thesis.

The main focus of research during the last months fall into the following categories:

- How many different call types do exist in Ross seals?
- What do typical calls look like?
- Are there any patterns of calling rate and the use of different calls?
- How many animals are calling?
- Are individual Ross seals distinguishable by their calls?
- How does their vocal activity change in the presence of other species and predators?



## 2. Material and methods

### 2.1 PALAOA – an underwater listening station

The PALAOA station (**P**erenni**AL** **A**coustic **O**bservatory in the **A**ntarctic Ocean, Fig.2.1) was designed to autonomously obtain year-round underwater recordings of a wide frequency and dynamic range, while providing real-time data access.

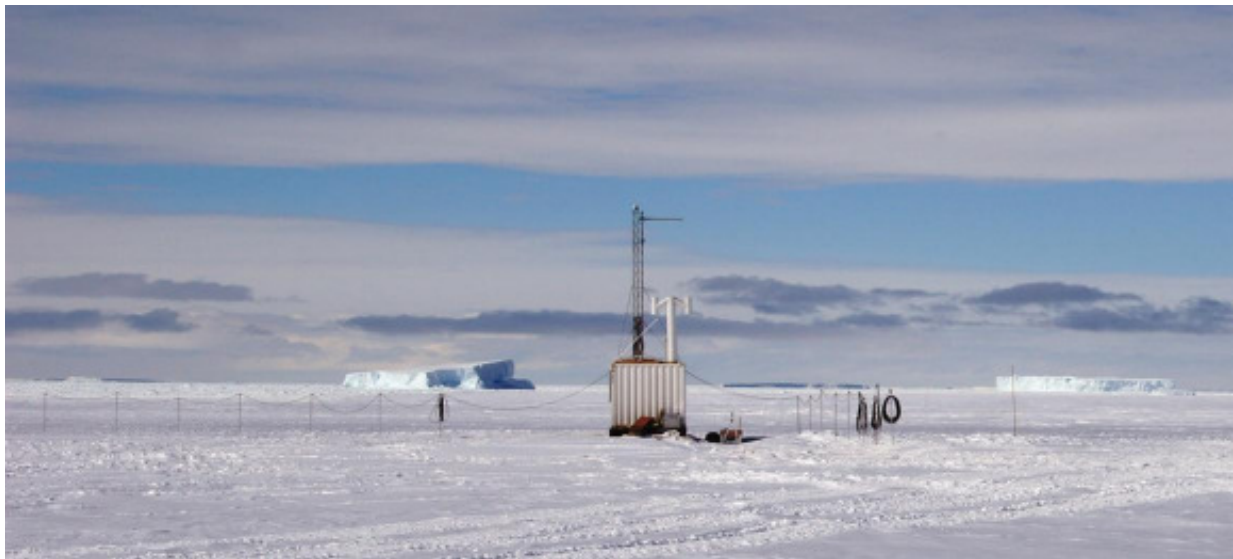


Figure 2.1: The central container of PALAOA on the ice shelf with wind generator, mast with WLAN and webcam, and the elevated hydrophone cables (Photo by Peter Henning).

#### 2.1.1 Location

PALAOA is located at 70.3°S, 8.1°W on the Ekström Ice Shelf in the eastern Weddell Sea, Antarctica, about 15 km north of the German Neumayer Station (Fig.2.1.1A), which is operated by the Alfred Wegener Institute for Polar and Marine Research (AWI) in Bremerhaven. The Ekström Ice Shelf reaches more than 200 km out onto the ocean. This glacier advances seaward with a speed of 100-150 m per year, resulting in occasional ice break-offs at its edge. At the PALAOA site, the free-floating ice shelf is approximately 100 m thick with about 160 m of water below (Fig.2.1.1C). The ice edge (Fig.2.1.1B) is located at a distance of 1-3 km from PALAOA, with Atka Bay and a little inlet positioned at a distance of 1.5 km to the East. The ice shelf is exposed to diurnal tidal movement of up to 2 m in amplitude.



Figure 2.1.1A: The location of PALAOA on the Ekström Ice Shelf, about 15 km north of the German Neumayer Base. This floating ice shelf reaches about 200 km into the sea, advancing approx. 100-150 m per year. The ice edges around PALAOA are at distances of 1-3 km to the open ocean to the North, Atka Bay to the East, and a little inlet extending south of it (IKONOS-2 satellite image provided by Space Imaging Europe).



Figure 2.1.1B: Environment at the PALAOA site. The edge of the Ekström Ice Shelf towers approx. 10 m above sea level. All marine life can be found either in the ocean or on pack ice floes (i.e. seals in the left hand corner) and icebergs (i.e. penguins in the center of the picture. Photo by Lars Kindermann).

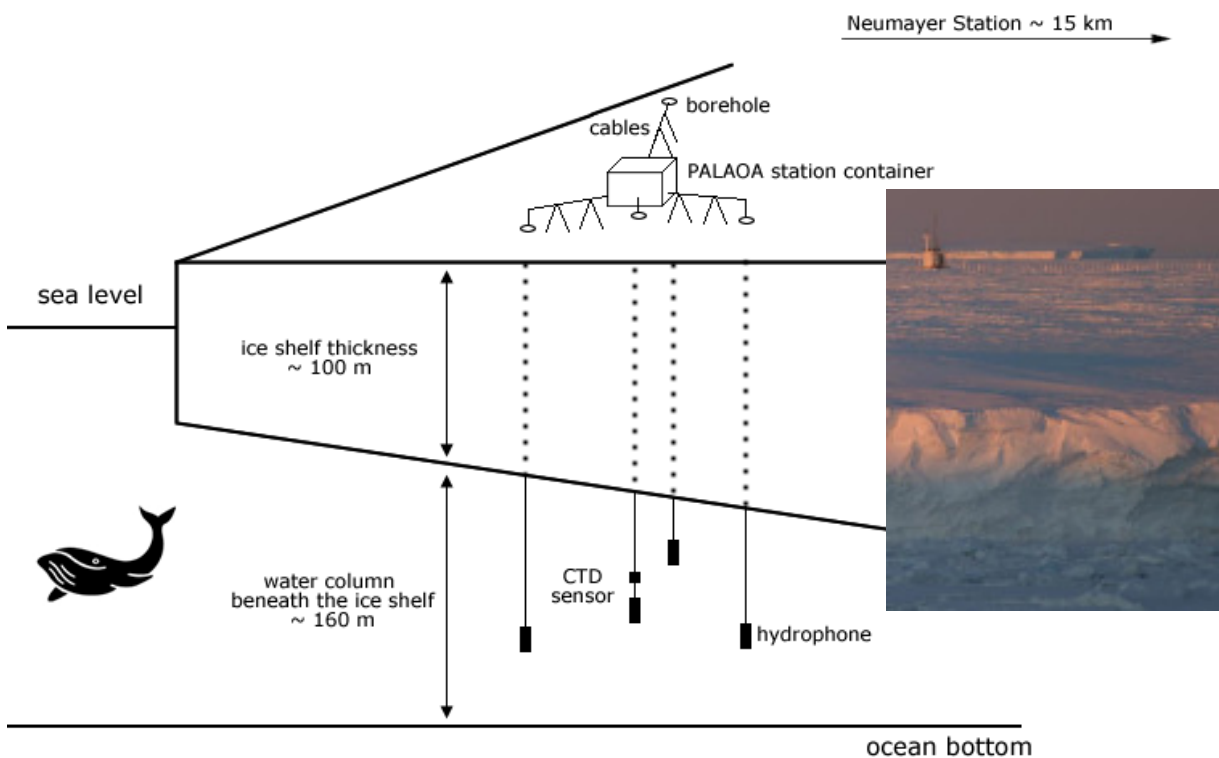


Figure 2.1.1C: Schematic of the PALAOA setup with its centred container and four boreholes through which the hydrophones had been lowered into the water column. At this site, the floating ice shelf is about 100 m thick (10 m above and 90 m below sea level), with 160 m of water below. The ice edges around PALAOA are at distances of 1-3 km, decreasing by occasional break-offs. Station viewed from Atka Bay on a photo by Lars Kindermann.



### 2.1.2 Description and function

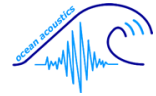
PALAOA is designed for perennial, autonomous operation with real-time data access to broadband (10 Hz – up to 96 kHz), high resolution (digitized at up to 24 bit) underwater recordings from up to four calibrated hydrophones deployed through the ice shelf.

PALAOA's frequency resolution permits the detection of the full range of marine mammal vocalizations, from infrasonic mysticete vocalizations to ultrasonic odontocete echolocation clicks. The system's dynamic resolution permits the detection of signals as weak as the low-frequency ocean background noise at sea-state zero, and incidents of high amplitude such as iceberg calving. PALAOA is in operation since December 2005. It consumes about 50 W, which are supplied by 24 12-V batteries. These are charged by solar panels (max. 400 W), and a Savonius wind generator (max. 180 W) to provide a continuous power supply to the station. A methanol fuel cell (50 W) is activated in case neither sun nor wind is available during the austral winter. Those batteries powering the acoustic system (preamplifiers and sound device) are galvanically isolated in turn to reduce electric interference (Boebel et al., 2006). The setup of the station's container comprising the electronics is shown in Fig. 2.1.

Two different kinds of hydrophones were used: three Reson TC4032 and one Reson TC4033, as shown in Fig.2.1.2A. Both hydrophones are rated for a frequency range of 5-120 kHz. Unfortunately, two of the TC4032 stopped working within the first year, probably due to an assembly fault.



Figure 2.1.2A: The two types of hydrophones deployed at PALAOA: the Reson TC4032 with built-in pre-amplifier (left) and the Reson TC4033 (right; both photos by Reson).



The four hydrophones were deployed in a tetrahedral array through the ice shelf. This array permits the localization of the sound source by means of measuring the signal's time delay between the different hydrophones. The central hydrophone is deployed next to the station's container, while the three others are placed in a triangle around it (Fig.2.1.2B). The distances between those three and the central hydrophone measure 300 m, the distance between two hydrophones along the perimeter of the triangle measures 520 m. To prevent melt-in, the hydrophone cables are elevated from the borehole to the central container.

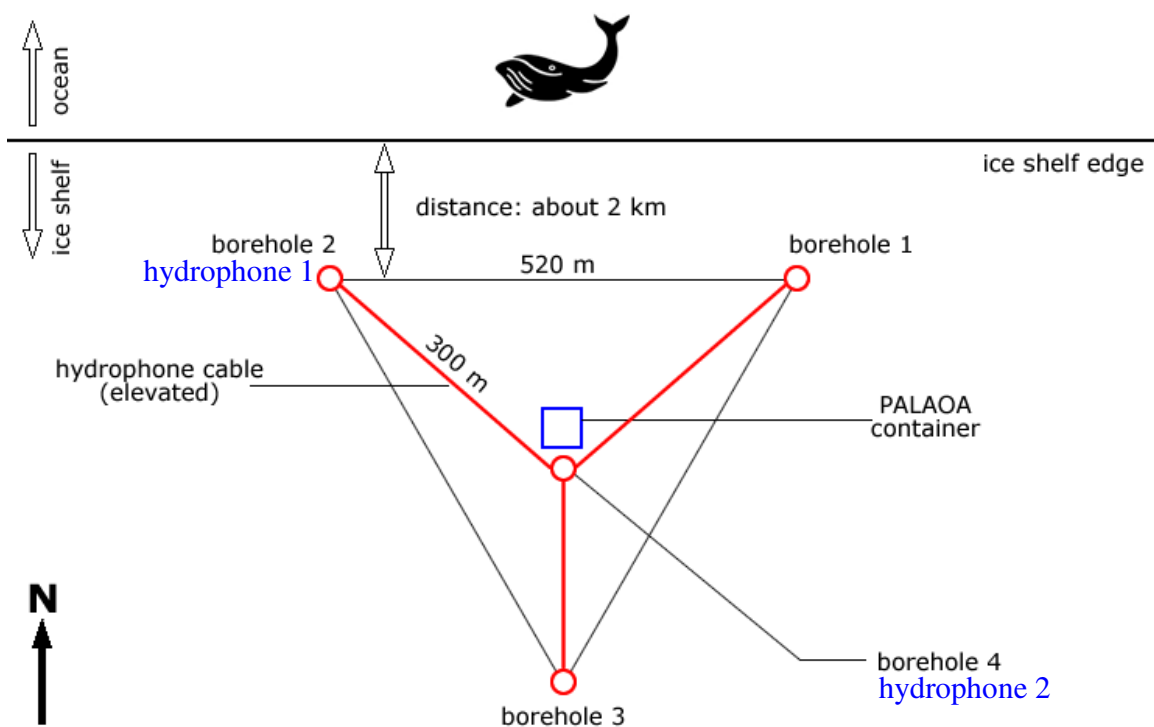
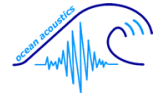


Figure 2.1.2B: Flat view of the PALAOA setup. The central hydrophone is deployed next to the container, with the other three forming an equilateral triangle around it. The distances between the outer hydrophones measure 520 m respectively, while all of them are at a distance of 300 m from the central hydrophone. In this study, all stereo recordings are obtained from hydrophone 1 in borehole 2 (the TC4032), and hydrophone 2 in borehole 4 (the TC4033), as shown in blue.

In this thesis, the amplitude is always given as dB full scale (FS), which equals the amplitude of 143 dB *re* 1 $\mu$ Pa/Hz (Zero Peak). At this time being, no estimation of the source level can be made since the distance to the sound source is unknown and sound propagation models for shallow ice-covered underwater mediums are not yet available.



### 2.1.3 Data acquisition

The signals from the hydrophones are amplified and bandpass filtered (10 Hz - 100 kHz) by a Reson VP2000 preamplifier. The data is digitized by two different devices: for continuous data acquisition of standard quality, a BARIX Instreamer audio-to-network device generates a stereo mp3 stream (32 kHz sampling frequency, 16 bit resolution, 192 kBit/s compression) at 192 kBit. At Neumayer, the mp3 data stream is saved into one-minute files, which are labelled with date and time. A further compressed audio stream (24 kBit/s, OGG-Vorbis format) is constantly transmitted via satellite to the AWI in Bremerhaven, allowing live monitoring of the underwater soundscape (Boebel et al., 2006). It can publicly be accessed on the AWI webpage ([www.awi.de/acoustics](http://www.awi.de/acoustics)).

On demand, very high quality audio data is digitized by a professional studio sound card (MOTU Traveller), and recorded by an embedded computer to 192 kHz, 24 bit wav files, each one minute in length.

The higher quality mp3 and wav files cannot be transmitted via the low bandwidth satellite link (128 kBit/s). Instead, they are stored on disks and back-up tapes, which are transported to Bremerhaven twice per year. By now, more than four terabytes of acoustic data have been saved at the AWI data silo, which is accessible as a network directory within the institute, permitting an easy data access. Every day, 1440 new minute-files are added automatically. On 6 December 2007, after almost two years of operation, the recordings cover almost 74% of the course of a year, as shown below in Fig.2.1.3. Gaps still exist for the austral winter because the extreme environmental conditions caused some system failures. This dataset will be published under an open access license in the "World Data Centre for Marine Environmental Data" hosted at AWI. For this study, the entire dataset was screened in order to find Ross seal vocalizations. Two types of files have been used for different purposes: high quality wav files for detailed call characterization (chapter 2.3) and standard quality mp3 files for counting calls within the one-minute files (chapter 2.4 and chapter 2.5), since this required no high temporal or frequency resolution.

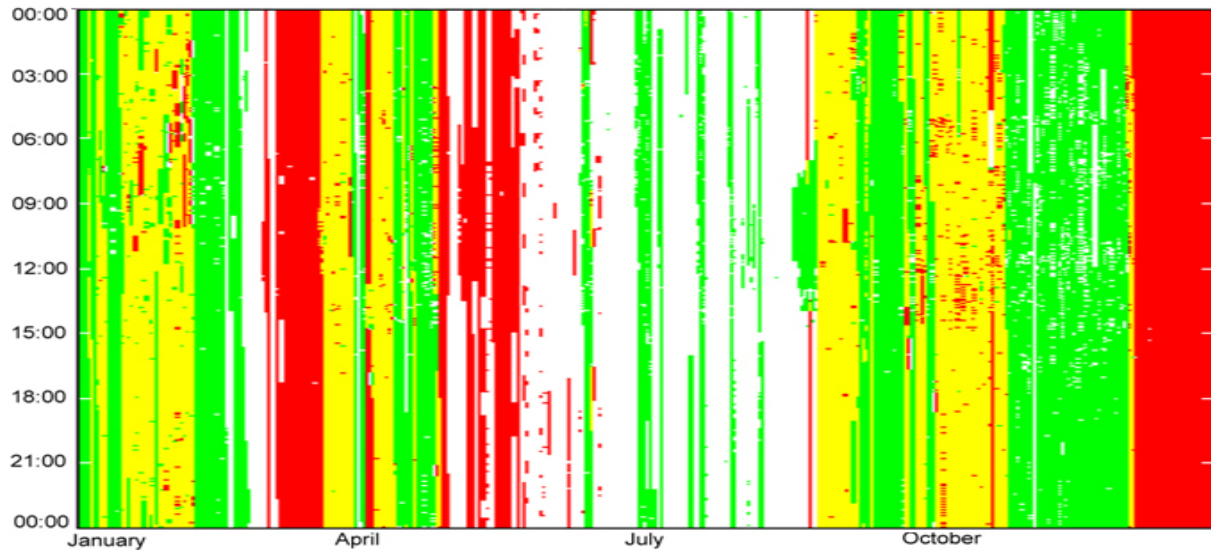
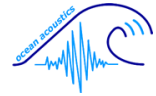
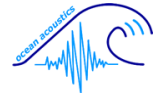


Figure 2.1.3: Timeline of PALAOA with date on the x-axis and daytime on the y-axis. Red areas were covered in 2006, green areas were covered in 2007, and yellow areas were covered in both years. 73.7% of a year have been covered until 6 December 2007. The white gaps are due to technical difficulties and energy shortage, especially during austral winter.

## 2.2 Software and settings

Adobe Audition 2.0 was used to analyze the Ross seal calls. Audition can display the waveforms, spectra, and spectrograms of multiple audio channels. The signals were neither filtered nor modified prior to the visualization of the spectral call contours.

In this thesis, measurements of call parameters were mainly obtained using spectrograms based on short-time fast-fourier transform (FFT). For detailed characterization of individual calls and call counting, the FFT length was set to yield a temporal resolution of 0.085 sec and a frequency resolution of 2.93 Hz.



## 2.3 Acoustic measurements

### 2.3.1 Differentiation of call types

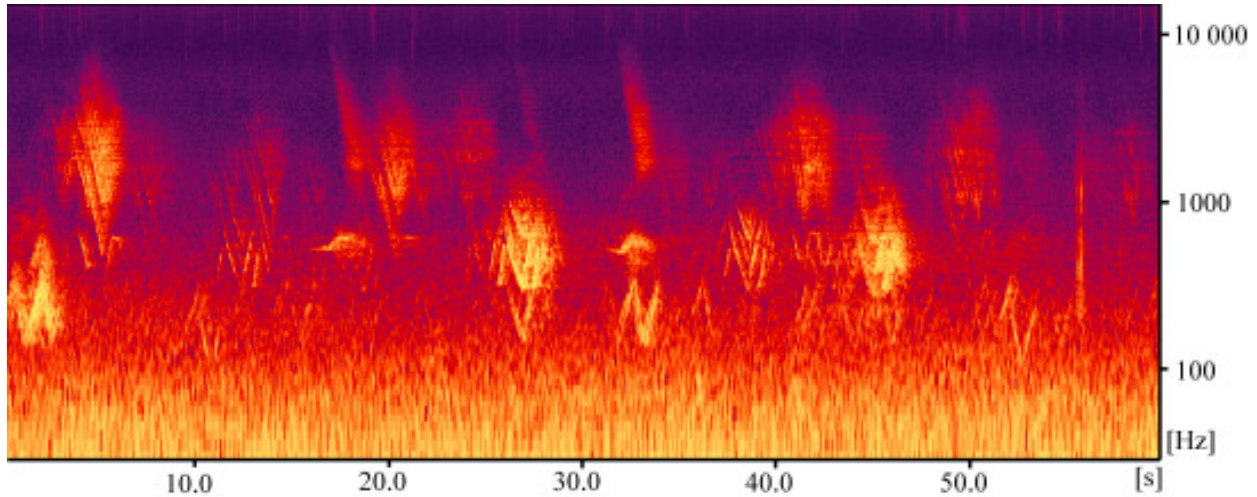
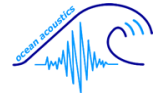


Figure 2.3.1A: Spectrogram of a typical PALAOA sound file with time on the x-axis and frequency on a logarithmic scale on the y-axis. The colours code for the intensity with bluish/purple for almost silence and light yellow for sounds with high amplitude. The constant low-frequency background noise is due to the ocean sounds (tide, waves etc.)

#### Pre-results:

It is not possible to view, count, and characterize animal vocalizations without having some sort of systematic and differentiation into call types, subtypes etc. For Ross seal vocalizations this has not been described before. Hence, it is necessary to shortly introduce the call types that were found while conducting the acoustic measurements as pre-results for better understanding the methods used for this thesis.

A first preview of the data suggested that – hitherto undefined – various call types apparently occupy different frequency ranges (Fig.2.3.1). Owing to their close acoustic resemblance to the sound of a siren, they were already referred to as “siren calls” by Watkins and Ray (1984). Therefore, the calls were named in accordance to their spectral position: the High siren call (also referred to as High) in the upper frequency range (sometimes with a so-called Bowl sound attached to it), the Low siren call (also referred to as Low) in the lower frequency range, and the Mid siren call (also referred to as Mid) in between the other two. In addition, a yet undescribed acoustic signature was named the “Whoosh” in resemblance to its auditory quality. The Whoosh comprises of two different components, a broadband component (WBC) and a tonal component (WTC), that always occur together.



In the following, all acoustic measurements taken, based on 50 individual calls of each type, are presented and explained along with a spectrogram as an example to represent the other call types.

For all spectrograms, a logarithmic frequency scale was chosen over the whole course of this thesis (Fig.2.3.1B). That way, the spatial distribution of the different call types allowed an easier visual access for counting and characterizing the calls.

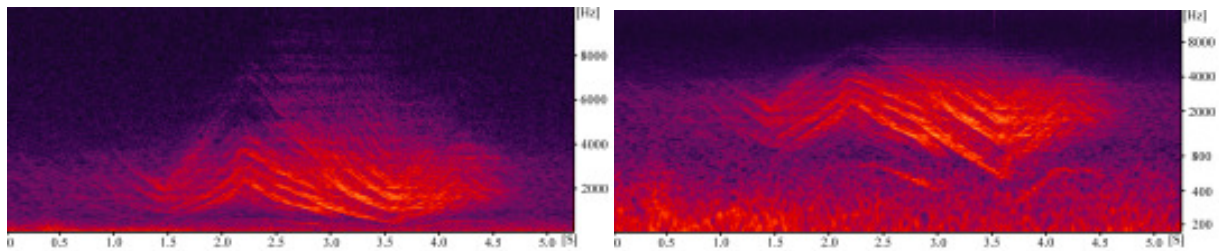


Figure 2.3.1B: Spectrograms of Ross seal vocalizations show the siren calls as slightly curved structures (left), however, when displayed on a logarithmic scale, the curved sweeps become an almost straight line (right). Spectrogram settings as described in Fig.2.3.1A.

Call characterization was performed on calls that could easily be identified aurally and visually in spectrograms (Fig.2.3.1A) while avoiding overlapping calls. The calls for analysis were randomly chosen. However, as the association between a call and a specific individual is unknown – as is the overall number of vocally active seals and their distance to PALAOA – it remains unclear whether the extracted calls are representative for the local population. Animals could have been oversampled and thus the independence of data be influenced. Nevertheless, these call characterizations, obtained from spectrograms give a first impression on the acoustic features of Ross seal vocalizations and allow comparisons among scientists all across Antarctica.

### 2.3.2 Duration

The total duration of a call is measured in seconds (Fig.2.3.2A). For the siren calls this was not easily accomplished since these calls fade in, rise in amplitude and at the end fade out again. Therefore, the determination of the start and the end point is subject to the intensity of the background noise. These points had to be chosen individually for each call. Strict standards as to when structures really belong to a call had to be applied to in order to minimize the observer related error.

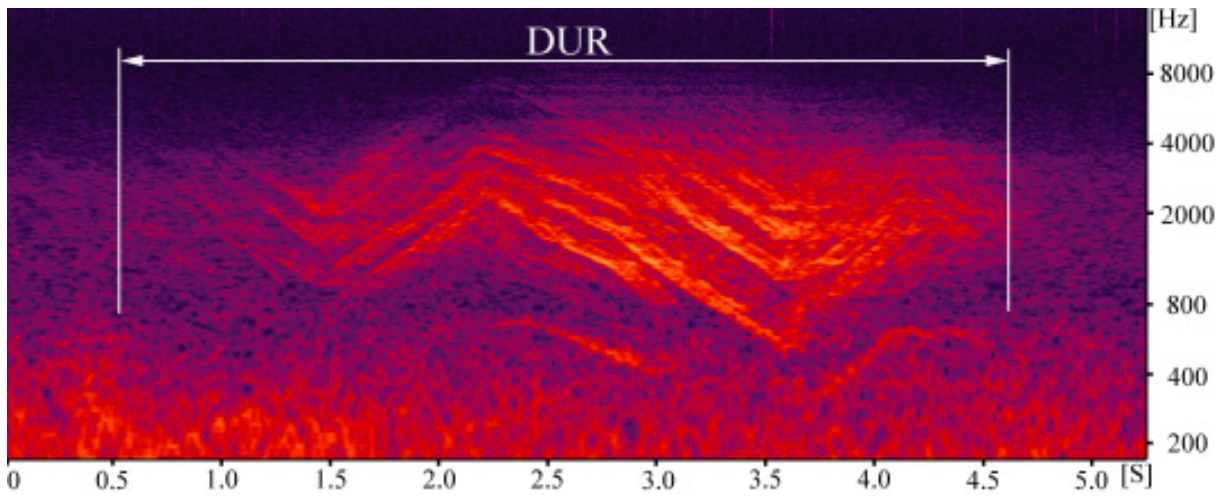
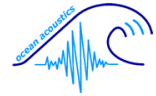


Figure 2.3.2A: Call duration (DUR) in seconds for a High siren call, as measured in the other siren calls as well. See Fig.2.3.1 for the description of the spectrogram settings.

Attached to some of the High siren calls a so-called Bowl sound can be found. The total duration (DUR) of the Bowl parts comprises of the sum of the durations of the two single parts minus the missing centre part (DUR1 and DUR2, as seen in Fig.2.3.2B). Bowls are also subject to fading-in and fading-out, as in the siren calls, but usually the start and the end were easily discerned from the background. Additionally, the frequency gap (GAP) between the Bowl and the High is determined as the difference between the maximum frequency of the Bowl and the minimum frequency of the High.

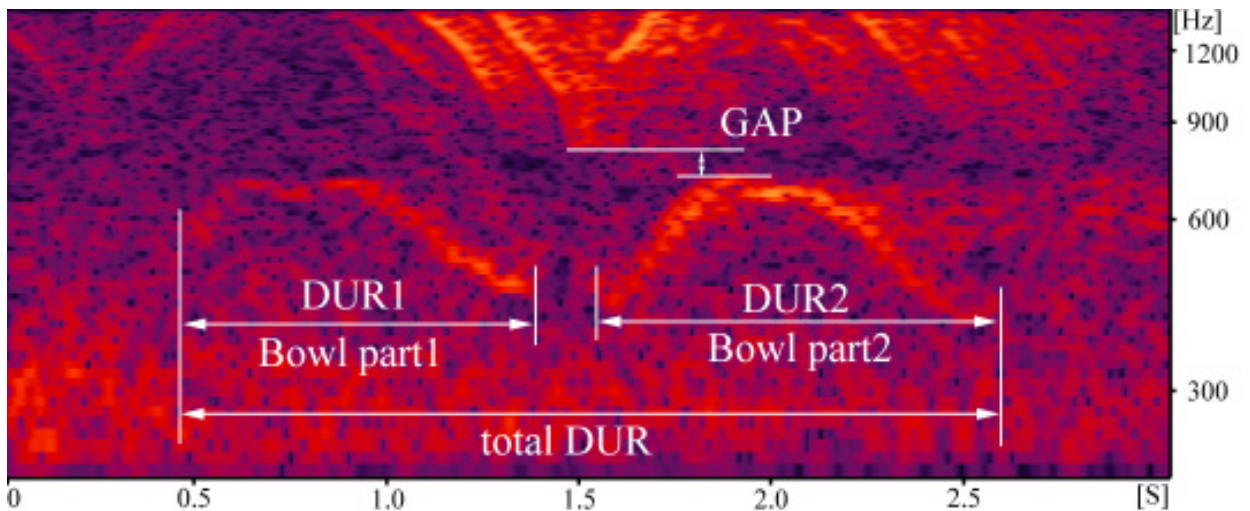
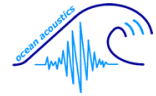


Figure 2.3.2B: Total call duration (DUR) in seconds for a Bowl comprises of the sum of the duration of its two parts (DUR1 and DUR2) minus the missing centre part. The spatial gap (GAP) in Hz between the Bowl and the High siren call is obtained by subtracting the Bowl's maximum frequency from the High's minimum frequency. See Fig.2.3.1 for the description of the spectrogram settings.



For the two Whoosh components the total duration in seconds is determined as described for the siren calls. The duration of the Whoosh Broadband Component (WBC) is particularly difficult to determine due to its slow fading-in and its diffuse ending. The duration (DUR1) is given as first clear sign of the call until most of it ends in a broad section, as shown in Fig.2.3.2C. The duration (DUR2) of the Whoosh Tonal Component (WTC) is easier to extract due to its distinct starting and ending points (Fig.2.3.2C).

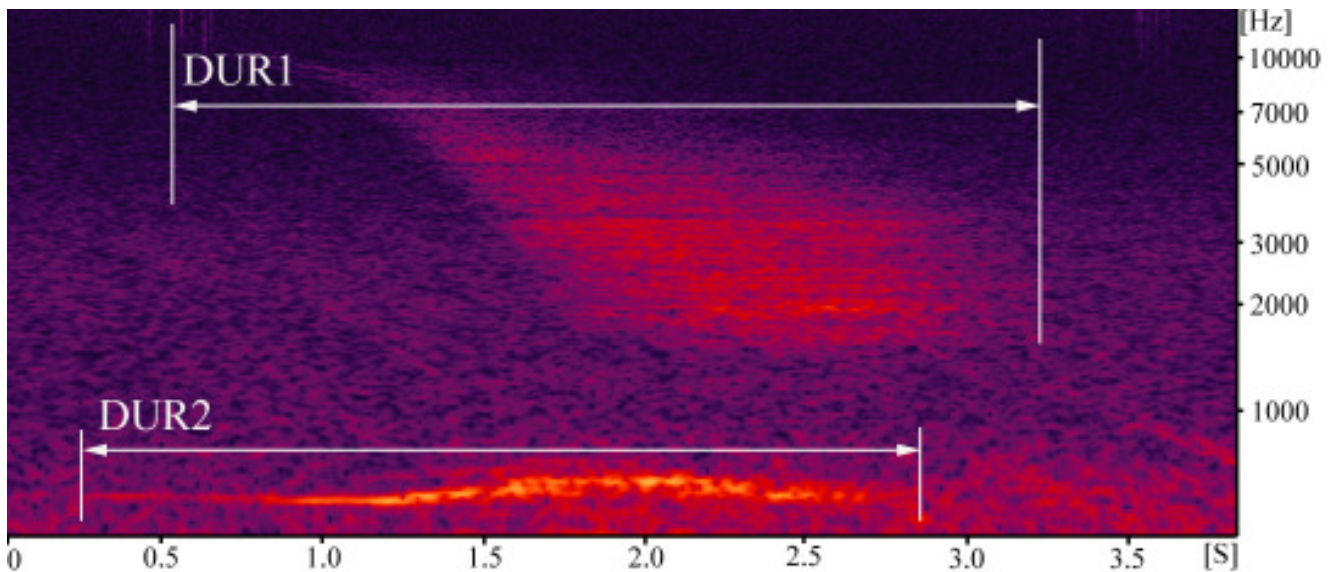


Figure 2.3.2C: Call duration in seconds for a Whoosh Broadband Component (DUR1) and a Whoosh Tonal Component (DUR2). For DUR1 the start is set at the first clear sign of the call until the broad diffuse section ends. See Fig.2.3.1 for the description of the spectrogram settings.

### 2.3.3 Minimum frequency, maximum frequency, and frequency range

The overall minimum (min) and maximum frequencies (max) in Hz are determined by measuring the lowest and highest visible frequency of the call. Here again, the highest frequencies of the siren calls and the WBC appear to fade out into the background noise. Depending on its intensity, it is possible to detect more or less of a call's higher frequency harmonic structures. The total frequency range (FR) in Hz can then be calculated by subtracting the minimum frequency from the maximum frequency (max-min, see Fig.2.3.3A). This very same parameter can also be given in octaves, calculated by taking the logarithm to the basis 2 of the quotient from maximum and minimum frequency ( $\log_2(\text{max}/\text{min})$ ).

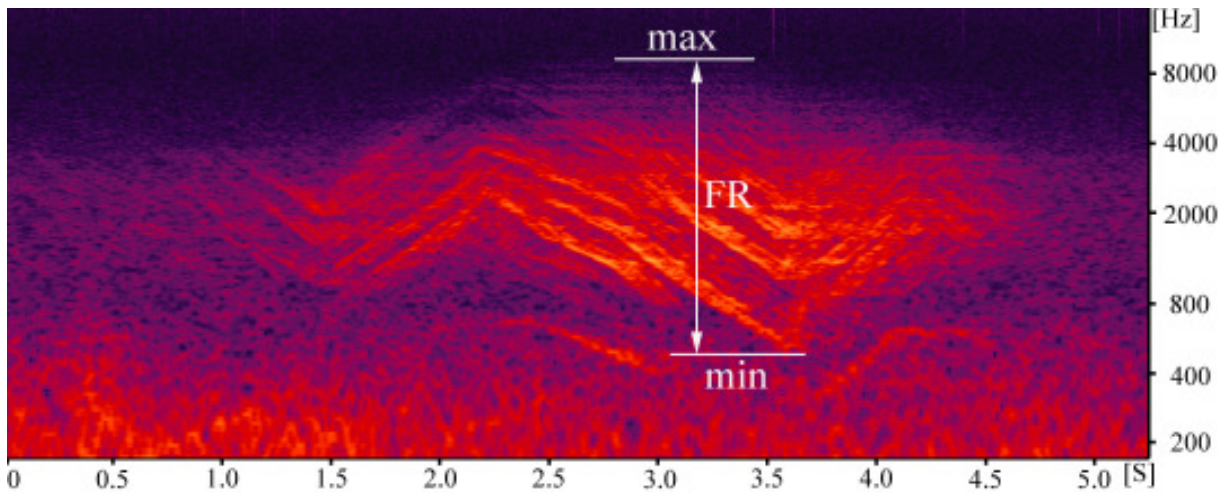
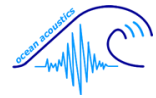


Figure 2.3.3A: Minimum (min) and maximum frequencies (max) in Hz for a High siren call. The other siren calls are treated the same way. The total frequency range (FR) in Hz is calculated by subtracting min from max. See Fig.2.3.1 for the description of the spectrogram settings.

If not identical to min and max, the start frequencies (SF1 and SF2) and end frequencies (EF1 and EF2) in Hz are determined for the two Bowl parts (Fig.2.3.3B), the WTC, and Low siren calls (Fig.2.3.3C). The frequency range for each call part (FR1 and FR2) in Hz or octaves can then be calculated as described above.

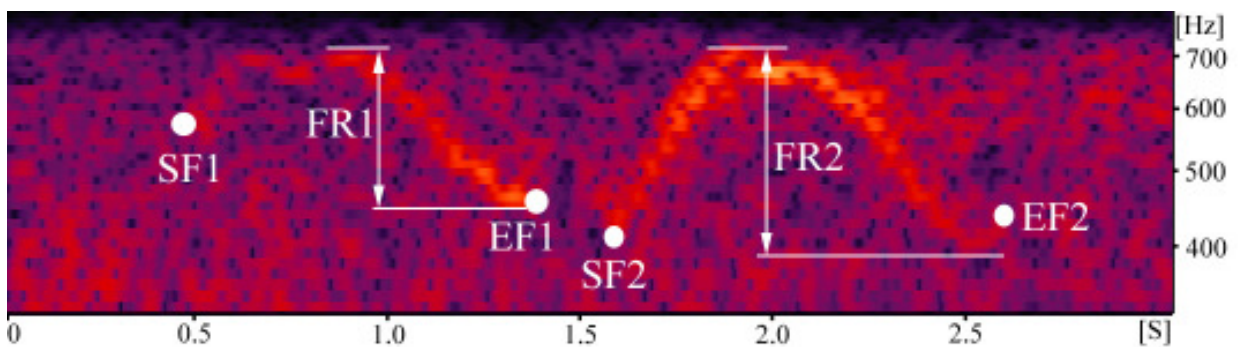
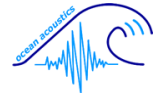


Figure 2.3.3B: Start (SF1 and SF2) and end frequencies (EF1 and EF2) in Hz for the two parts of a Bowl sound. The frequency range is calculated as described in Fig.2.3.3A. The same is done for the WTC. See Fig.2.3.1 for the description of the spectrogram settings.



In Low siren calls the start frequency (SF) is measured along with the end frequency (EF), the frequencies of the upswEEP peaks (1.Peak and 2.Peak), and the lowest points of the downsweeps (1.Low, see Fig.2.3.3C). The total frequency range in Hz can then be calculated by subtracting the minimum frequency (the lowest of the low downsweep points) from the maximum frequency (the highest of the upswEEP peaks).

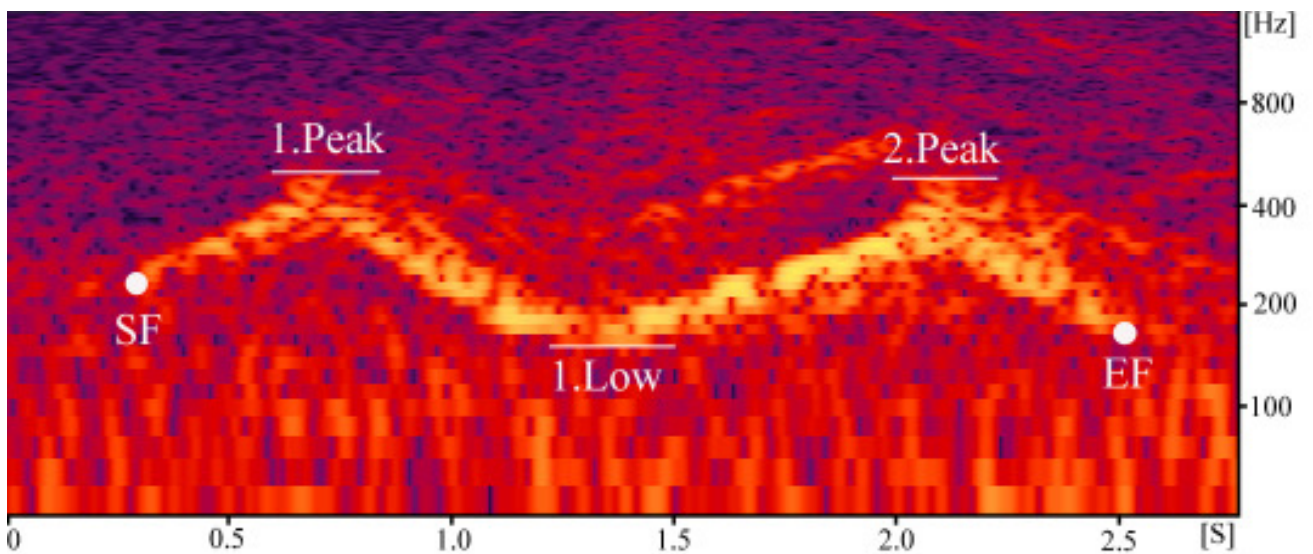


Figure 2.3.3C: Start (SF) and end frequency (EF) in Hz for the Low siren call. Additionally, the upswEEP peaks (1. and 2. Peak) and the lowest point of the downsweeps (1.Low) are determined. FR is calculated by subtracting the lowest Low from the highest Peak. See Fig.2.3.1 for the description of the spectrogram settings.

### 2.3.4 Elements, subtypes, and sweep rates

The complex siren calls were broken down into their sweeps, or so-called elements. The call elements are measured separately. The subtype of the siren calls is chosen depending on the number of elements (ups and downs, as explained in Table 2.3.4). The example in Fig.2.3.4A would be of subtype 4 with two upswEeps (a starting up (SU) and a complete up (U)) and two downsweeps (a complete down (D) and an ending down (ED)). It is also noted with what type of sweep a call started. In addition to the elements defined above, the elements ending up (EU) and starting down (SD) occurred in siren calls.

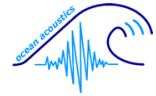


Table 2.3.4: Siren calls are sub-divided into subtypes depending on their number of elements (sweeps). This table shows the different forms a subtype can have. For call characterization it was noted whether the call started with an up- or a downsweep.

Subtype	Call appearance
1	/ or \
2	^ or v
3	∨ or ∨
4	∧∧ or ∨∨
5	∧∨ or ∨∧
6	∧∧ or ∨∨
7	∧∨∨ or ∨∧∧
	etc.

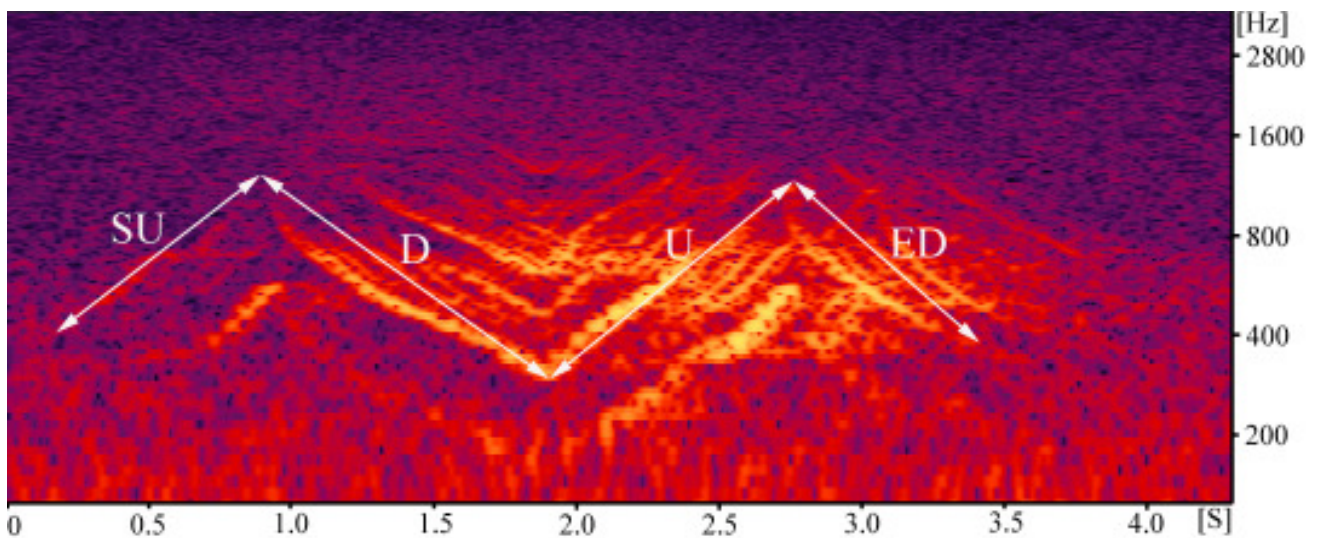


Figure 2.3.4A: Siren calls are broken down into their elements (number of sweeps). The Mid siren call shown here would be of subtype 4, with a starting upsweep (SU), a complete downsweep (D), a complete upsweep (U), and an ending downsweep (ED). See Fig.2.3.1 for the description of the spectrogram settings.

In Fig.2.3.4B the sweep rates of single siren call elements are determined. For each sweep rate, the minimum and maximum frequency and the duration of the element is required. The starting up rate (SUR) is the result of the logarithm to the basis 2 of the frequency range  $\Delta F$  (max-min) divided by the duration ( $t_1$ ). In the very same way all the other sweep rates (downsweep rate (DR), upsweep rate (UR), and ending downsweep rate (EDR)) are calculated. In other siren call subtypes, starting downsweep rate (SDR) and ending upsweep rate (EUP) occurred as well.

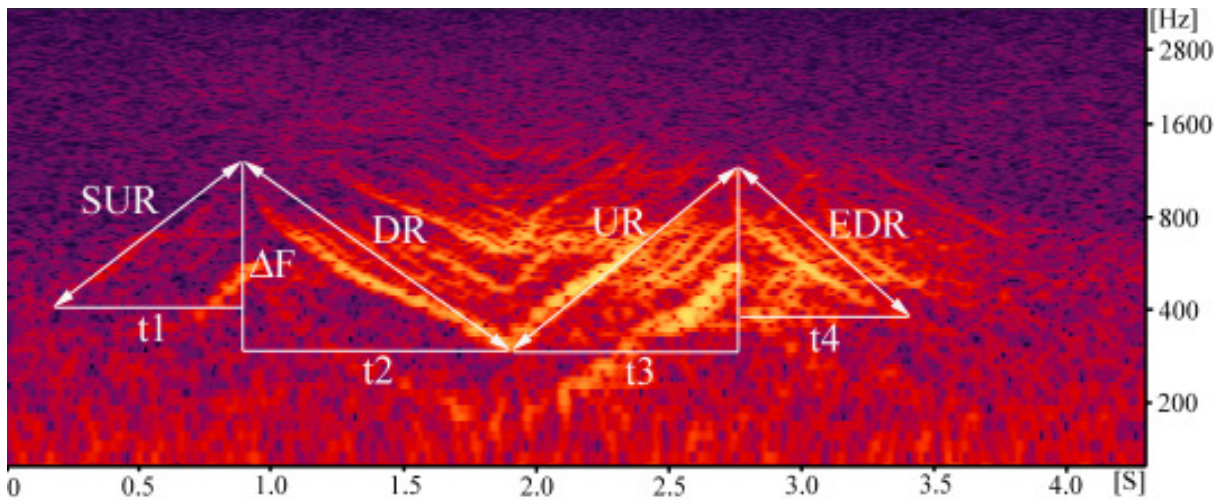
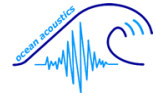


Figure 2.3.4B: Sweep rates of a subtype 4 Mid call. The starting up rate (SUR) is calculated using  $\log_2(\text{max-min})/t_1$ . This way, the other sweep rates (downsweep rate (DR), upsweep rate (UR), and ending downsweep rate (EDR)) are calculated as well. See Fig.2.3.1 for the description of the spectrogram settings.

### 2.3.5 Inter-harmonic intervals

In siren calls, the four most prominent (of greatest amplitude, if present) harmonic structures were chosen to calculate the inter-harmonic intervals (IHI1- IHI4) in Hz as shown in Fig.2.3.5. The upper and lower frequency limits of each of these four harmonics were determined at a distinct time. For example, the IHI1 is the lower frequency limit of the second harmonic subtracted from the upper frequency limit of the first harmonic (upper-lower), the same way the frequency range was calculated in 2.3.3.

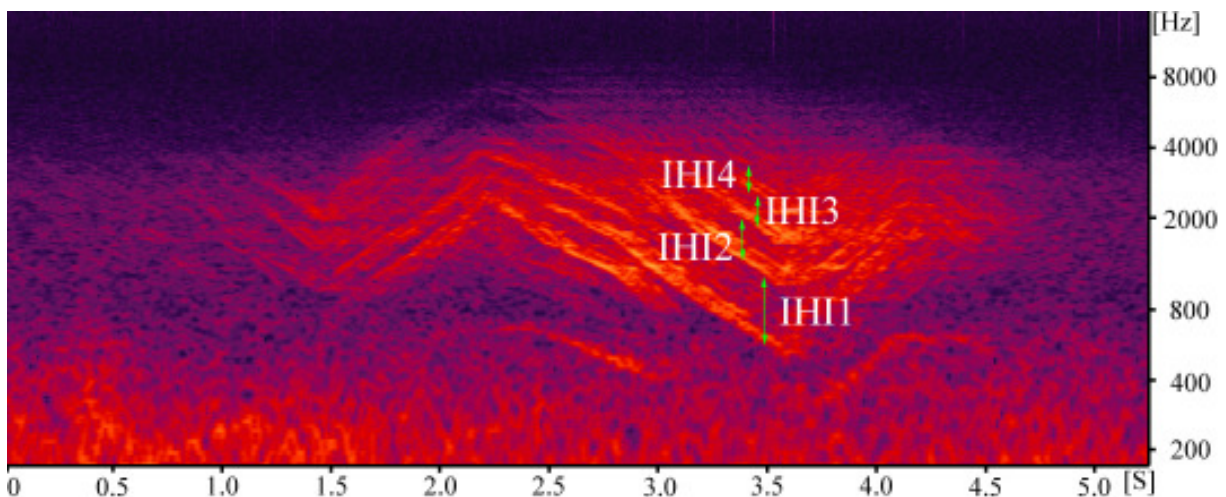
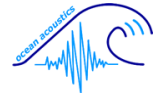


Figure 2.3.5: The first four inter-harmonic intervals (IHI) of a High siren call. The IHIs (green arrows) result from the lower frequency limit being subtracted from the upper frequency limit. See Fig.2.3.1 for the description of the spectrogram settings.



### 2.3.6 Peak frequency and bandwidth

Another method to determine the frequency range, or bandwidth, of a call is using the spectral display, as shown in Fig.2.3.6A, with frequency in Hz on the x-axis and amplitude in dB FS (full scale=143 dB *re* 1 $\mu$ Pa/Hz) on the y-axis.

The background noise (green line) is measured prior to the call. The call itself is summarized over its full length (red line). The bandwidth (BW) is determined by the frequency range where the red line exceeds the noise level (green line). The peak frequency (PF) is extracted visually along with its corresponding amplitude.

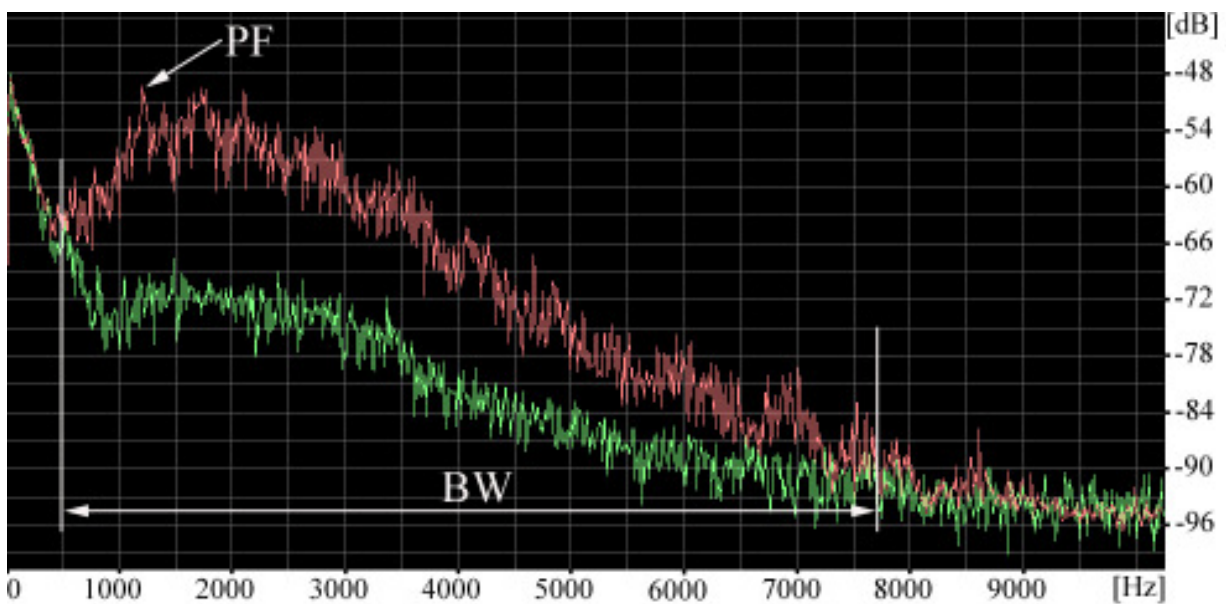
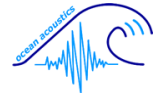


Figure 2.3.6A: Spectrum of a High siren call with frequency in Hz on the x-axis and amplitude in dB FS (full scale equals the amplitude of 143 dB *re* 1 $\mu$ Pa/Hz) on the y-axis. The background noise (green line) is measured prior to the call. The call itself is summarized over its full length (red line). The Bandwidth (BW) is determined by the frequency range where the red line exceeds the green line. The peak frequency (PF) is extracted visually.



To determine the WBC's bandwidth and peak frequency in a reproducible manner, spectra were calculated at the temporal centre of the diffuse horizontal downsweep part (PF1, as seen in Fig.2.3.6B) and again one second before that (PF2).

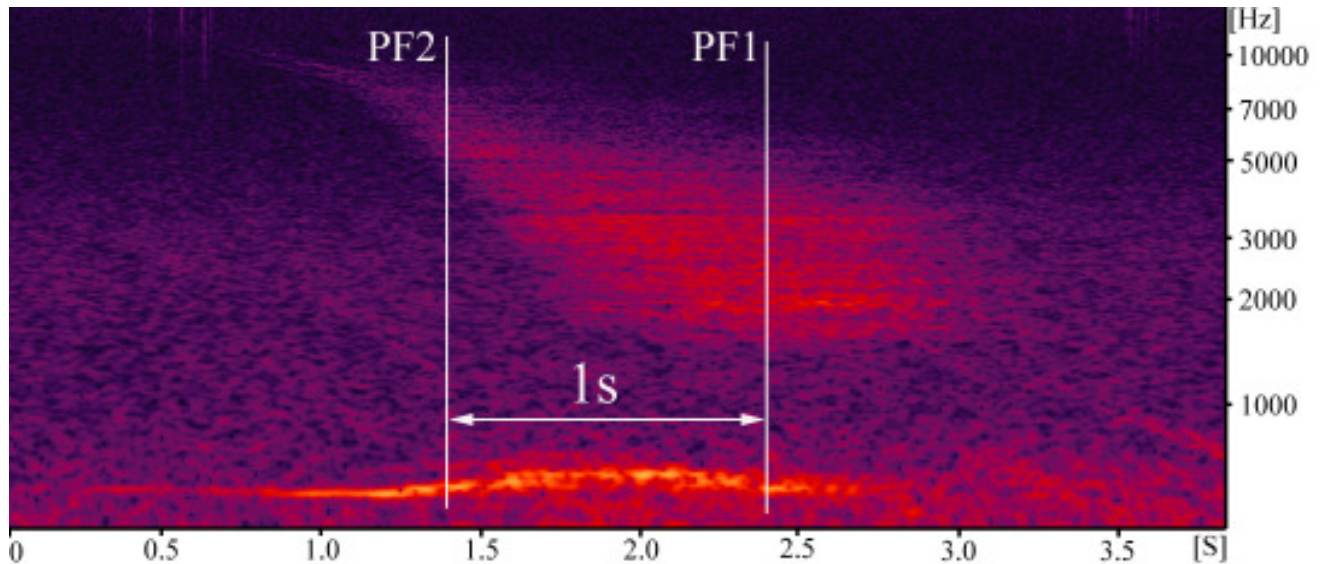


Figure 2.3.6B: To determine the peak frequency in the WBC, two positions are chosen for measurement. The first (PF1) is located in the temporal centre part of the diffuse horizontal downsweep, the second exactly one second (PF2) prior to the first one. See Fig.2.3.1 for the description of the spectrogram settings.

For the WBC, the green line in Fig.2.3.6C represents the first spectrum at time PF1 of Fig.2.3.6B, while the red line represents the second measurements at time PF2 of Fig.2.3.6B. Corresponding bandwidths (BW) were determined by the frequency range, which exceeds the underlying background noise, as already explained in Fig.2.3.6A. The peak frequencies (PF1 and PF2) are visually extracted. In this spectrum, the prominent peak of the WTC, which is explained further down, is marked as well.

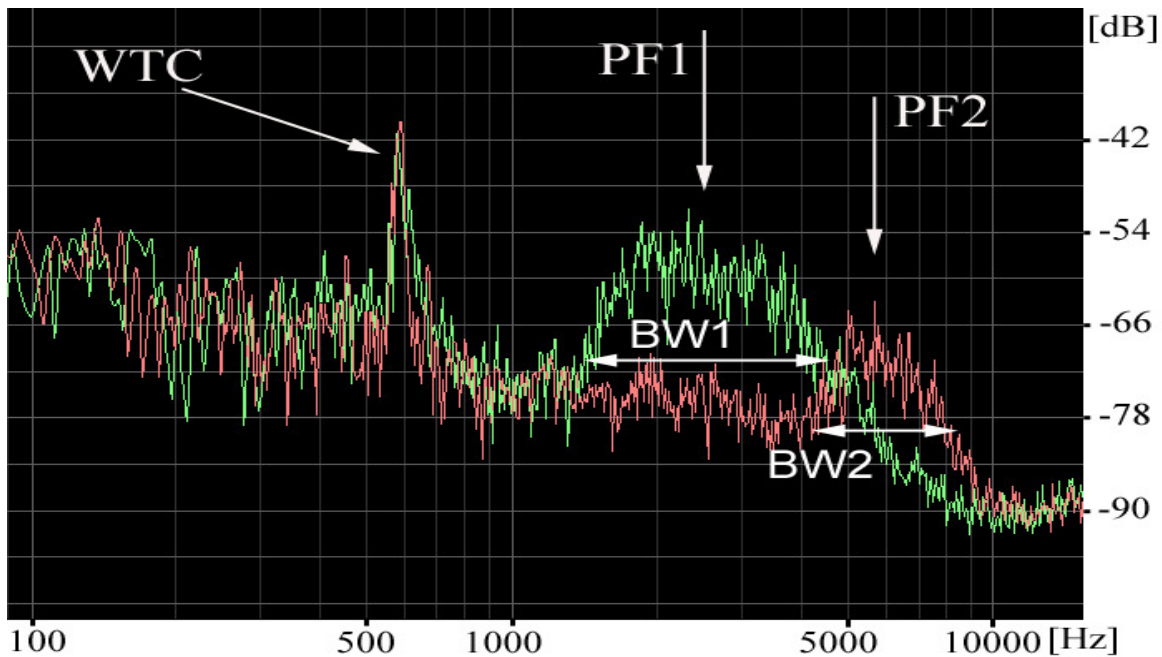
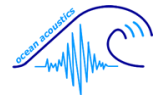


Figure 2.3.6C: The WBC is measured at two positions (PF1 resulting in the green line and PF2 resulting in the red line) as mentioned in Fig. 2.3.6B. For each position, the bandwidths (BW1 and BW2) and the peak frequencies (PF1 and PF2) are determined, as explained in Fig.2.3.6A, along with the description of the setting of the spectrum. The WTC is explained below.

As already mentioned earlier, the WTC forms a very distinct spectral peak as shown in Fig.2.3.6D. The WTC's bandwidth (BW), peak frequency (PF), and amplitude at peak frequency are determined, as described in Fig.2.3.6A.

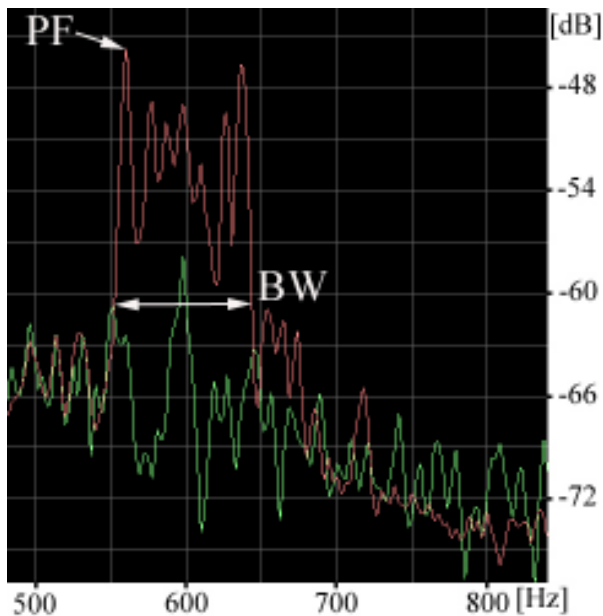
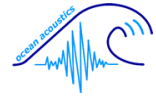


Figure 2.3.6D: A more detailed view of the WTC's spectral peak. The narrow bandwidth (BW), the peak frequency (PF), and its corresponding amplitude in dB FS are determined, as explained along with the description of the setting of the spectrum in Fig.2.3.6A.



### 2.3.7 Echoes

In Fig.2.3.7 two examples of echoes and/or multipath transmissions are given. Often it is not clear whether two similar looking calls are overlapping, or whether multipathing might be caused by reflections at the ocean boundaries (ice walls, sea surface, sea floor). However, the time shift between the first and the following signatures is quite small and the latter look exactly like the first. Therefore, such an event was labelled “echo present”.

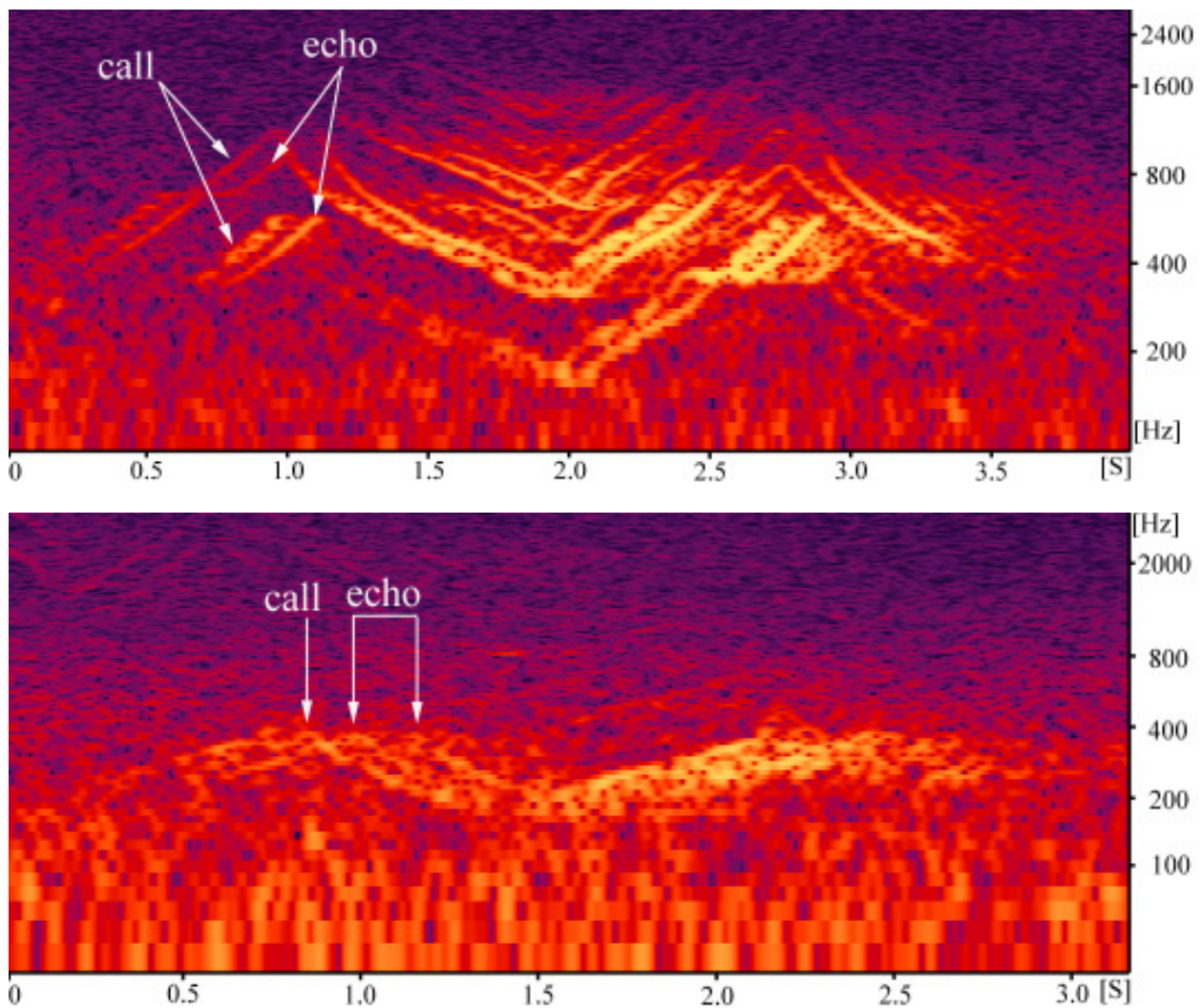
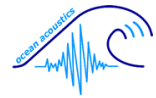


Figure 2.3.7: Two examples of a call echo. A Mid siren call is reflected once (top), while a Low siren call produces two echoes (below). See Fig.2.3.1 for the description of the spectrogram settings.



### 2.3.8 Special features

Additional to the usual measurements some special features of Ross seal calls are noted. In Mid siren calls distinct edges (E1-E3) occur at the upsweeps that are sampled with their frequency and duration respectively. Also, the levelled peaks of the basic call, the low part peaks (LPP1-LPP2), are listed with their corresponding frequencies (Fig.2.3.8A).

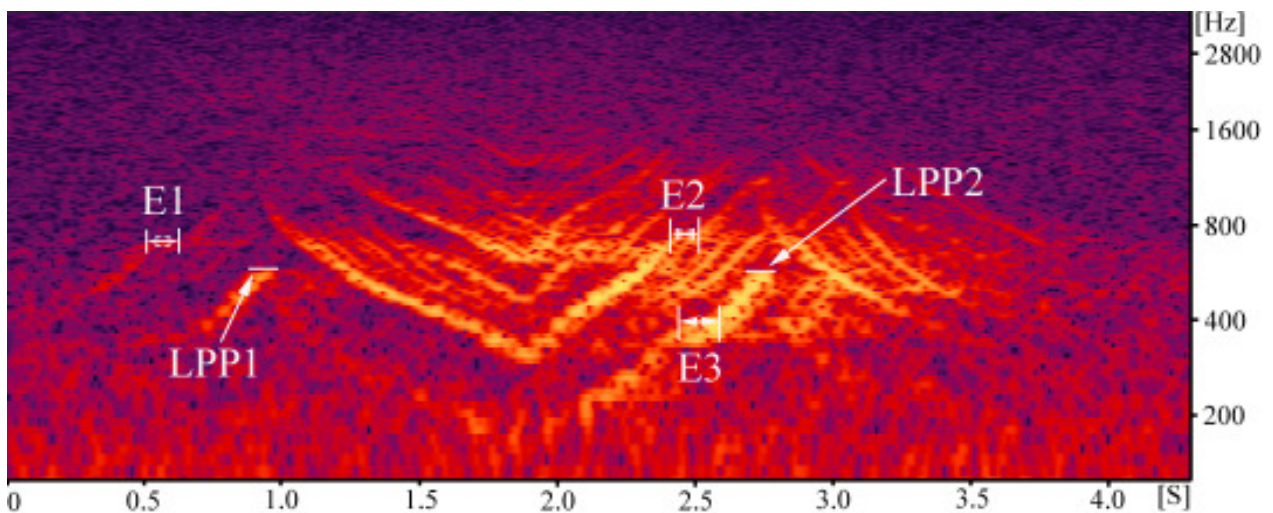


Figure 2.3.8A: Distinct edges (E1-E3) can be found in the upsweeps of Mid siren calls. Their frequency and duration is noted, as well as the so-called Low Part Peaks (LPP1-LPP2) that form the highest part of the basic call. See Fig.2.3.1 for the description of the spectrogram settings.

Fig.2.3.8B shows an example of a little attached dot (Dot) in front of a Low siren call. The distance (Dis) in seconds between the dot and the actual beginning of the call is determined along with the dot's frequency.

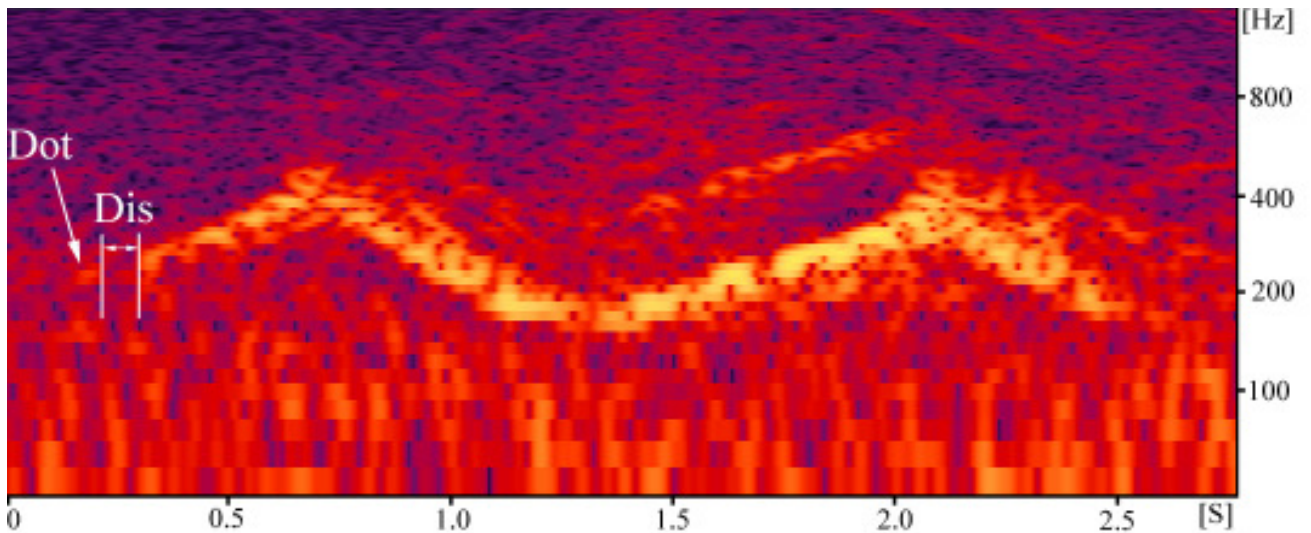
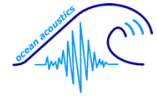


Figure 2.3.8B: A little attached dot (Dot) in front of a Low siren call. Its frequency and its temporal distance in seconds (Dis) to the actual call are determined. See Fig.2.3.1 for the description of the spectrogram settings.

Another feature specific to Low siren calls are the diffuse turning points (DTP) as shown in Fig.2.3.8C. This is the case when the lowest and/or highest turning points of the sweeps cannot be seen visually, as if the call is locally interrupted or disturbed by masking noise. It is listed whether such DTPs are present and in which position they occur.

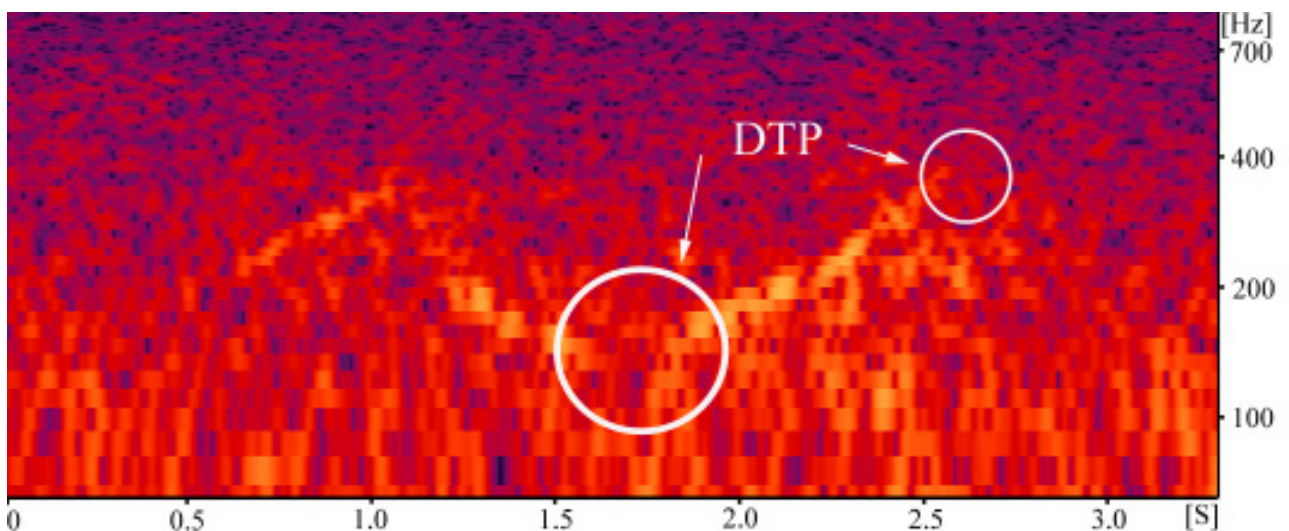


Figure 2.3.8C: Diffuse turning points (DTP) in Low siren calls look as if the call is interrupted at this point. They occur at either the highest or lowest turning point of the Low call. Their presence is noted along with their position. See Fig.2.3.1 for the description of the spectrogram settings.

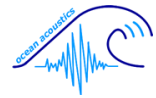


Fig.2.3.8D highlights the “visible bands” of the WBC as indicated by arrows on the right. Only the first three bands – starting from low to high frequencies – were retrieved, even though sometimes more than three were visible.

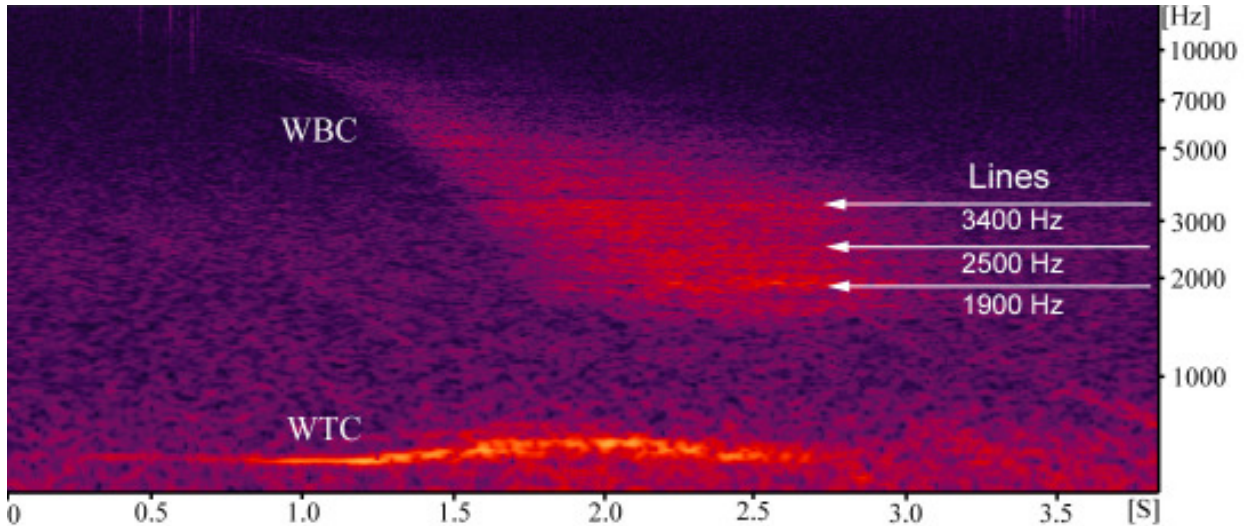


Figure 2.3.8D: Visible bands of the WBC on the right side. Starting from low to high frequencies, the first three bands are counted and noted along with their frequency. See Fig.2.3.1 for the description of the spectrogram settings.

The gap in the Whoosh is defined as the frequency distance between the WBC and the WTC. It is measured by subtracting the maximum frequency of the WTC from the minimum frequency of the WBC, as shown in Fig.2.3.8E.

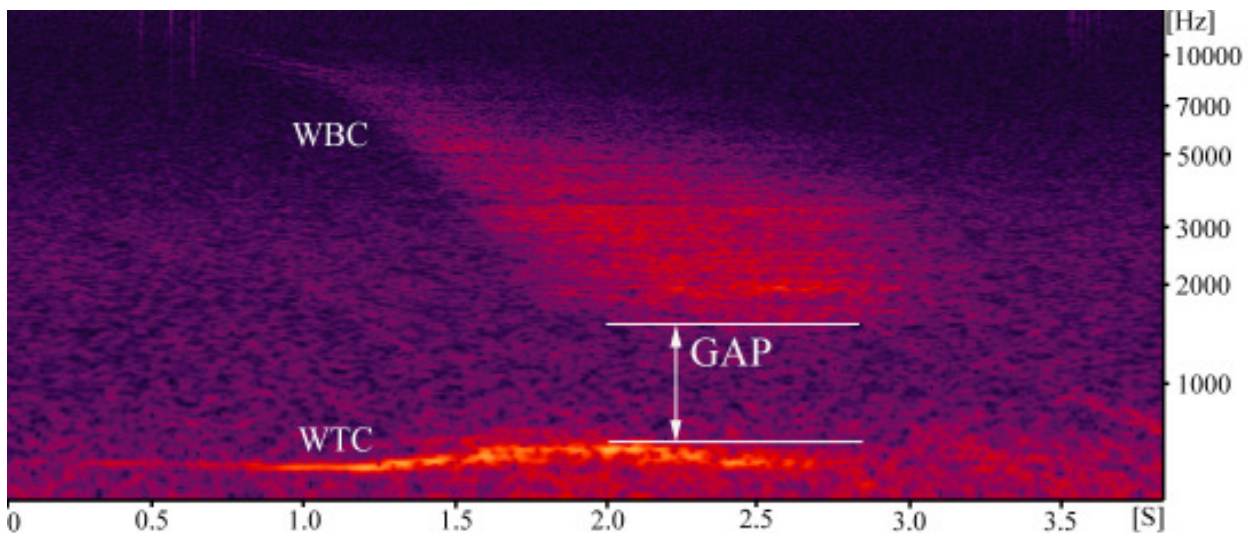
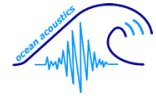


Figure 2.3.8E: The gap is the distance between the WBC and the WTC in Hz. It is determined by subtracting the maximum frequency of the WTC from the minimum frequency of the WBC. See Fig.2.3.1 for the description of the spectrogram settings.

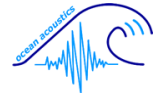


### **2.4 Seasonal call counts**

For this study, it was of interest in what time periods Ross seals are present at PALAOA. It was known from the very first recordings of 2005, that this species can be heard in mid December. Starting at this point, the mp3 dataset was scanned systematically to find the first occurring Ross seal call. All four call types (High, Mid, Low, and Whoosh) of the first two consecutive minutes after midnight were counted. The midnight-period was selected as this seemed to be the time of greatest calling activity (as explained in chapter 2.5). When calls ceased in early February, the exact time of the last call occurrence was determined by backtracking. The calls' seasonal variability was determined for two consecutive seasons: beginning at PALAOA's setup in December 2005 through February 2006, and again in December 2006 through February 2007. The resulting numbers were plotted using Microsoft's Excel.

### **2.5 Diurnal call counts**

Spectrograms of different times of day immediately indicate variations in calling activity with phases of higher and lower activity. To quantify this diurnal variability, the total number of calls per one-minute-file was counted in a chosen time window (see below). Information on call type (High, Mid, Low, or Whoosh), background noise, technical notes, and acoustic presence of other marine mammals was retained as well. Only calls that could definitely be identified as Ross seal calls were included in this census. The period of this analysis was chosen due to the availability of additional CTD data (conductivity, temperature, and pressure for depth), which is collected every 30 minutes. Thus, the census starts at midnight on 23 January 2007, and proceeds for 10 consecutive days (until 1 February 2007), when the seals would leave the area again (as the seasonal counts had indicated, as explained in chapter 2.4). In addition, weather conditions were compiled from the meteorological observatory at the Neumayer base, while digital images, obtained by the PALAOA webcam, monitored sea ice conditions.



To estimate whether the calling rate of a one-minute-file is representative for an entire period, all 60 minute files of the first full hour on 23 January were analyzed. To test whether the obtained standard deviation is independent of the overall daytime, a 12 hour period (01:00 to 13:00) was analyzed at an interval of 6 files per hour. Finally, the remaining period was examined by counting the calls of one file every 30 minutes until midnight of 30 January, followed by a one hour interval up to 2 February, when hardly any calls could be detected anymore. The resulting call numbers were plotted using Microsoft's Excel.

### **2.6 Localization of the sound source**

The tetrahedral design of the PALAOA hydrophone array allows localizing a sound source by looking at the differences of arrival times on each one of the four deployed hydrophones. Unfortunately, two hydrophones failed their function within a year after deploying due to an assembly defect, which leaves intact only two hydrophones (hydrophone 1 and hydrophone 2, as shown in Fig.2.1.2B). These two hydrophones permit the bearing of a sound source rather than its position.

Fig.2.6A and Fig.2.6B demonstrate the method. An acoustic event is visible in the spectrograms of both channels (Fig.2.6A; upper channel = hydrophone 1, bottom channel = hydrophone 2) but with a small difference in its time of arrival. This delay of time of arrival is determined by selecting a prominent feature of the respective sound event, which is visible on both channels (e.g. sharp edges, peaks etc.). In Fig.2.6A, this offset is indicated by a horizontal white line between two vertical white lines, which point to that feature (Fig.2.6B).

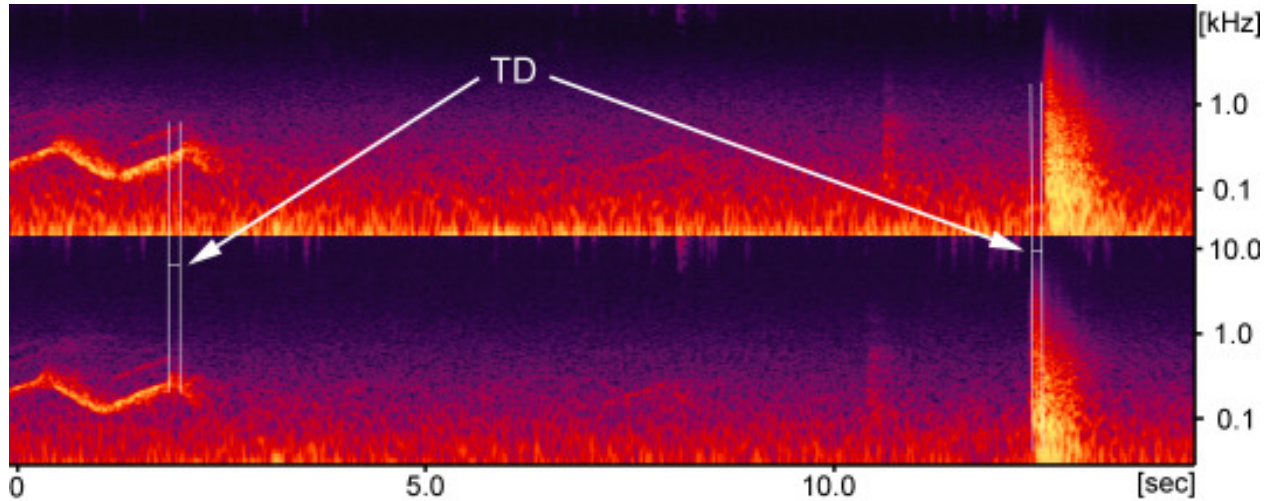


Figure 2.6A: Illustration of the different times of arrival of two sound events in a stereo spectrogram with time on the x-axis and frequency on a logarithmic scale on the y-axis. Both the Ross seal call on the left and the loud ice crack on the right side of the spectrogram arrive first at the bottom channel (hydrophone 2), and with a minimal time delay (horizontal white line between the vertical white lines) also at the upper channel (hydrophone 1).

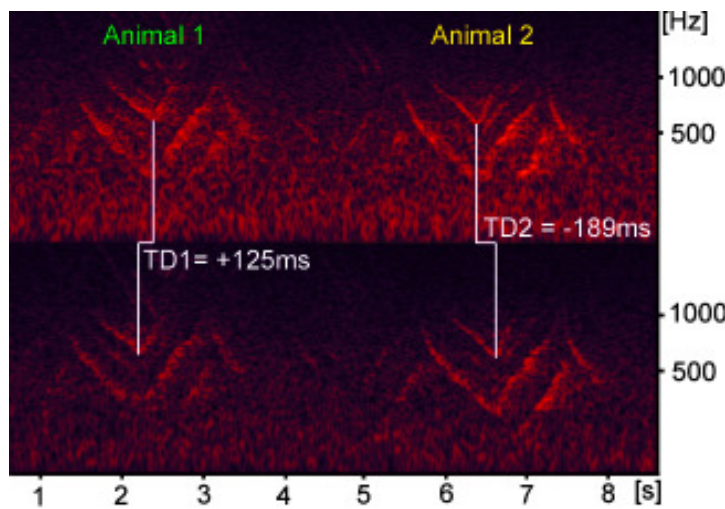
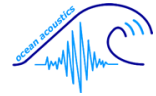


Figure 2.6B: Spectrogram of two Ross seal calls. The lower edge is chosen as a prominent feature to determine the differences in time of arrival. The left call arrived earlier on hydrophone 2 (bottom) by a time delay (TD1) of 125 ms, whereas the right call arrives earlier at hydrophone 1 (top) by a time delay (TD2) of 189 ms. Therefore it can be assumed that these calls are emitted by two different animals, or at least come from two different directions. Description of the spectrogram settings as in Fig.2.6A.



### 2.6.1 Estimation of the number of calling seals

Based on the time delays at which sound arrives at the two hydrophones, the speed of sound underwater (1442.1 m/s at the local conditions), and the exact distance and alignment of the two hydrophones (300 m, NO-SW), it is possible to calculate the direction of the incoming call.

A sound source that is located at exactly the same distance from both hydrophones, would not produce any time delay (0 ms), whereas the delay would be maximal (208 ms, which is the time span the sound needs to travel the distance of 300 m) at one hydrophone, if the sound source would be exactly behind the other hydrophone. Other time delays fall within the range of -208 ms to 208 ms (as calculated by the formula:  $\sin(\alpha) = t \cdot 1442 / 300$ ). Positive numbers indicate that the signal arrives first at hydrophone 2, while negative numbers indicate a first arrival at hydrophone 1 (as shown in Fig.2.6B). However, this method leaves a left-right ambiguity in relation to the axes drawn through the hydrophones. But taking into account the geometry of the ice boundaries around PALAOA, this ambiguity can be resolved. Signals that come from the southern direction would propose a sound source located below the 100 m thick ice shelf, and pack ice seals, such as the Ross seal, are rather unlikely to dive underneath the ice shelf. For easy analysis, differences in time of arrival were drawn on a circle and overlaid to a satellite image (Fig.2.6.1).

This method of sound source localization contributes to an estimation of the minimum number of calling animals, assuming that two vocalizing seals would not be too close to each other or on a straight line viewed from the hydrophones.

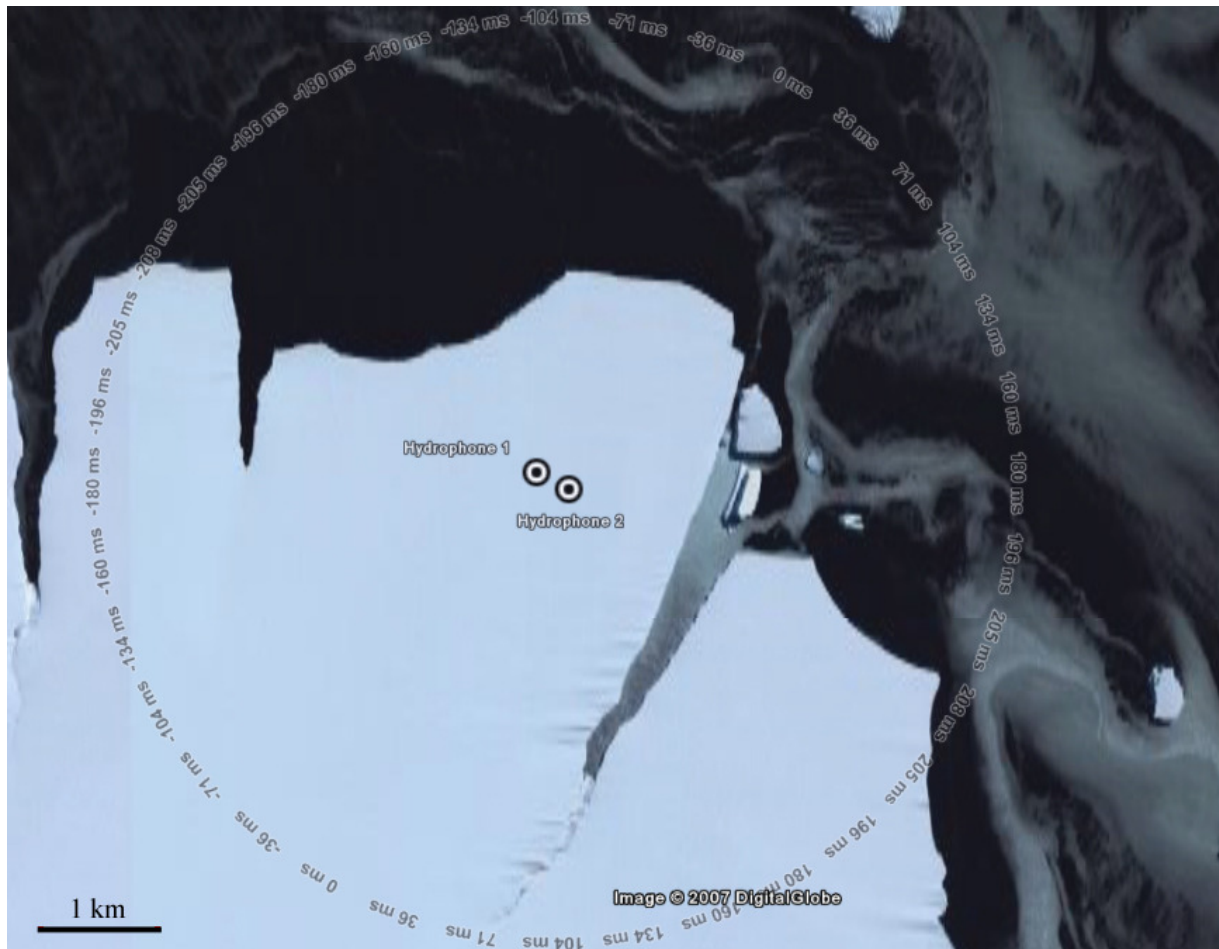
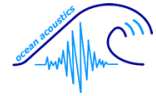


Figure 2.6.1: This localization circle visualizes the relation between differences of time delays and the direction of the sound source. If a calling animal is located right amidst the two hydrophones, the delay would be 0 ms. On the other hand, if it is located behind one hydrophone in a straight line connecting both devices, the time delay would be maximal with 208 ms. All other values lie in between those extremes, hence drawn-in measurements of the time delays assign the direction of the incoming call (satellite image by DigitalGlobe, 2007).

### 2.6.2 Individual calling patterns

In order to explore the possibility of individual calling patterns, the directions of the above mentioned time delays of four randomly chosen one minute-files were each given a colour. Thus all measured call types could be coloured and plotted in chronological order to reveal any patterns of call usage. The same has been done for five consecutive minutes as well.



### 2.7 Problems of visual measurements

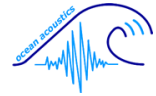
PALAOA provides – at least for Ross seal bioacoustics – an amount of acoustic data without precedent, and with no prior analytic work existing in this regard. Therefore, the analysis presented in this thesis goes well beyond pre-described methods in order to explore the possibilities, strengths, and weaknesses of the current dataset and various analysis approaches. There was no standard approach on how to start the measurements, how to accomplish those, or even how to distinguish the different call types.

Measurements of the various call parameters are not less problematic, since they are performed visually on the basis of spectrograms. However, these are subject to changing background noise (which, in turn, depends mostly on environmental factors, as described below) and the choice of settings. Therefore, all the values measured or counted or calculated are, in fact, quite subjective and might not be reproduced in a similar way by another observer. Being aware of this, it was attempted to judge objectively throughout this study in order to minimize observer related errors.

Another impact on the visual measurements is the ambient noise of the recordings. PALAOA, as described in chapter 2.1, passively records in the Southern Ocean, which still is a “quiet” location concerning anthropogenic noise pollution, as opposed to highly frequented other oceans. Nevertheless, it is a natural environment. Especially the ice but also other marine mammals contribute to an almost constant background noise. This adds up to the weather-dependent “normal” ocean noise caused by tidal movements, waves etc. Low frequency calls (< 500 Hz) are often masked by this noise.

### 2.8 Statistical analysis

Basic descriptive statistics and the diagrams of call frequencies were made using Microsoft’s Excel. The boxplots were created in SigmaPlot 8.0, the scatterplots and a principal component analysis in MATLAB 7.2.0. A principal component analysis (PCA) is one approach to simplify multidimensional data and to visualize it. PCA is defined as an orthogonal linear transformation that transforms the data to a new coordinate system so that the greatest variance lies on the first coordinate (first principal component)



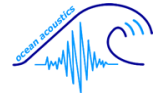
independently of the projection of the data. The second greatest variance then lies on the second coordinate, etc. PCA can be used to reduce dimensions in a dataset by retaining the characteristics that contribute most to its variance. It does so by keeping lower-order principal components and ignoring higher-order ones (Wikipedia).

A second multivariate approach was performed using a tree-based method - the classification tree. This visually accessible, tree-structured, non-parametric analysis is created in CART (Classification And Regression Trees; De`ath and Fabricius, 2000) using the free software R (Ihaka and Gentleman, 1996; under <http://www.r-project.org>) which produces a decision tree by separating the data into groups (so called nodes) through a series of binary splits. Each split is based on a value for a single variable. The criteria for splitting are set by splitting rules that are applied at each node. The optimal tree would be the smallest possible tree (with the fewest variables) but with the highest predictive accuracy concerning the data. The length of the vertical lines at each split represents the total variation explained by that split, and the earlier a split occurs the more variability it contains.

Call numbers were tested for Gaussian distribution using the Kolmogorov-Smirnoff-Test in SigmaStat 8.0.

Cross correlation coefficients between the call rate, tidal current, and global radiation were computed in MATLAB to estimate their influence on each other. Prior to this computation, the time series were normalized to zero mean and any linear trend was removed. Due to a possible delay between peaks in call rate and the respective factor, the maxima and minima of the cross correlation function were used. These calculate the cross correlation as a function of time lags between two time series. In addition, direct correlations between the factors mentioned above were calculated using the Pearson Product Moment Correlation Test in SigmaStat.

A Fast Fourier Transform (FFT) in MATLAB was added to clarify the correlations.



## 3. Results

### 3.1 Description of call types

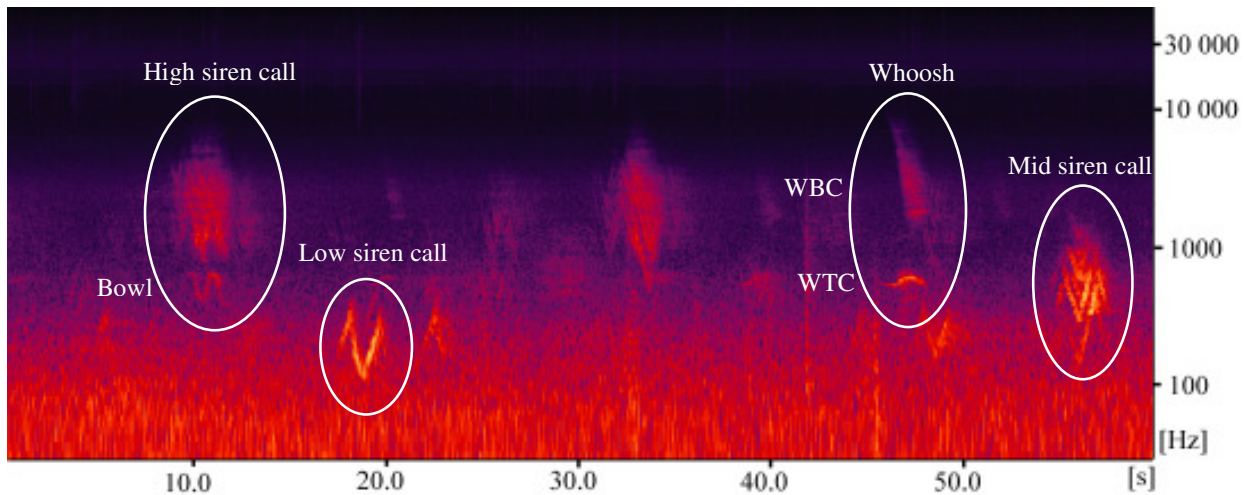
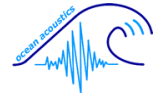


Figure 3.1: Spectrogram of a typical PALAOA sound file presenting all four Ross seal call types. A High siren call with Bowl attachment, a Mid siren call, a Low siren call, and the Whoosh, comprising of the two components WBC and WTC. The x-axis shows the time and the y-axis the frequency on a logarithmic scale. The colours code for the intensity with bluish/purple for almost silence and light yellow for sounds with high amplitude.

The main result of this thesis is the discovery, description, and nomenclature of four different Ross seal calls. Some of these have already been mentioned in chapter 2 for better understanding and explanation of the measurements taken.

In the following chapter, the four different call types - High siren call (also referred to as High), Mid siren call (also referred to as Mid), Low siren call (also referred to as Low), and the Whoosh (comprising of the Whoosh broadband component WBC and the Whoosh tonal component WTC) - will each be looked at in detail. Single elements of the three siren call types are highlighted separately. Call attachments, if existent, are added in each section. The chapter concludes with comparisons among the four call types. A description of differentiation proves that these four call types really are distinct from one another.



### 3.1.1 High siren call

Highs consist of alternating up- and downsweeps (48% of the calls starting with an up, 52% starting with a down; see Fig.3.1.1A). Subtypes 2-9 occur, but subtypes 4 (36%), 5 (34%), and 6 (14%) dominate with 4-10 strong harmonics and sidebands at a relatively constant rate. The mean four inter-harmonic intervals vary widely. They are 849 Hz ( $\pm 211$ ), 689 Hz ( $\pm 164$ ), 631 Hz ( $\pm 168$ ), and 556 Hz ( $\pm 122$ ) respectively. The minimum frequency is 592.18 Hz ( $\pm 145.47$ ) and the maximum frequency is 7129.38 Hz ( $\pm 1803.55$ ), resulting in the typical frequency range of Highs of 6537.20 Hz ( $\pm 1798.59$ ) or 3.58 oct ( $\pm 0.51$ ) and a mean call duration of 3.37 sec ( $\pm 0.68$ ). The peak frequency is 1585.42 Hz ( $\pm 226.09$ ) with an amplitude at peak frequency of -57.28 dB ( $\pm 4.83$ ). dB is given as dB FS with full scale=143 dB *re* 1 $\mu$ Pa/Hz (Zero Peak). 40% of the calls have an added Bowl sound as attachment (as described below).

A complete upsweep (U) has a sweep rate of 3.02 oct/s ( $\pm 0.59$ ) and a complete downsweep (D) a rate of 2.12 oct/s ( $\pm 0.41$ ). The diffuse starting upsweep (SU) does so at a rate of 2.66 oct/s ( $\pm 0.66$ ), a starting downsweep (SD) at a rate of 2.28 oct/s ( $\pm 0.33$ ), an ending upsweep (EU) at a rate of 2.91 oct/s ( $\pm 0.84$ ), and an ending downsweep (ED) at a rate of 2.23 oct/s ( $\pm 0.50$ ). A summary of the measurements of High siren calls and their single elements are provided in the attached tables Tab.6.1 and Tab.6.2 of the appendix.

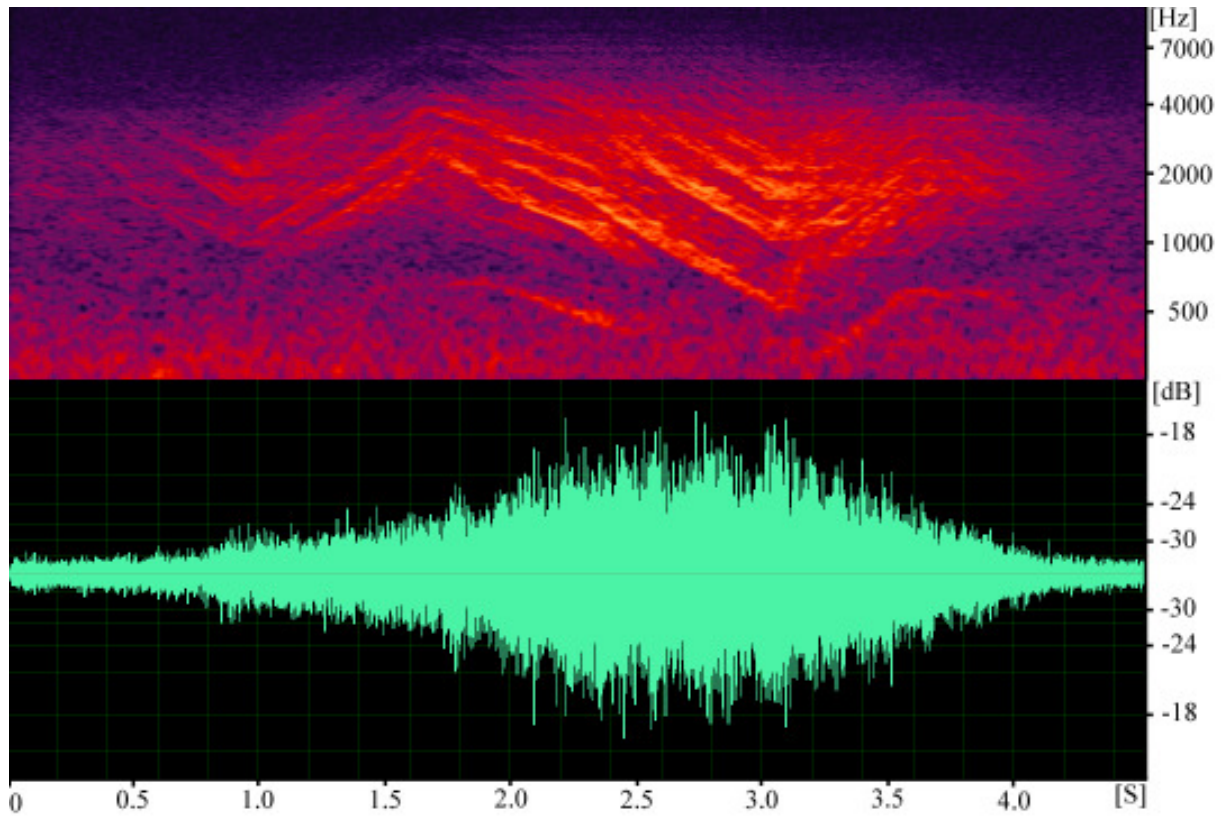
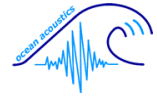
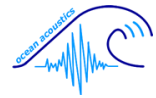


Figure 3.1.1A: Spectrogram (top) and waveform of a typical High siren call. The x-axis of both plots is the time in seconds, while the y-axis of spectrogram and waveform give frequency on a logarithmic scale and amplitude in dB FS (full scale equals the amplitude of 143 dB *re* 1  $\mu$ Pa/Hz) respectively. The High's waveform (below) does not show the different sweeps, meaning the amplitude does not change significantly between the sweeps.



Among the High siren calls some “pure” calls occur. Usually their appearance in a spectrogram shows quite thick lines, sometimes with a ladder-like pattern in it. 58% (n=29) of the Highs measured in detail show fine thin lines instead (Fig.3.1.1B). Of these with fine lines only 2 calls (7%) own a Bowl component.

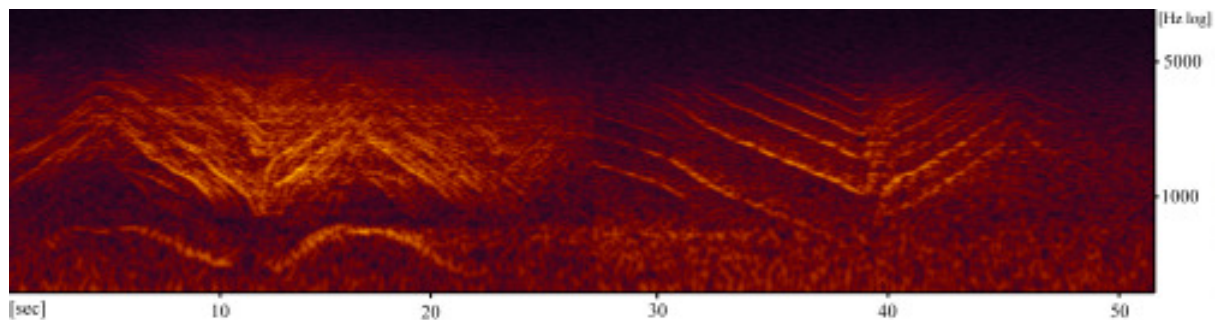


Figure 3.1.1B: Comparison of High calls with “thick lines” and Bowl (left) and one with “thin lines” and no Bowl component (right), with duration in seconds on the x-axis and frequency on logarithmic scale on the y-axis.

### Bowl attachment

Whenever present, the Bowl attachment is characterized as well. The Bowl’s tonal sound is frequency modulated as well, but varies with a much slower rate than the High. In most instances, the Bowl is interrupted in its low frequency part as shown in Fig.3.1.1C.

The Bowl attachment is found in 40% of all High siren calls. It also consists of alternating ascending and descending parts. 90% of these Bowls are “interrupted” at their lowest part forming two separated elements. In no instances just one part of the Bowl was detected, but in 10% of the Highs with attachment an uninterrupted Bowl version occurred. Therefore, it is suspected that the two Bowl parts belong together.

The Bowl’s minimum frequency is 371.95 Hz ( $\pm 72.21$ ) and the maximum frequency is 706.90 Hz ( $\pm 29.12$ ), resulting in the frequency range of 334.95 Hz ( $\pm 80.96$ ) or 0.95 oct ( $\pm 0.27$ ) and a mean duration of 2.18 sec ( $\pm 0.35$ ). The first element has an upsweep rate of 3.50 oct/s ( $\pm 2.19$ ) and a downsweep rate of 1.30 oct/s ( $\pm 0.45$ ), while the second element shows an upsweep rate of 2.49 oct/s ( $\pm 0.44$ ) and a downsweep rate of 2.30 oct/s ( $\pm 0.14$ ). A summary of the Bowls’ measurements is provided in the attached table Tab.6.3 of the appendix.

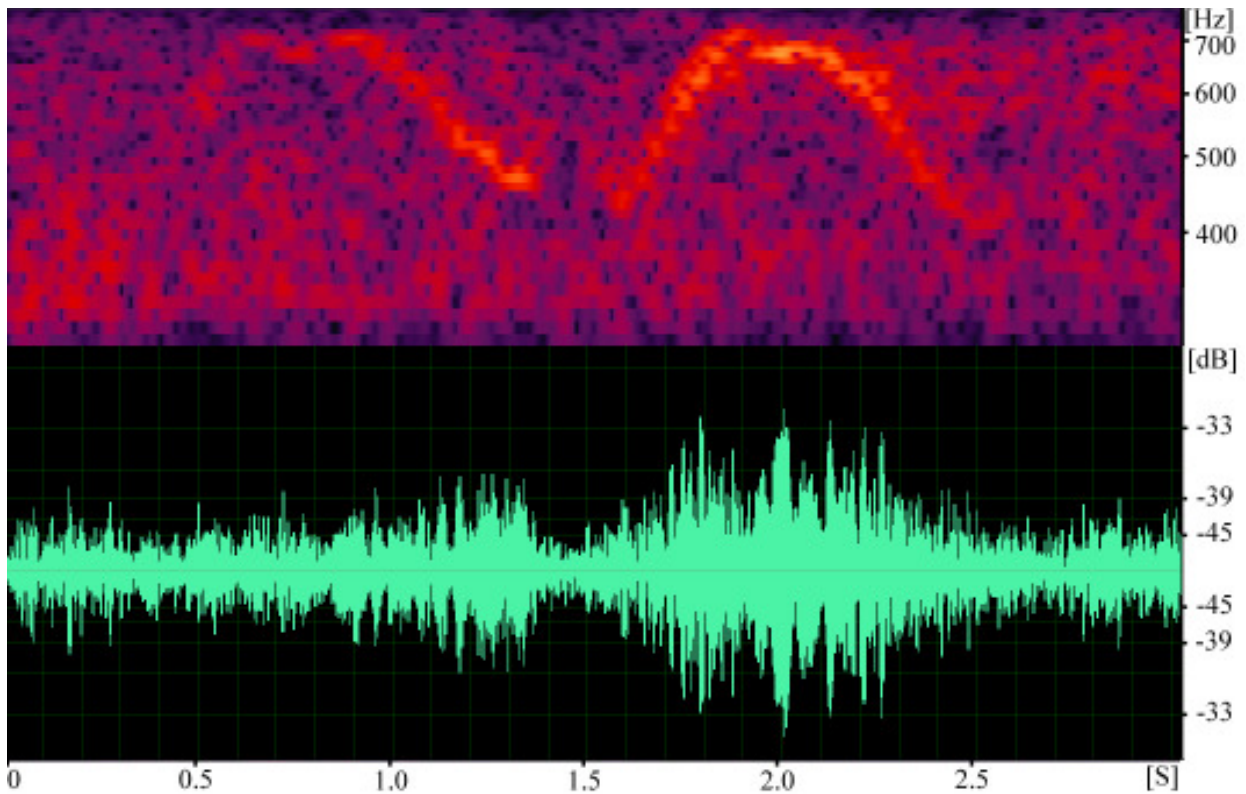
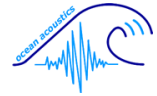
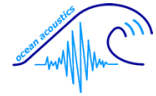


Figure 3.1.1C: Spectrogram of a typical Bowl (top). Unlike in Highs, the waveform of the Bowl shows a distinct increase in amplitude in both Bowl parts, the second one being even higher than the first one in this example. Thus the middle part of the second Bowl part has the highest amplitude, which descends towards the end (below). The explanation of the axis as described in Fig. 3.1.1A.

### 3.1.2 Mid siren call

As seen in Fig.3.1.2A, Mids, similar to Highs, consist of alternating up- and downsweeps (92% of the calls starting with an up, 8% starting with a down), that cause the siren-like sound. Subtypes 3-8 occur, but subtypes 4 (82%), 6 (8%), and 3 (6%) dominate with 4-9 strong harmonics at a relatively constant rate. For Mids the mean four inter-harmonic intervals are 224 Hz ( $\pm 58$ ), 212 Hz ( $\pm 59$ ), 191 Hz ( $\pm 44$ ), and 705 Hz ( $\pm 138$ ) respectively. The minimum frequency is 168.42 Hz ( $\pm 35.45$ ) and the maximum frequency is 2010.38 Hz ( $\pm 596.62$ ), resulting in the typical frequency range of Mids of 1841.96 Hz ( $\pm 599.83$ ) or 3.55 oct ( $\pm 0.48$ ) and a mean call duration of 3.29 sec ( $\pm 0.42$ ). The peak frequency is 498.98 Hz ( $\pm 94.04$ ) with an amplitude at peak frequency of -44.93 dB ( $\pm 13.58$ ). dB is given as dB FS, as explained in 3.1.1.



98% of the Mid calls have three distinct edges at their upsweeps. These edges are measured at the frequencies of 761.13 Hz ( $\pm 126.41$ ), 773.76 Hz ( $\pm 79.98$ ), and 401.09 Hz ( $\pm 47.95$ ), and have a mean duration of 0.11 sec ( $\pm 0.03$ ), 0.11 sec ( $\pm 0.02$ ), and 0.11 sec ( $\pm 0.03$ ) respectively. The low part peaks (LPP) can be found on the left side at 628.66 Hz ( $\pm 139.67$ ), and on the right side at 628.96 Hz ( $\pm 149.68$ ).

A complete upswEEP (U) has a sweep rate of 2.40 oct/s ( $\pm 0.42$ ) and a complete downswEEP (D) a rate of 2.29 oct/s ( $\pm 1.06$ ). The diffuse starting upswEEP (SU) does so at a rate of 2.08 oct/s ( $\pm 0.58$ ), a starting downswEEP (SD) at a rate of 1.59 oct/s ( $\pm 0.17$ ), an ending upswEEP (EU) at a rate of 2.29 oct/s ( $\pm 0.43$ ), and an ending downswEEP (ED) at a rate of 2.42 oct/s ( $\pm 0.38$ ). A summary of the measurements of Mid siren calls and their single elements are provided in the attached tables Tab.6.4 and Tab.6.5 of the appendix.

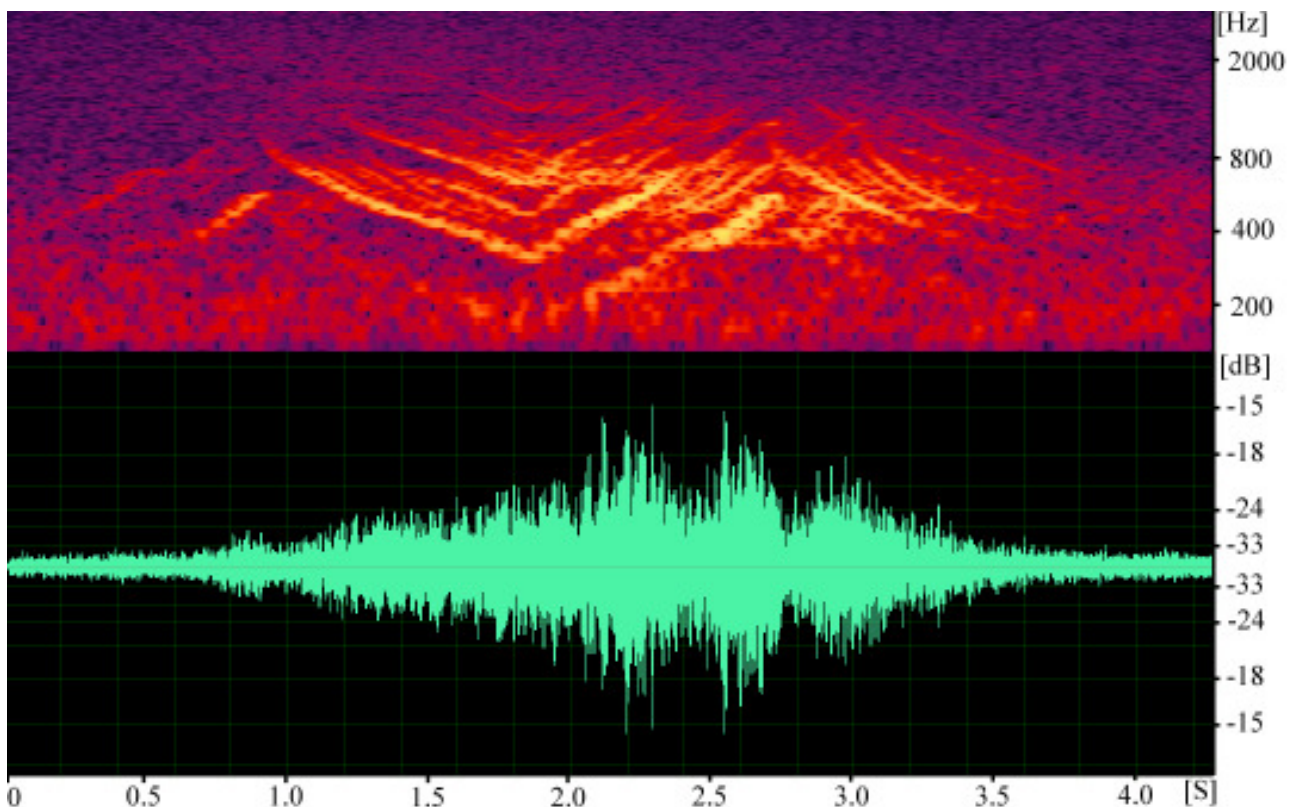
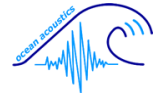


Figure 3.1.2A: Spectrogram of a typical Mid siren call (top). As in Highs, the Mid's waveform (below) does not show the different sweeps but seems to indicate the distinct edges, as described in the text above. The explanation of the axis as described in Fig.3.1.1A.



### Mid attachment

While taking the measurements of the Mid calls' elements, a tiny attachment was noticed in 14% (n=7) of the calls. It has the shape of an “umbrella” and occurs at the right upper corner of the Mid call at a frequency of 1452.29 Hz ( $\pm 579.71$ ) and with a mean duration of 0.33 sec ( $\pm 0.15$ ) as shown in Fig3.1.2B. A summary of the Mid-attachments' measurements is provided in the attached table Tab.6.6 of the appendix.

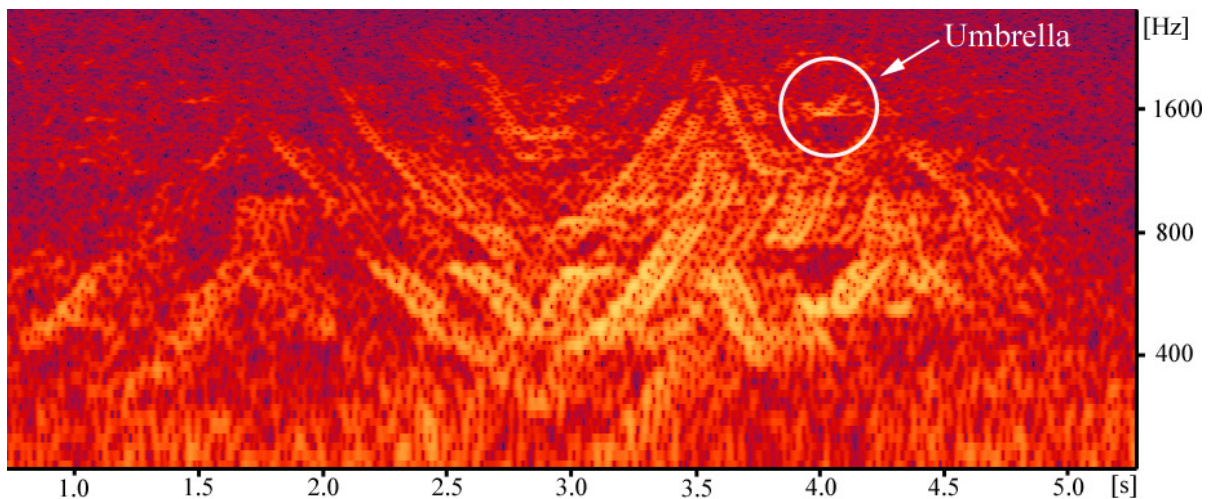
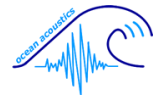


Figure 3.1.2B: The little umbrella-like attachment found in 14% of the measured Mid calls. Description of the axis as given in Fig.3.1.1B.

### 3.1.3 Low siren call

Lows consist of alternating up- and downsweeps (100% of the calls starting with an up, see Fig.3.1.3A). Subtypes 2-5 occur, but subtypes 4 (68%), 2 (18%), and 3 (12%) dominate. If present, only parts of a maximum of two harmonic are visible. 38 (76%) of the Lows have only one harmonic. Three of those (8%) have a faint second harmonic with an inter-harmonic interval of 258 Hz ( $\pm 15$ ). The minimum frequency is 132.54 Hz ( $\pm 21.69$ ) and the maximum frequency is 449.14 Hz ( $\pm 60.85$ ), resulting in the typical frequency range of Lows of 316.60 Hz ( $\pm 60.87$ ) or 1.77 oct ( $\pm 0.26$ ) and a mean call duration of 2.00 sec ( $\pm 0.46$ ). The start frequency is 234.22 Hz ( $\pm 36.72$ ), the first peak can be found at 439.24 Hz ( $\pm 51.72$ ), the first low is at 131.20 Hz ( $\pm 21.54$ ), and the second peak at 407.56 Hz ( $\pm 72.47$ ). The call ends with a mean end frequency of 221.08 Hz ( $\pm 58.43$ ). The peak frequency is 225.84 Hz ( $\pm 49.82$ ) with an amplitude at peak frequency of -45.68 dB ( $\pm 4.23$ ). dB is given as dB FS, as explained in 3.1.1.

### 3. Results



A diffuse turning point (DTP) on peak points can be found in 58% (n=29) of the calls, and on low points in 34% (n=17) of the calls.

A complete upsweep (U) has a sweep rate of 2.13 oct/s ( $\pm 0.33$ ) and a complete downsweep (D) a rate of 2.89 oct/s ( $\pm 0.43$ ). The diffuse starting upsweep (SU) does so at a rate of 2.29 oct/s ( $\pm 0.65$ ), an ending upsweep (EU) at a rate of 2.43 oct/s ( $\pm 1.99$ ), and an ending downsweep (ED) at a rate of 3.37 oct/s ( $\pm 1.53$ ). Starting downsweeps (SD) do not occur. A summary of the measurements of Low siren calls and their single elements are provided in the attached tables Tab.6.7 and Tab.6.8 of the appendix.

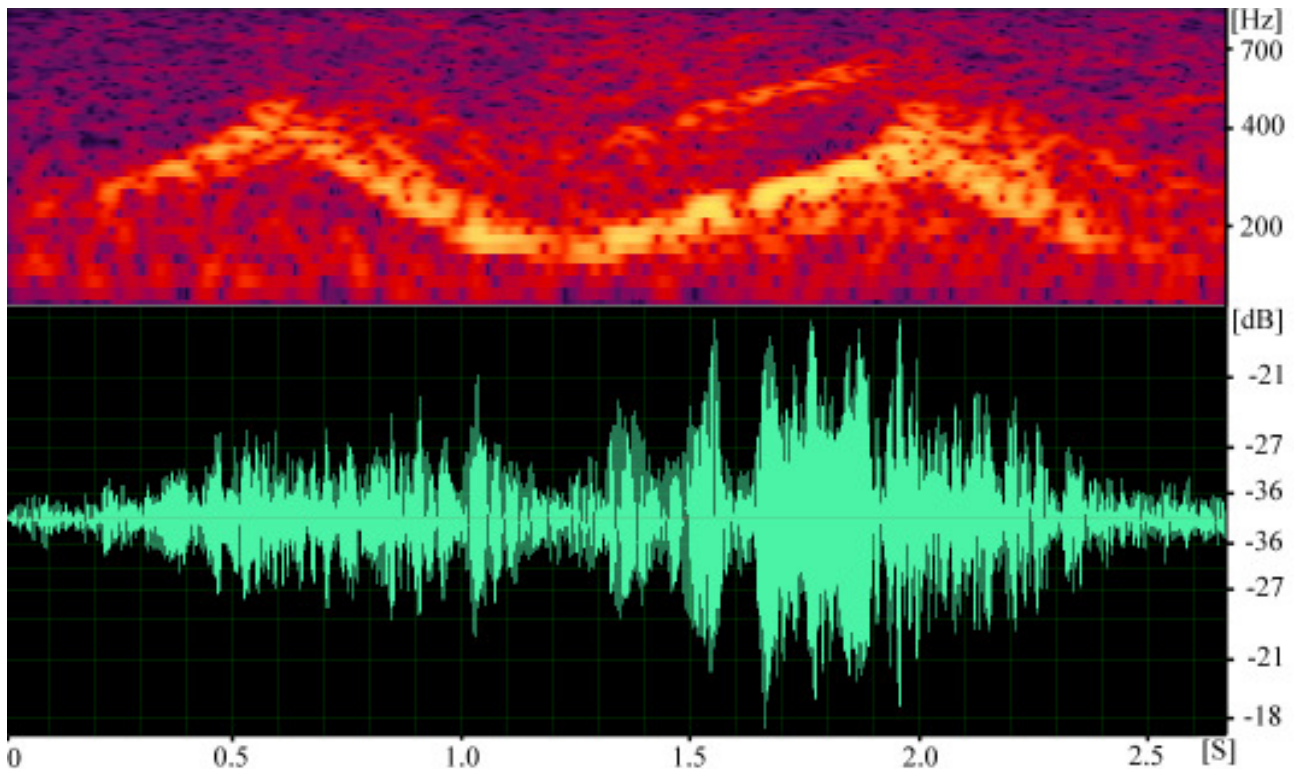
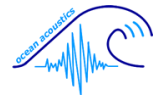


Figure 3.1.3A: Spectrogram of a typical Low siren call (top). As in Highs, the Low's waveform (below) does not show the single sweeps but the amplitude increases during the second part of the call, as it does in Bowl sounds. The explanation of the axis as described in Fig.3.1.1A.



### 3.1.4 Whoosh components

The Whoosh always comprises two distinct components, as shown in Fig.3.1.4A. The Whoosh broadband component (also referred to as WBC) represents a hissing fast downsweep, covering the highest frequency range associated with Ross seal vocalizations. The Whoosh tonal component (also referred to as WTC) has some similarity to the Bowl (the High call attachment, as explained in chapter 2.3.2): in the spectrogram: it lies underneath the WBC, it sounds like a Bowl sharing almost the same frequency range, and the WTC comprises a single upsweep, followed by a plateau and eventually a downsweep.

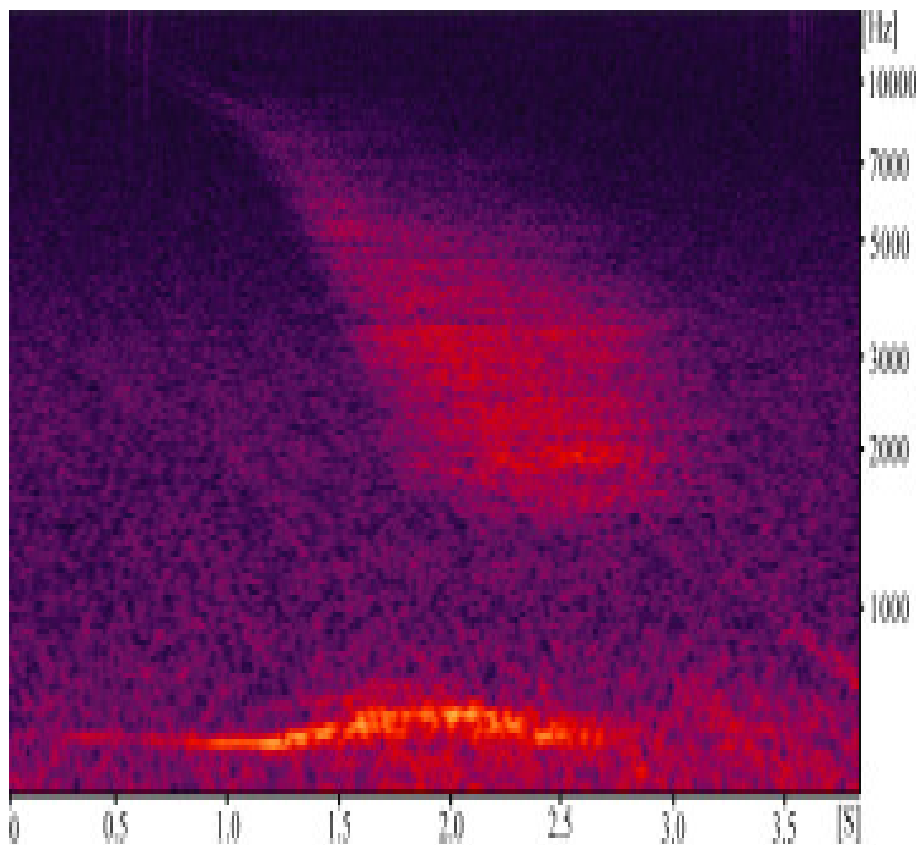
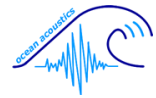


Figure 3.1.4A: Spectrogram of the two Whoosh components, the WBC in then upper, and the WTC in the lower frequency range, which always occur together. Description of the axis as given in Fig.3.1.1B.



### A) Whoosh broadband component

The Whoosh broadband component (WBC) is a diffuse downsweep at relatively constant rate (Fig.3.1.4B). The maximum frequency also embodies the start frequency, which is 10 996.54 Hz ( $\pm 1305.36$ ). The minimum frequency can also be given as the end frequency, which is 1439.26 Hz ( $\pm 104.70$ ). This results in the WBCs' frequency range of 9557.28 Hz ( $\pm 1324.30$ ) or 2.93 oct ( $\pm 0.23$ ) and a mean call duration of 2.51 sec ( $\pm 0.30$ ). The peak frequency measured at the so called mid part is 2296.00 Hz ( $\pm 168.98$ ), and the one measured one second earlier (as described in the chapter 2.3.6) is 5892.00 Hz ( $\pm 840.76$ ).

100% of the observed calls are coupled with the Whoosh tonal component (WTC). If they were not seen together, then due to bad signal-to-noise ratio or overlapping calls. A summary of the WBC's measurements is provided in the attached table Tab.6.9 of the appendix.

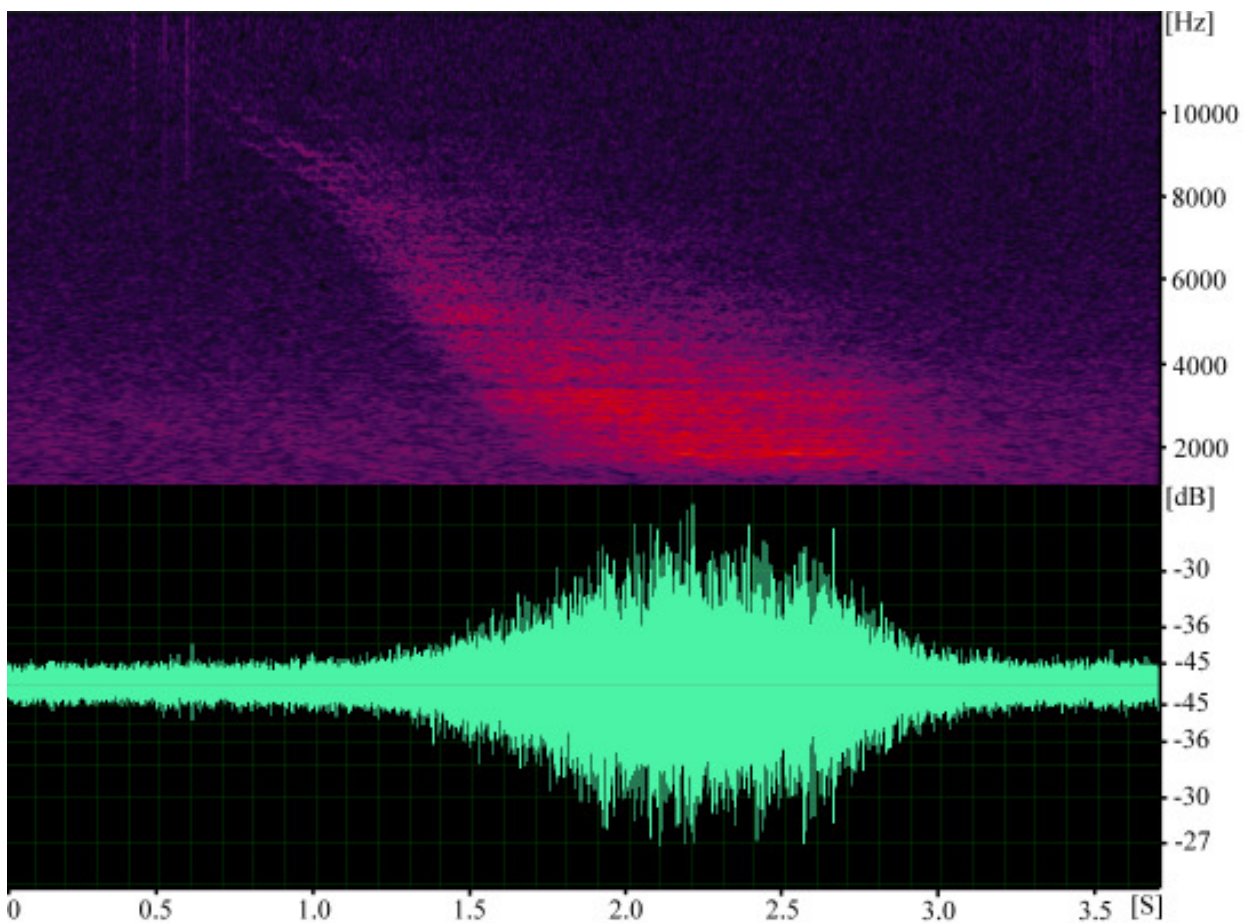
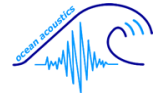


Figure 3.1.4B: Spectrogram of a typical WBC (top). The sweep can be clearly seen in the WBC's waveform (below). The explanation of the axis as described in Fig. 3.1.1A.



### B) Whoosh tonal component

The Whoosh tonal component (WTC) is always coupled with the WBC, as mentioned above. It consists of a single, short ascending tonal sound (100% starting with an upswEEP) with a frequency-plateau and eventually descending at the end, as shown in Fig.3.1.4C. The start frequency is 574.18 Hz ( $\pm 11.42$ ) and the end frequency is 591.50 Hz ( $\pm 47.31$ ), resulting in the typical narrow frequency range of WTCs of 129.84 Hz ( $\pm 21.53$ ) or 0.31 oct ( $\pm 0.05$ ) and a mean duration of 2.33 sec ( $\pm 0.44$ ). The peak frequency is at 605.64 Hz ( $\pm 30.80$ ) with an amplitude at peak frequency of -50.66 dB ( $\pm 4.87$ ). dB is given as dB FS, as explained in 3.1.1. The upswEEP at the beginning of the call has a rate of 0.60 oct/s ( $\pm 0.17$ ), and the gap between the WBC and the WTC measures 883.18 Hz ( $\pm 91.81$ ). A summary of the WTC's measurements is provided in the attached table Tab.6.10 of the appendix.

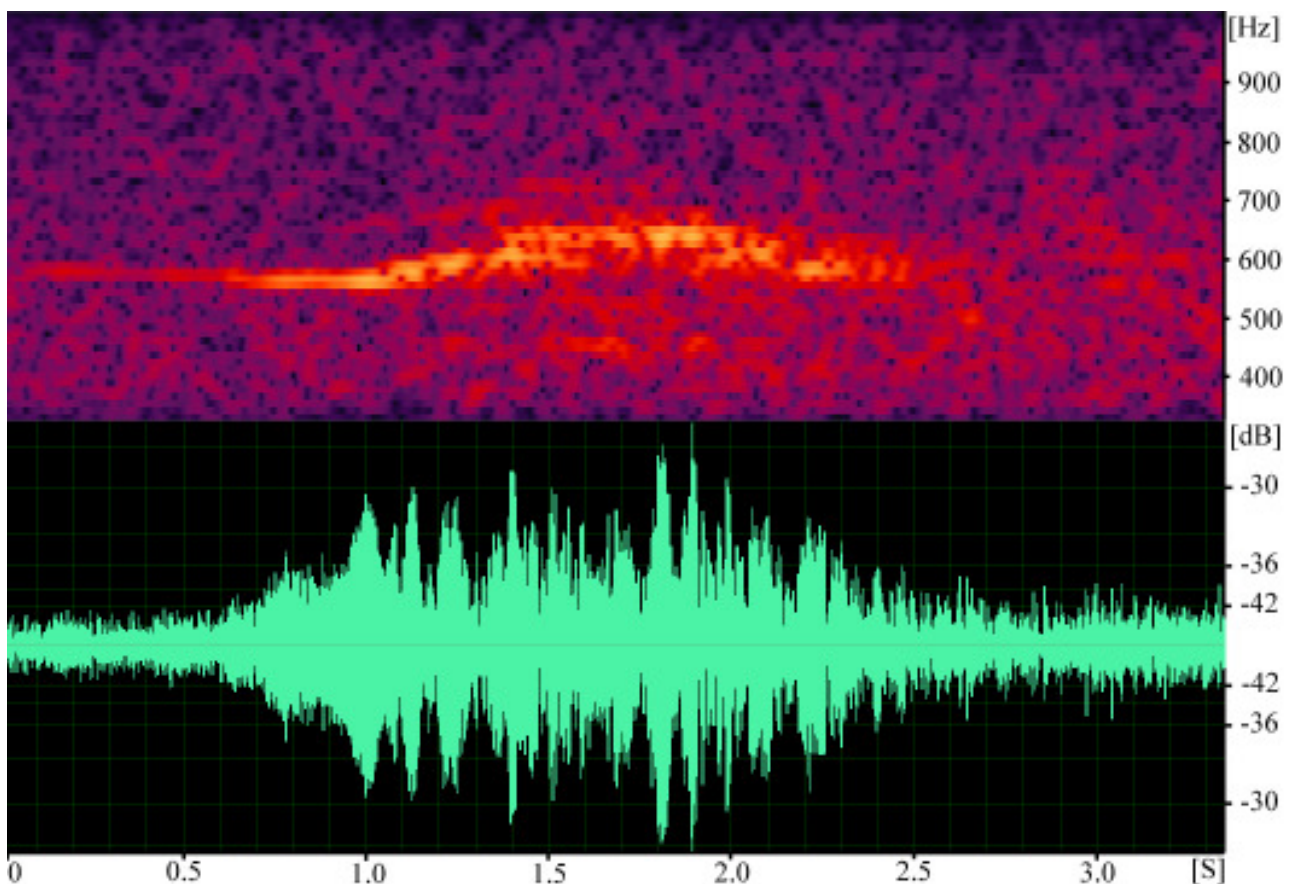
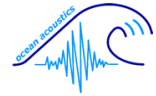


Figure 3.1.4C: Spectrogram of a typical WTC (top). The WTC's waveform (below) indicates a rather discontinuous nature with highly variable sound pressure levels. The start and the end of the waveform are not clearly discernable, and hence do not serve as useful parameter for call detection. The explanation of the axis as described in Fig. 3.1.1A.



### 3.2 Differentiation of call types

In this chapter the different parameters of the four call types are compared.

In the following boxplots (Fig.3.2A-Fig.3.2H) the eight parameters (duration, minimum frequency, maximum frequency, peak frequency, amplitude at peak frequency, subtypes, downsweep rate, and upsweep rate), that were measured in all call types, are combined to give an visual impression of the relative values just presented in chapter 3.1, and for comparison among the different call types. If one parameter is not available for a certain call type, it was omitted. The variable “frequency range” was also omitted, since it closely resembles that of the maximum frequency, considering that it only represents the differences between maximum and minimum frequencies. Presented here are the calls High, Mid, Low, and both Whoosh components, WBC and WTC, separately. The boxes represent 50% of the data, containing the mean (dashed line) and the median (solid line). The whiskers on each side of the box stand for the 5<sup>th</sup> and 95<sup>th</sup> percentile; the black dots mark any additional outliers. These figures serve as the first indication of which parameters are worthwhile to consider to separate the different call types from each other. For each parameter  $n=50$  if not otherwise stated.

Fig.3.2J and Fig.3.2L show the scatterplot of two (minimum frequency and maximum frequency) out of the nine parameters of all four call types, as mentioned above. Only the pairing of most interest is shown here. Those remaining plots that contain any additional valuable information are provided in the appendix.

Fig.3.2K shows a visually accessible classification tree that was received after five variables (duration, frequency range, minimum frequency, maximum frequency, and peak frequency) were tested for the four different call types.

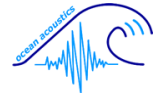


Fig.3.2A gives the duration in seconds for all call types for comparison. Highs and Mids have a relatively similar duration with 3.37 ( $\pm 0.68$ ) sec and 3.29 ( $\pm 0.42$ ) sec respectively. Lows, on the other hand, are much shorter with 2.00 ( $\pm 0.46$ ) sec and the WBC with 2.51 ( $\pm 0.30$ ) sec. The WTC and Bowl are shown separately in Fig.3.2AA. Both exhibit approximately the same duration as Lows with 2.33 ( $\pm 0.44$ ) sec and 2.18 ( $\pm 0.35$ ) sec respectively.

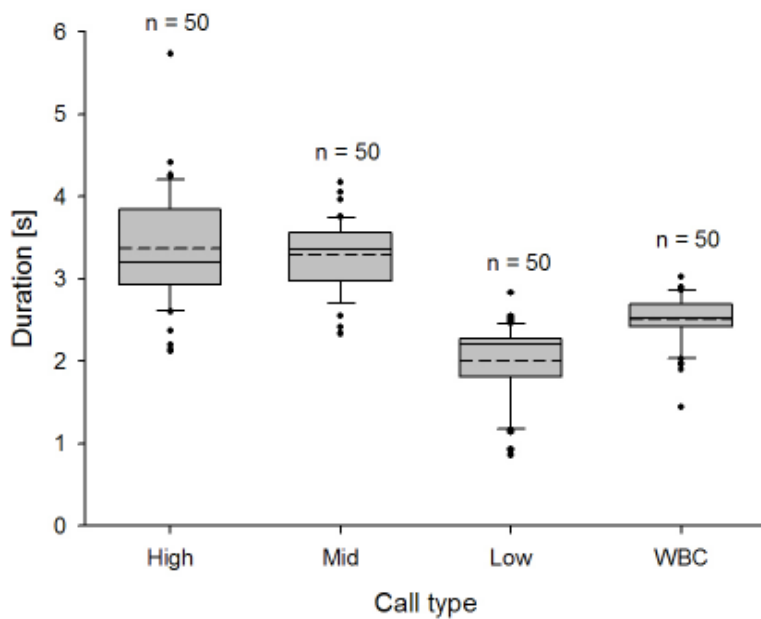


Figure 3.2A: The duration in seconds on the y-axis and the four call types on the x-axis: High (with the Bowl component separately in Fig.3.2AA), Mid, Low, and both Whoosh components (the WTC separately in Fig.3.2AA). The boxes represent 50% of the data, containing the mean (dashed line), and the median (solid line). The whiskers on each side of the box stand for the 5<sup>th</sup> and 95<sup>th</sup> percentile respectively, and the black dots mark any outliers (n=50 if not otherwise stated).

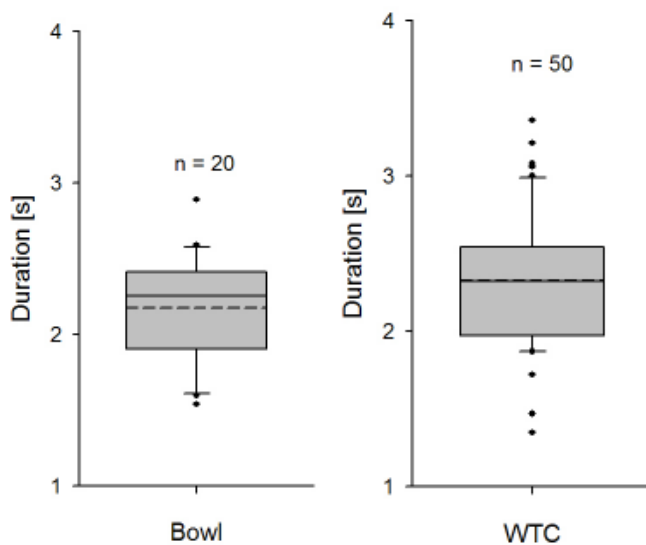


Figure 3.2AA: The duration in seconds for the two components Bowl and WTC. Description of the boxplots as given in Fig.3.2A.

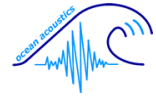


Fig.3.2B gives the maximum frequency in Hz for all call types and their components. It shows clear differences in the four call types, with the WBC being the highest at 10 996.54 Hz ( $\pm 1305.36$ ) and then dropping down in the order Highs at 7129.38 Hz ( $\pm 1803.55$ ), Mids at 2010.38 Hz ( $\pm 596.62$ ), Bowls at 706.90 Hz ( $\pm 29.12$ ), WTC at 678.26 Hz ( $\pm 16.95$ ), and Lows at 449.14 Hz ( $\pm 60.85$ ).

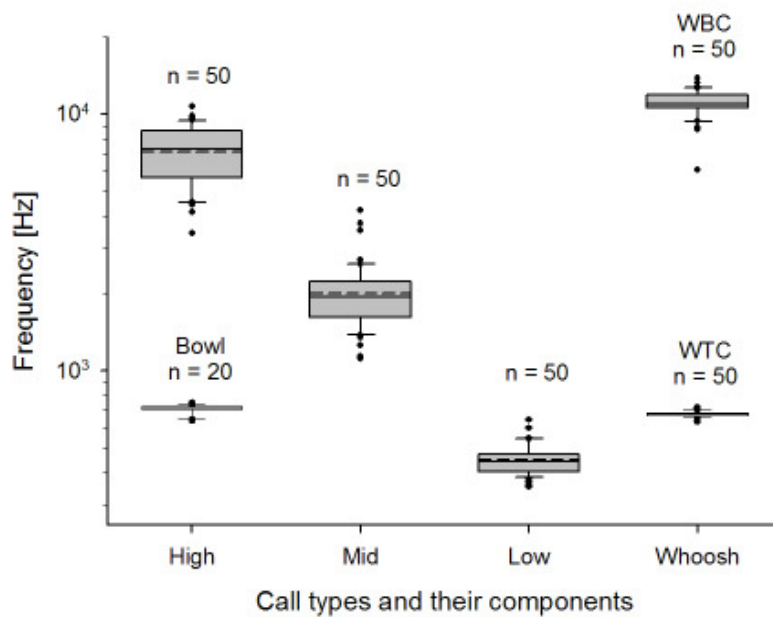


Figure 3.2B: Comparison of the maximum frequencies in Hz for the four call types High (with Bowl component), Mid, Low, and both Whoosh components, WBC and WTC. Description of the boxplots as given in Fig.3.2A.

Fig.3.2C gives the minimum frequency in Hz for all call types and their components. It is, just like the maximum frequency, quite different for the four call types, with the two Whoosh components being the highest again: the WBC has its minimum frequency at 1439.26 Hz ( $\pm 104.70$ ) and the WTC at 678.26 Hz ( $\pm 16.95$ ). Highs follow at 592.18 Hz ( $\pm 145.47$ ), Bowls at 424.40 Hz ( $\pm 47.67$ ), Mids at 168.42 Hz ( $\pm 35.45$ ), and Lows at 132.54 Hz ( $\pm 21.69$ ).

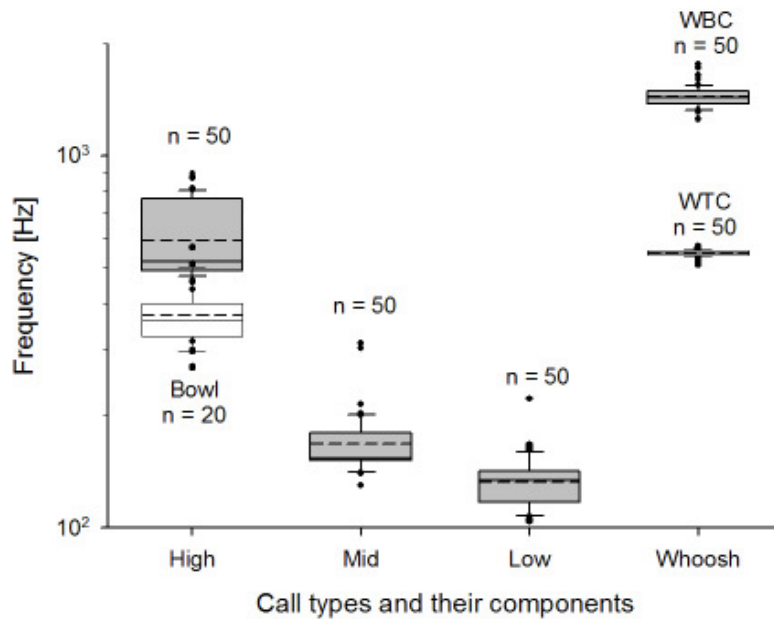


Figure 3.2C: Comparison of the minimum frequencies in Hz for the four call types High (with Bowl component), Mid, Low, and both Whoosh components, WBC and WTC. Description of the boxplots as given in Fig.3.2A.

Fig.3.2D gives the peak frequency in Hz for the three siren call types. The Highs at 1585.42 Hz ( $\pm 226.09$ ) are the highest, followed by Mids at 498.98 Hz ( $\pm 94.04$ ), and finally the Lows at 225.84 Hz ( $\pm 49.82$ ). Additionally, the WTC is given separately on the right side with its peak frequency being 605.64 Hz ( $\pm 30.80$ ).

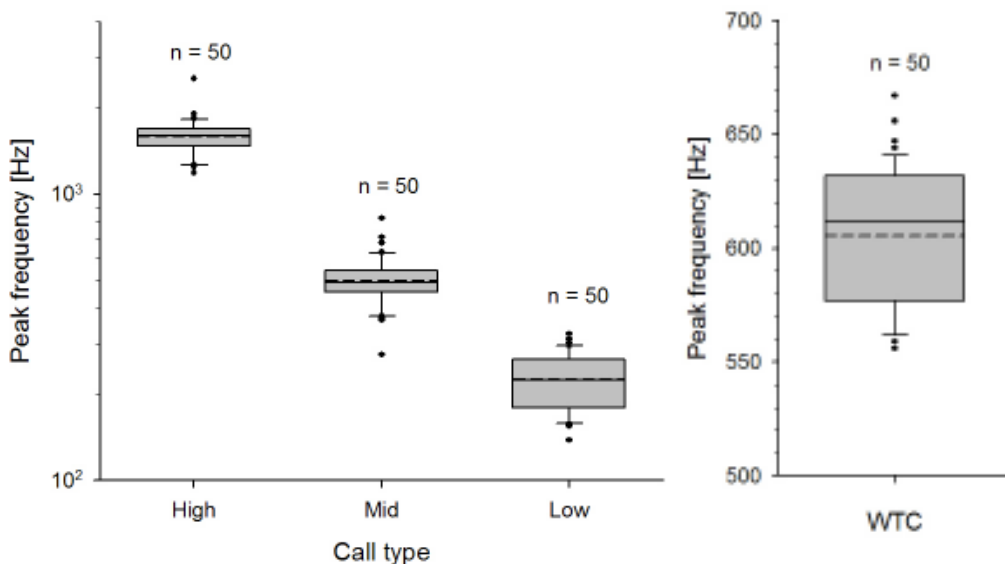


Figure 3.2D: Comparison of the peak frequencies in Hz for Highs, Mids, and Lows (left) and the WTCs (on the right; note the different frequency scale). Description of the boxplots as given in Fig.3.2A.

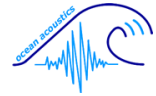


Fig.3.2E gives the amplitude at peak frequency in dB FS for the three siren call types. The amplitude is quite similar in the Mids at  $-44.93$  dB ( $\pm 13.58$ ), and Lows at  $-45.68$  dB ( $\pm 4.23$ ), but higher in Highs at  $-57.28$  dB ( $\pm 4.83$ ). Additionally, the WTC is given separately on the right side with its greatest amplitude at  $-50.66$  dB ( $\pm 4.87$ ).

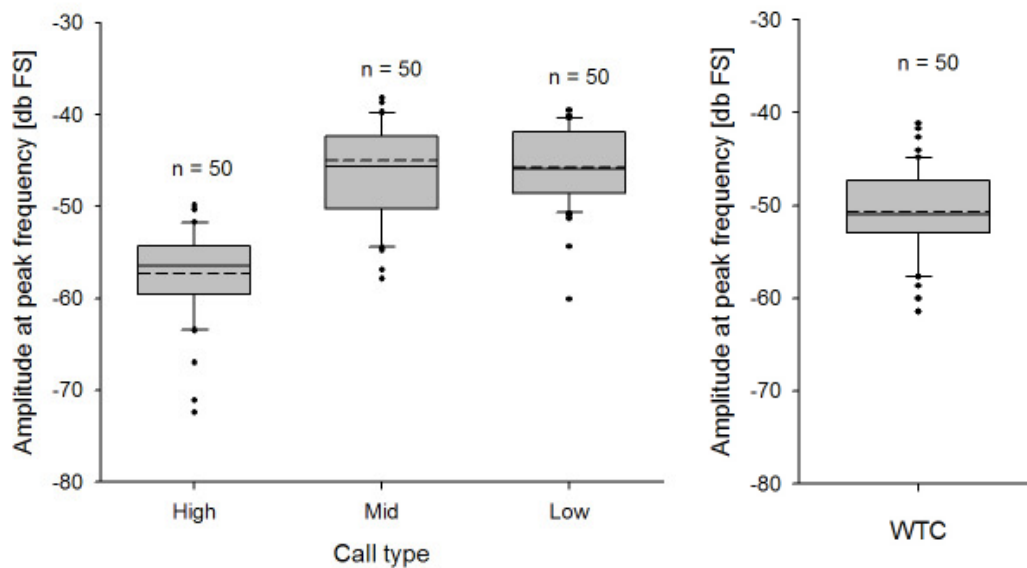


Figure 3.2E: Comparison of the amplitude at peak frequency in dB FS for Highs, Mids, and Lows (left), and the WTCs (right). Description of the boxplots as given in Fig.3.2A.

Fig.3.2F gives the subtypes (number of upsweeps and downsweeps) of the three siren call types. Highs and Mids have potentially higher subtypes with  $4.84$  ( $\pm 1.22$ ) and  $4.20$  ( $\pm 0.83$ ) respectively, than Lows with  $3.54$  ( $\pm 0.81$ ).

### 3. Results

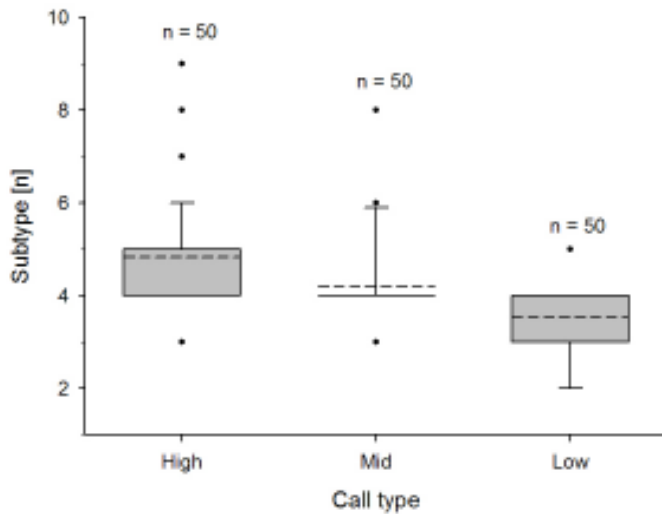
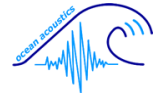


Figure 3.2F: Comparison of the subtypes of the three siren calls High, Mid, and Low. Description of boxplots as given in Fig.3.2A.

For comparison of sweep rates among different call types only complete sweeps (U and D) are considered. Starting and ending sweeps may not be complete due to their fading in and fading out-character.

Fig.3.2G gives the upsweep rate (U) in octaves per second of the three siren call types. The average upsweep rate of Highs and Mids are comparable at 3.02 oct/s ( $\pm 0.59$ ) and 2.40 oct/s ( $\pm 0.42$ ) respectively. The latter, however, lies a bit lower followed by Lows with the slowest upsweep rate of 2.13 oct/s ( $\pm 0.33$ ).

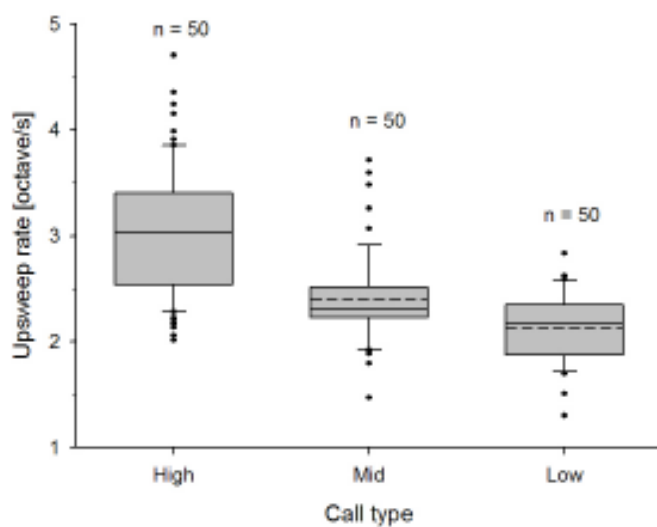


Figure 3.2G: Comparison of the upsweep rates in octaves per second for the three siren calls High, Mid, and Low. Description of the boxplots as given in Fig.3.2A.

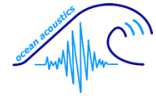


Fig.3.2H gives the downsweep rate (D) in octaves per second of the three siren call types. Surprisingly, the average downsweep rate of Lows at 2.89 oct/s ( $\pm 0.43$ ) is higher than the one of Highs and Mids at 2.12 oct/s ( $\pm 0.41$ ) and 2.29 oct/s ( $\pm 1.06$ ) respectively.

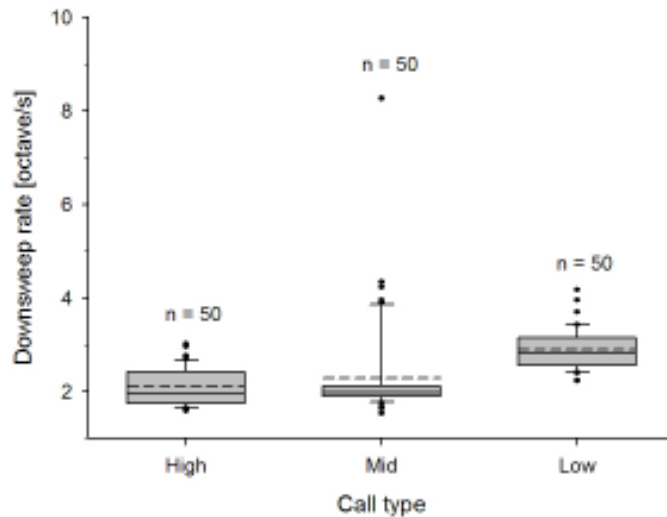


Figure 3.2H: Comparison of the downsweep rates in octaves per second for the three siren calls High, Mid, and Low. Description of the boxplots as given in Fig.3.2A.

The following figures (Fig.3.2J and Fig.3.2L) are an example of scatterplots received when two of the nine parameters (duration, frequency range, minimum frequency, maximum frequency, peak frequency, amplitude at peak frequency, subtypes, downsweep rate, and upswing rate) of all four call types are plotted against each other to reveal whether any one variable has an association with the others. Only the pairing that results in the best distinction between the calls is shown here. The remaining plots were studied but are not reproduced here. Those containing any valuable information are provided in the appendix (Fig.6.1-Fig.6.12). For each parameter  $n=50$  for each call.

### 3. Results

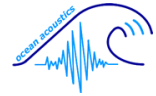


Fig.3.2J gives the scatterplot of minimum and maximum frequencies plotted against each other. These two parameters form distinct clusters and thus are ideal to clearly distinguish the four call types from one another.

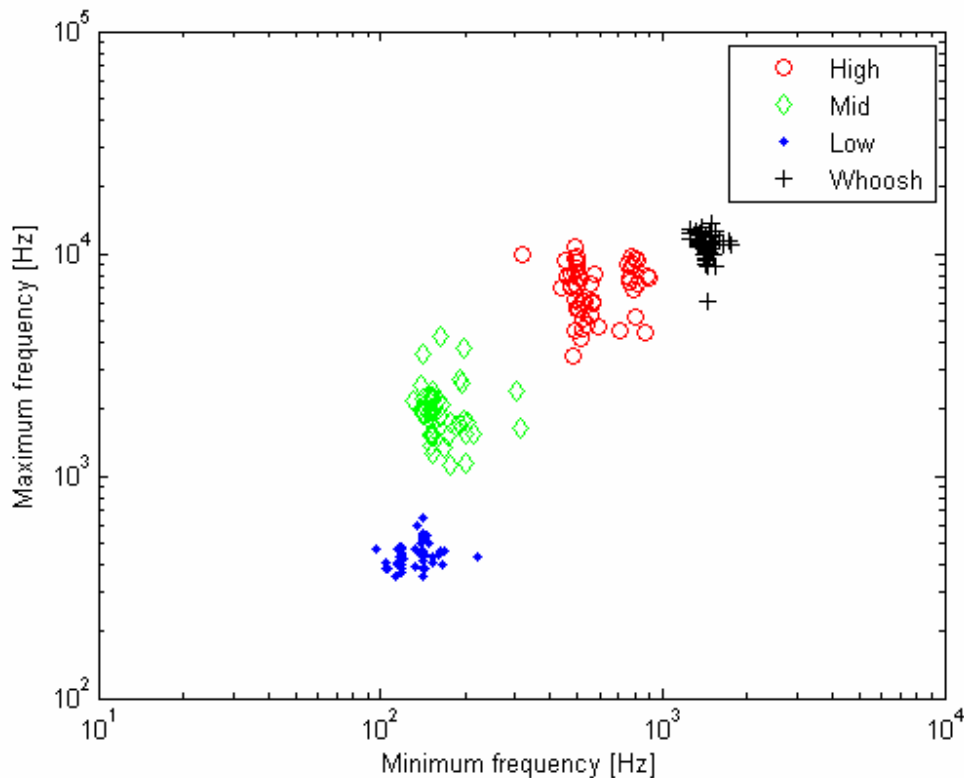
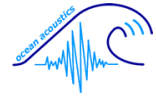


Figure 3.2J: The maximum frequency in Hz on the y-axis is plotted against the minimum frequency in Hz on the x-axis. The different call types are plotted in different colours (Highs in red circles, Mids in green diamonds, Lows in blue dots, and WBCs in black crosses). For the parameters  $n=50$  respectively.

The CART method resulted in a 3-node classification tree. The optimal version of the tree provides the highest predictive accuracy and the fewest variables (Fig.3.2K). Only two parameters (minimum and maximum frequency) out of originally five (duration, frequency range, minimum frequency, maximum frequency, and peak frequency) that were fed into the program, resulted in the shortest, yet most accurate tree. The percentage of correct classification was 100% for each of the four call types High, Whoosh (only the broadband component WBC), Low, and Mid. The length of the vertical lines at each split represents the total variation explained by that split.

The first node splits the calls at the minimum frequency of 315.5 Hz. Calls above this value go to the left, and the ones below to the right. The second node (left son of first

### 3. Results



node) splits them further at the minimum frequency of 1072 Hz. Calls below that value lead to Highs (H), and the ones above lead to Whooshes (W). The third node (right son of first node) makes the split at the maximum frequency of 879 Hz. Calls below that value belong to Lows (L), and the calls above to Mids (M). For each parameter  $n=50$  for each call type.

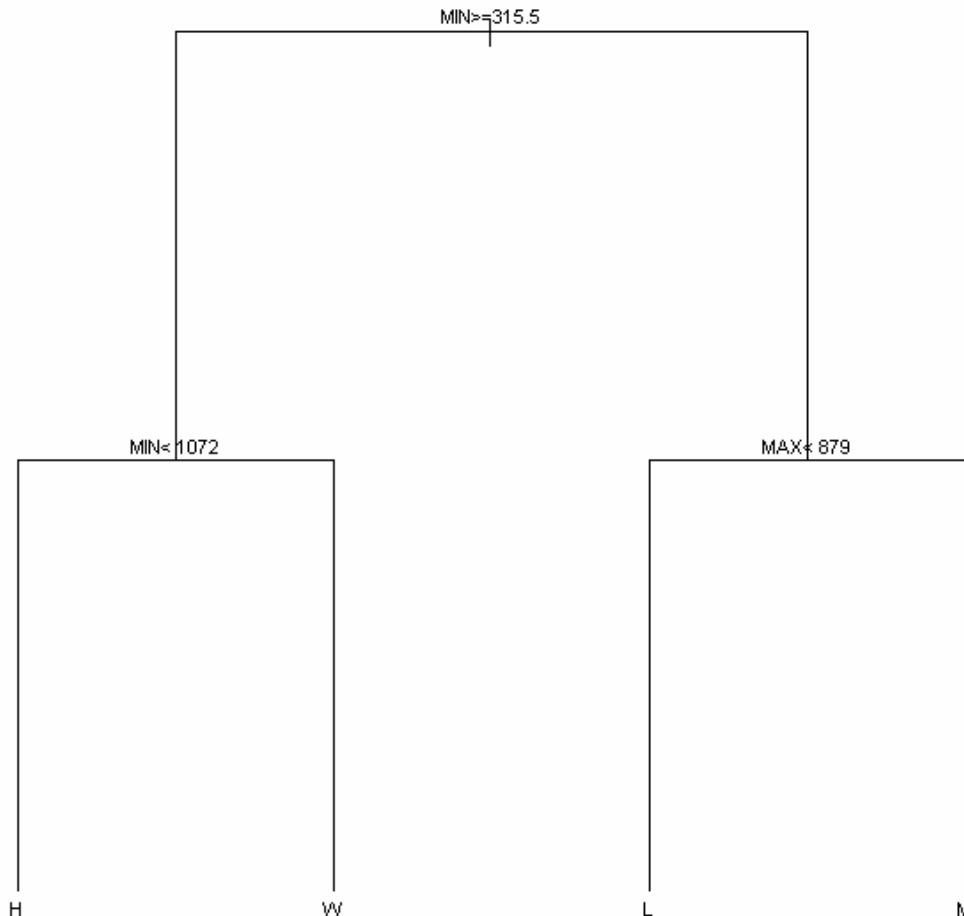


Figure 3.2K: The 3-node classification tree reveals that only the two variables (min and max frequency) are necessary to separate the four call types. The first node splits the calls at the minimum frequency of 315.5 Hz. Calls above this value go to the left, the ones below to the right. The second node splits them further at the minimum frequency of 1072 Hz. Calls below that value lead to Highs (H), the ones above lead to Whooshes (W, only WBC). The third node makes the split at the maximum frequency of 879 Hz with calls below that value belonging to Lows (L), the ones above to Mids (M). 100% correct classification was achieved for all call types ( $n=200$ ).

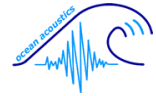


Fig.3.2L is the same scatterplot as shown in Fig.3.2J, however, now the splitting parameters of the classification tree above are included as black lines that separate the different call types quite nicely.

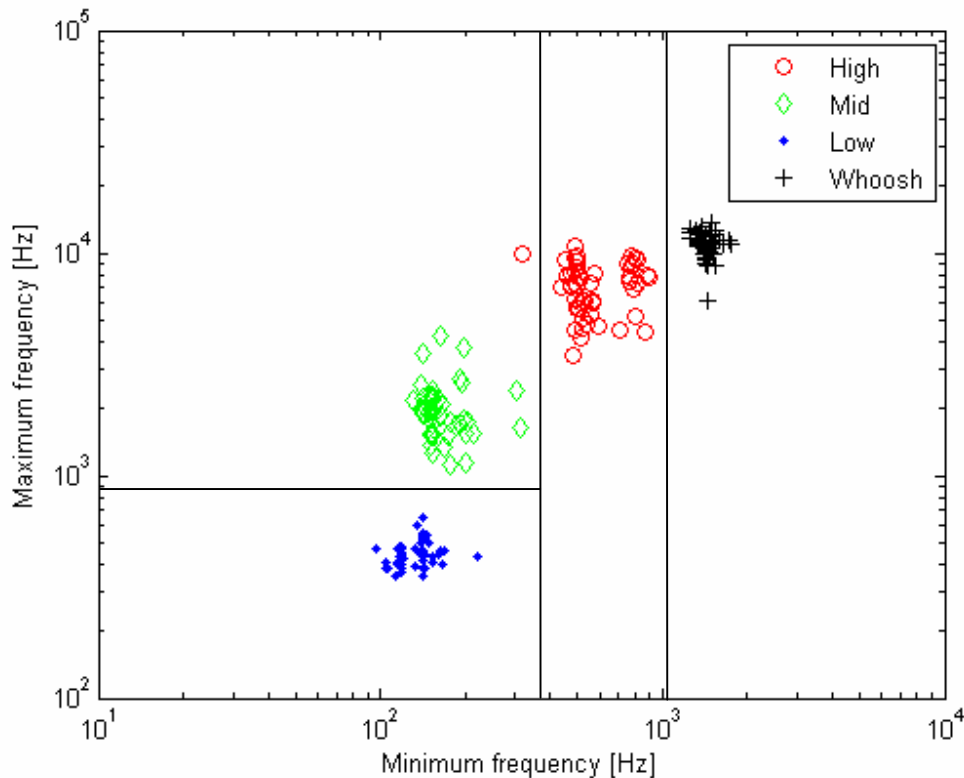
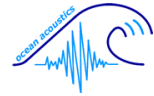


Figure 3.2L: The maximum frequency in Hz is plotted against the minimum frequency in Hz. The different call types are plotted as described in Fig.3.2J. The minimum and maximum frequencies are ideal to clearly distinguish the four different calls from each other, as indicated by the lines that mark the split parameters from the classification tree (Fig.3.2K).

A multivariate parametric principal component analysis (PCA) has been conducted as well. The results, plotted in a three-dimensional space, show no further separation and thus propose a similar clustering of the call parameters, as already shown in the scatterplots. Again, the minimum and maximum frequencies act as the major criteria to differentiate between the four call types.



### 3.3 Presence and acoustic environment of Ross seals at Atka Bay, Antarctica

In the first year, when PALAOA was installed and recordings were debugged of technical disturbances, Ross seals were already on site and calling very frequently. The first identified call occurred on 28 December 2005, at 11:42, and the last was heard 28 January 2006, at 00:10. The next austral summer was completely covered by recordings, showing that the seals already arrived at Atka Bay on 19 December 2006, at 20:58, and left this region again on 5 February 2007, at 05:11.

During that time frame Weddell seals and leopard seals were also present and acoustically quite active (Fig.3.3). In 2005, the Weddell seals (green line) had left or were vocally inactive, but leopard seals (blue line) joined the Ross seals (red line) for an overlapping duration of almost three weeks. The year following, the Weddell seals occurred together with the Ross seals for approximately two weeks. The leopard seals, again, stayed almost three weeks longer before disappearing from the recordings. As far as the data has been sighted, crabeater seals (yellow line) did not interfere with vocally active Ross seals.

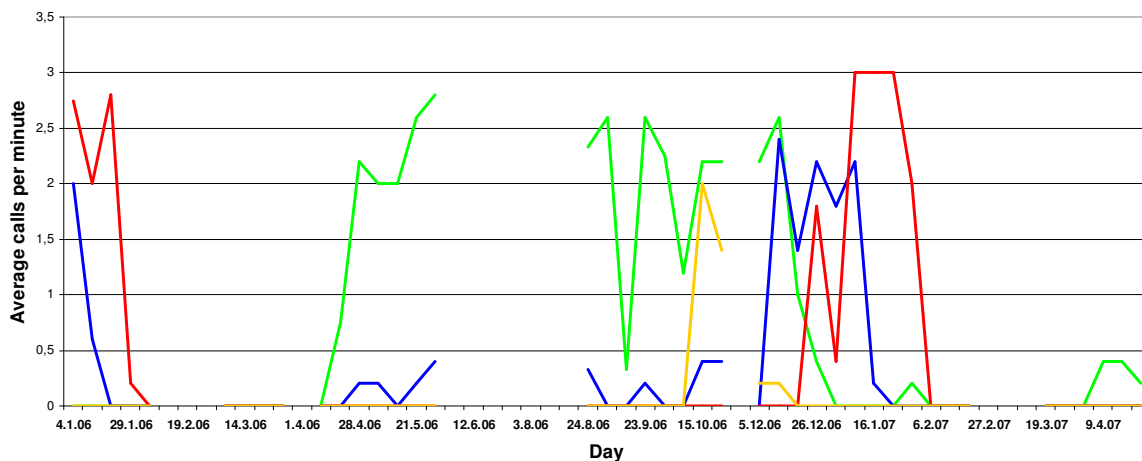
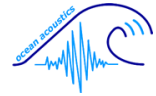


Figure 3.3: The acoustic environment of Ross seals at Atka Bay, Antarctica with the number of seal calls on the y-axis and time on the x-axis. The first counts in the huge PALAOA dataset revealed the three other pinniped species that occur along with Ross seals (red) during a one-year-period. But only Weddell seals (green) and leopard seals (blue) are vocal from Dec-Feb when Ross seals are present (crabeater seals are shown in yellow; overview dataset by I.C.van Opzeeland, AWI).



### 3.4 Seasonal calling pattern

The next diagram (Fig.3.4) can be seen as a quasi zoom-in of Fig.3.3 with only the timeframe of Ross seal presence in both summer seasons being shown in more detail. These counts began with the first detected call in December and ended with the last heard in February of both years (2005/2006 drawn in red, 2006/2007 drawn in blue). The time of counting at midnight coincides with the diurnal peak calling activity of the animals in order to get the maximum amount of calls (as described in chapter 3.5). The missing data in the 2005 season is due to the installation of PALAOA and initial technical problems that led to occasional recording failure. The sudden rise and drop of call numbers is quite impressive. In early January 2007, the activity changed from approximately 10 to up to 50 calls per minute within a few days only. The drop from 35 to about 10 calls per minute within one night at the beginning of February 2007 will be mentioned in more detail in chapter 4.5.

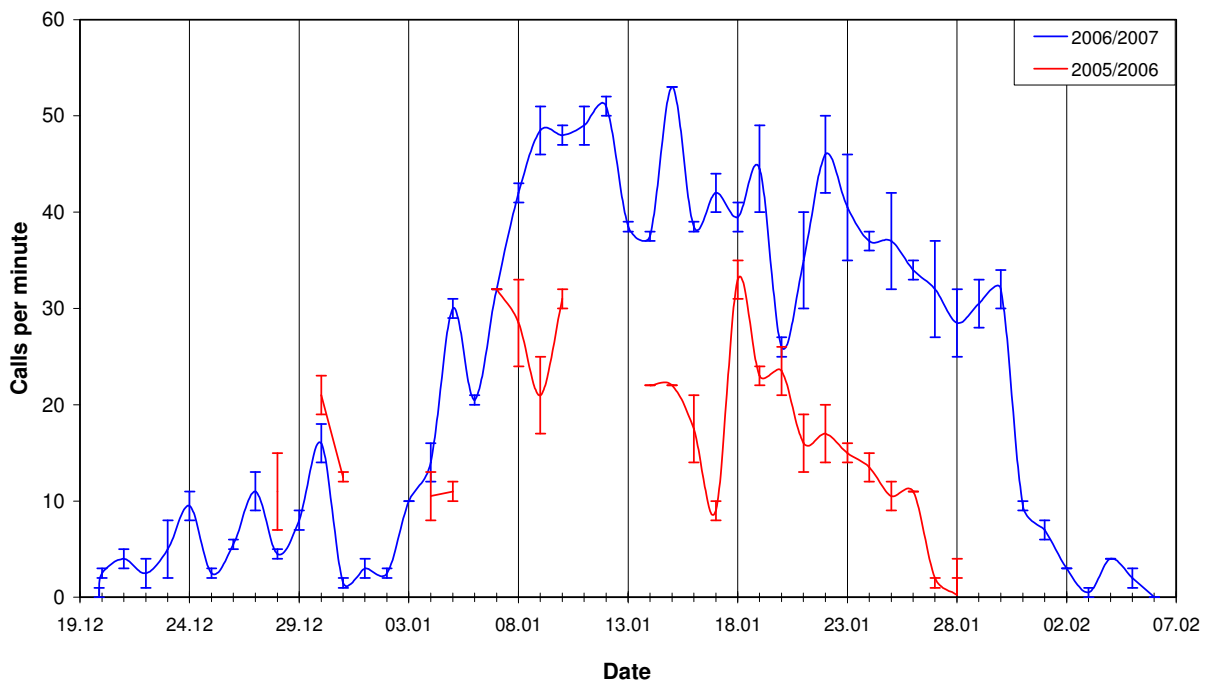
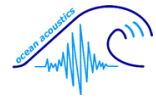
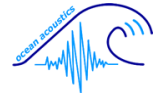


Figure 3.4: The calling activity of Ross seals (with calls per minute on the y-axis) over the whole period (x-axis) when they were present at Atka Bay, Antarctica. Two summer seasons are shown, 2005/2006 (red line) and 2006/2007 (blue line), with the absolute number of calls per minute measured twice a day at midnight. Each bar indicates the range of the two measurements.

### 3. Results



All calls are shown regardless of their type. A total of 3079 calls were counted (n=836 in 2005/2006, n=2243 in 2006/2007). The distribution of call types over the austral summer season for two consecutive years has the same activity pattern as their total number, as shown in Fig.3.4. Highs are most commonly used (45%, n=373 in 2005/2006; 39%, n=867 in 2006/2007), followed by Lows (21%, n=172 in 2005/2006; 31%, n=703 in 2006/2007), Mids (21%, n=179 in 2005/2006; 20%, n=445 in 2006/2007), and the two Whoosh components WTC (6.5%, n=55 in 2005/2006; 5%, n=109 in 2006/2007) and WBC (6.5%, n=57 in 2005/2006; 5%, n=119 in 2006/2007) respectively. The different numbers of the two Whoosh components result from them being counted separately, since the call differentiation had not been clear at the time of analysis. Unlike the good quality files chosen for call characterization, the files used for counting the calls often had higher background noise levels, and especially the WTC was masked by overlapping calls in its frequency range.



### 3.5 Diurnal calling pattern

A plot of the counted absolute numbers of all Ross seal calls in each minute-file, independent of their call type, clearly shows a diurnal calling activity, peaking mostly at night with up to 48 calls per minute (Fig.3.5A). The sudden drop in call numbers within just two hours (02:00-04:00) on 30 January 2007 is impressive. After this period only sporadic calls were detected before they ceased completely on 5 February 2007. This seasonal pattern has already been mentioned in chapter 3.4.

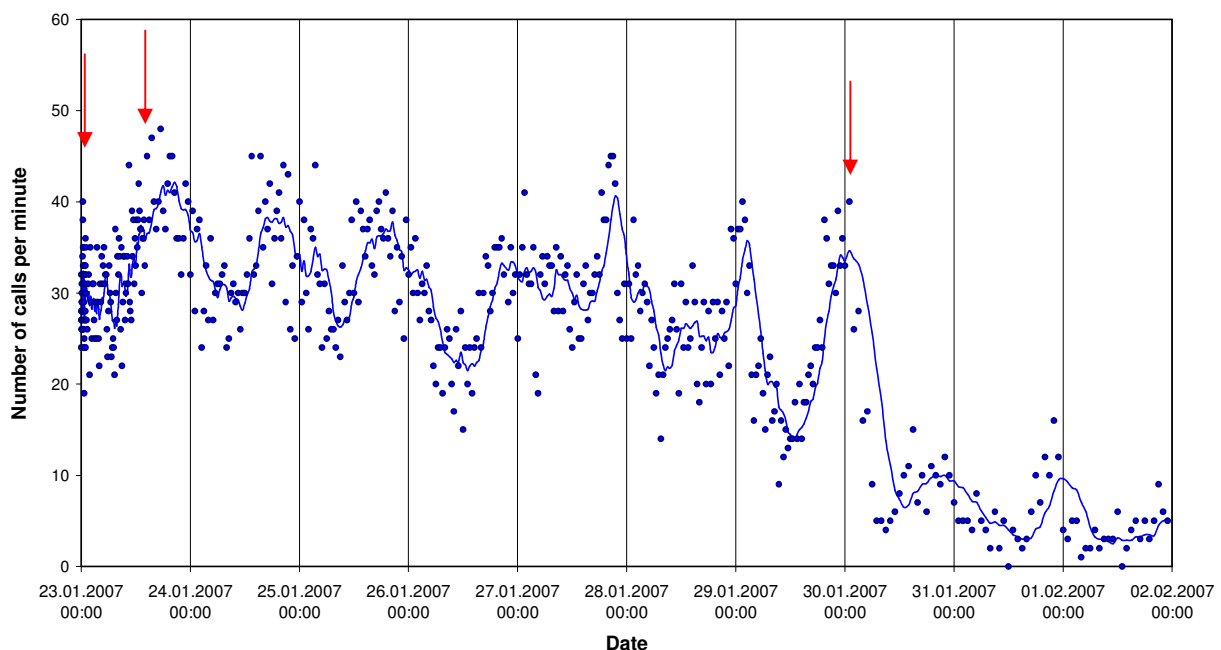


Figure 3.5A: The calling activity of Ross seals at Atka Bay, Antarctica, over a 10 day period in January 2007. Shown on the y-axis is the absolute number of calls per minute (blue dots,  $n=13\ 910$ ) with the time on the x-axis. The counting intervals were as follows: every minute (23.01.07 00:00 to 01:00, until first red arrow), every 10 minutes (23.01.07 01:00 to 13:00, until second red arrow), every 30 minutes (23.01.07 13:00 until 29.01.07, until third red arrow), and every hour (30.01.07 to 01.02.07). A clear diurnal pattern shows, with peak activities at night time. The blue line is the moving average of the call numbers.

In Fig.3.5B, the last days of call-counting with low calling numbers are left aside, and only the first seven days (23.01.07-29.01.07) with higher calling numbers are taken into consideration. The mean number of calls counted every 30 minutes at exactly the same time on all seven days specifies the nocturnal peak in calling activity. It always demonstrates more than 37 ( $\pm 6$ ) calls per minute around midnight opposed to only 24 ( $\pm 6$ ) calls per minute in midday.

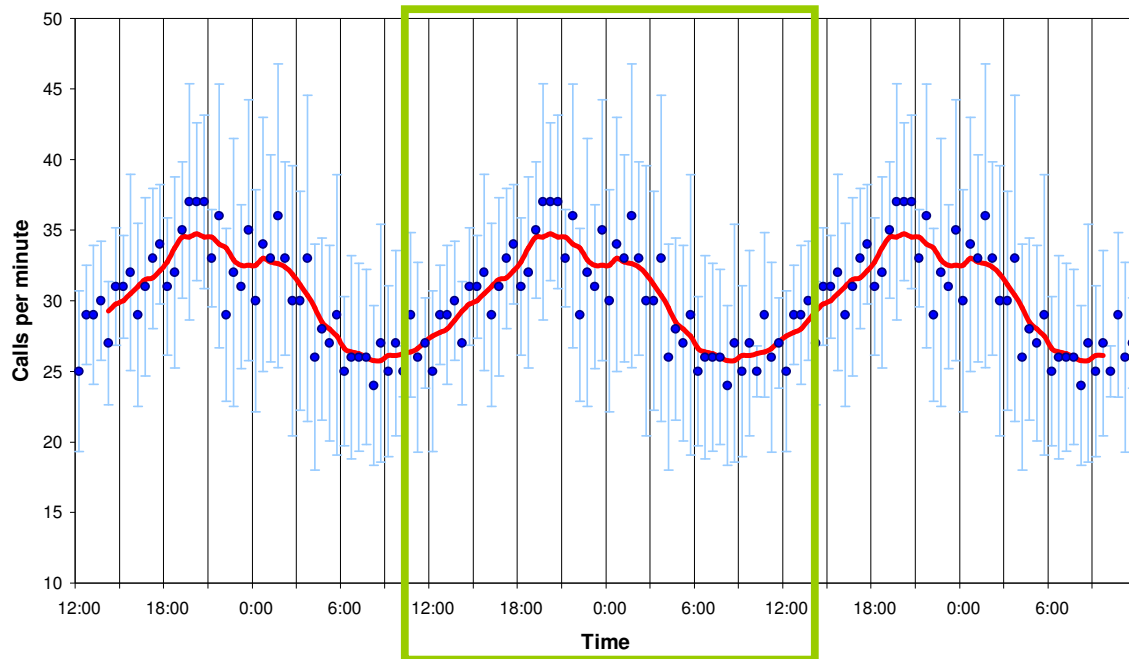
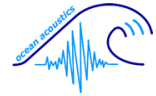


Figure 3.5B: The diurnal rhythm of calling activity of Ross seals at Atka Bay, Antarctica. Shown is the mean number of calls per minute (blue dots on the y-axis) measured every 30 minutes on seven consecutive days (23.-29.01.07 on the x-axis) but plotted into one 24-hour-interval (in the green frame). The data is tripled in order to make clear the diurnal nocturnal peak around midnight. Also shown are the minimum and maximum numbers of these counts (light blue bars), and the moving average (red line) of the mean.

In the graphs mentioned above, all calls are shown regardless of their type. A total of 13 910 calls were counted. Looking at the distribution of call types in that period, it appears that Highs are most commonly used (36%,  $n=5064$ ), followed by Lows (29%,  $n=4031$ ), Mids (21%,  $n=2919$ ), and then the two Whoosh components WTC (7%,  $n=951$ ) and WBC (7%,  $n=945$ ) respectively. The reasons for separating the Whoosh components are given in the previous chapter 3.4.

The diurnal pattern of the specific call types shows the same activity peak as the total call numbers (Fig. 3.5A).



The number of calls on 23-28 January were used for a FFT (Fast Fourier Transform) resulting in a single-sided amplitude spectrum (Fig. 3.5C). It reveals that a peak in calling activity occurs once a day. A minor peak occurs on approximately every second day.

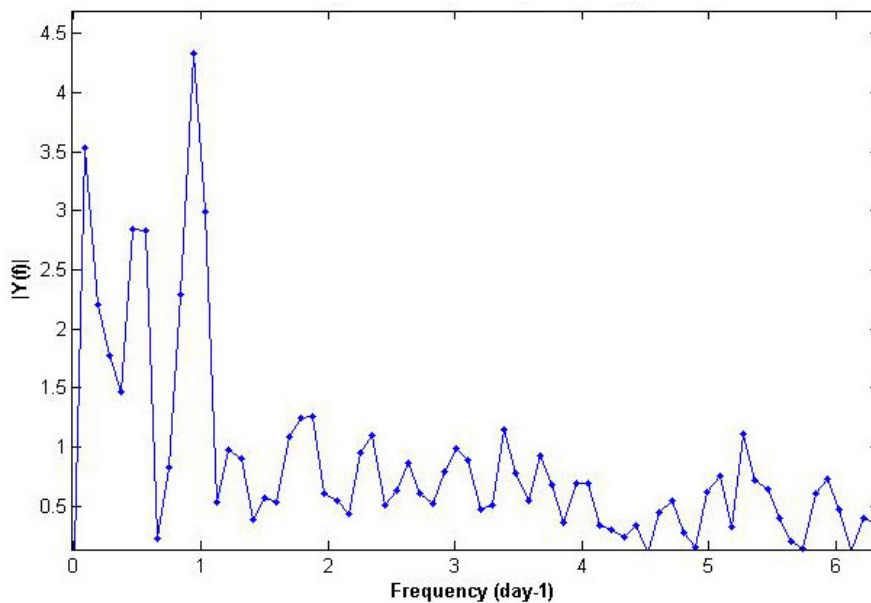


Figure 3.5C: This graph shows the FFT (Fast Fourier Transform) of Ross seal calls over a 6-day period before the calling rates dropped at the end of the season. The call frequencies per day are plotted on the x-axis, while the y-axis shows the  $y(f)$ . The high peak at 1 on the x-axis proves that calling activity is mainly driven by a daily cycle.

In search for reasons for this considerably regular calling pattern of Ross seals at the PALAOA site, global radiation (daylight), and tidal currents were considered and cross correlated to find the maximal and the minimal phase shifts, as explained in chapter 2.8. The significant negative correlation of calling activity and global radiation is shown in Fig.3.5D. Peaks in calling activity always occur during darkness or close to darkness around midnight. The cross correlation coefficient is  $r=-0.4$  at a four hour delay, indicating that calling activity peaks about four hours before (solar) midnight. The direct correlation coefficient is  $r=-0.18$  with  $p=0.0004$ .

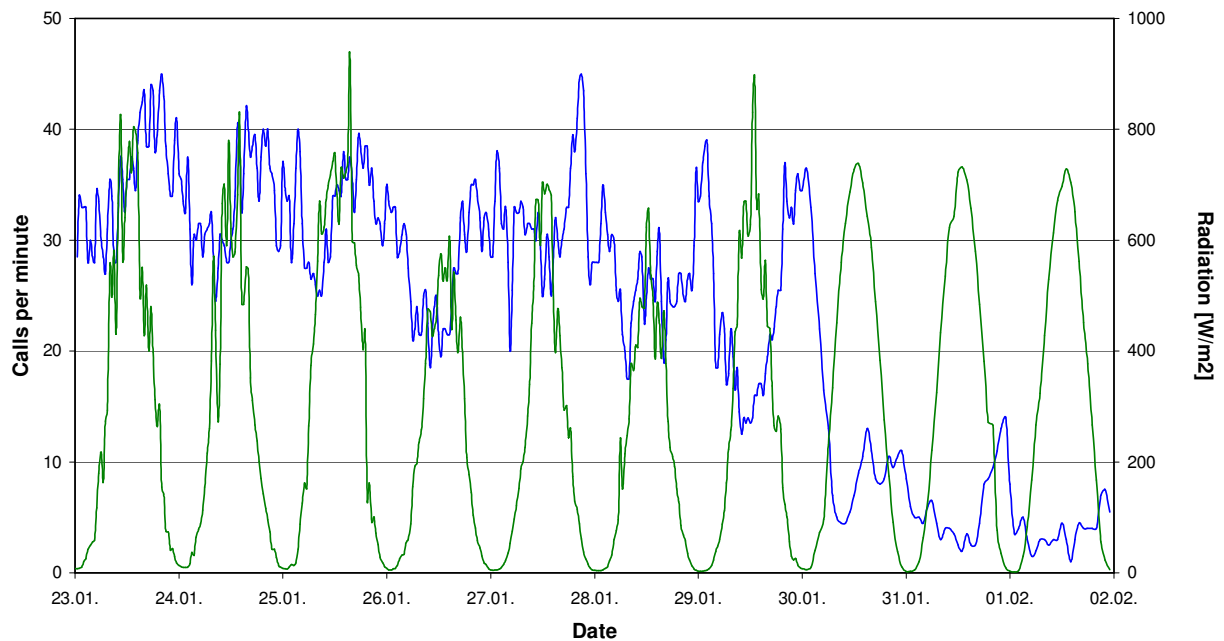
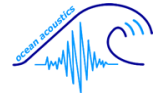


Figure 3.5D: This graph shows the diurnal calling pattern with calls per minute (blue line on the left y-axis) along with the global radiation in Watts per square meter (green line on the right y-axis) measured every 30 minutes (x-axis) at Neumayer base. The cross correlation coefficient is  $r=-0.4$ , the direct correlation coefficient is  $r=-0.18$  ( $p=0.0004$ ). The irregularities in radiation are caused by cloud coverage. Despite the low latitude it gets already dark for a short while at midnight at the end of January.

The significant correlation of calling activity and tidal movements is shown in Fig.3.5E. Even though it seems to match perfectly for the 28-30 of January (starting spring tide), the tidal pattern changes over the days (neap tide) and the calling activity does not follow it consistently. The cross correlation coefficient is  $r=0.2$  at a three hour delay, indicating that calling activity peaks about three hours after a peak in tidal currents. The direct correlation coefficient is  $r=0.14$  with  $p=0.004$ .

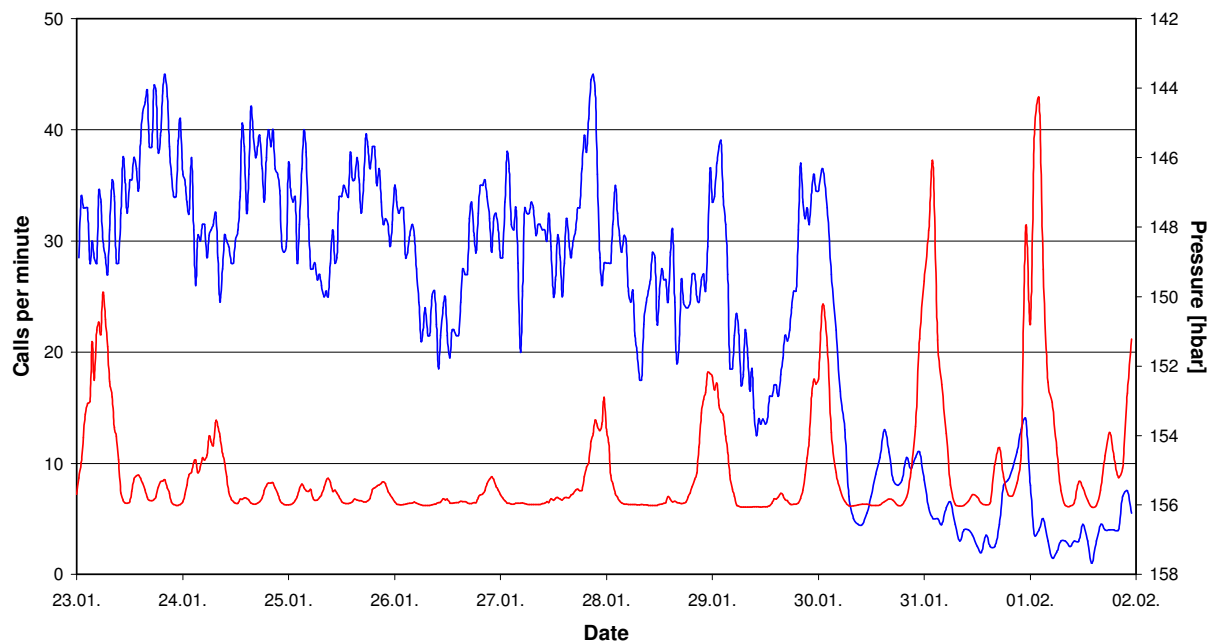
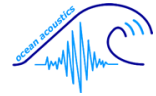
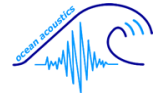


Figure 3.5E: This graph shows the diurnal calling pattern with calls per minute (blue line on the left y-axis) along with tidal movements (red line on the right y-axis) measured every 30 minutes (x-axis) by the CTD device directly at the PALAOA hydrophones. Not the tide itself is measured but the pressure in hecto bar, indicating the fluctuating depth of the instrument. The cross correlation coefficient is  $r=0.2$ , the direct correlation coefficient is  $r=0.14$  ( $p=0.004$ ).

### 3.6 Localization and individual calling patterns

With two hydrophones of PALAOA still working, it is possible to appoint a direction where a Ross seal call is coming from. The distance, however, cannot be predicted. Here (Fig.3.6.1A-E) the measured time delays are drawn into a map (colored lines) to show all possible directions of calls in chosen minute files. The directions derived from time delays at the hydrophones are correct, but a manual measuring error of  $\pm 70$ ms occurs. Each direction is given an assigned color, also representing a calling Ross seal. To scrutinize possible individual calling patterns, each direction, coded in its color, is additionally plotted by call type. The resulting pattern of the four call types are shown here as well. Each of the below schemata are of a one minute-file with  $n$  giving the number of calls in each file. “Grey calls” could not be assigned a specific direction.



Estimation of calling seals and individual calling patterns

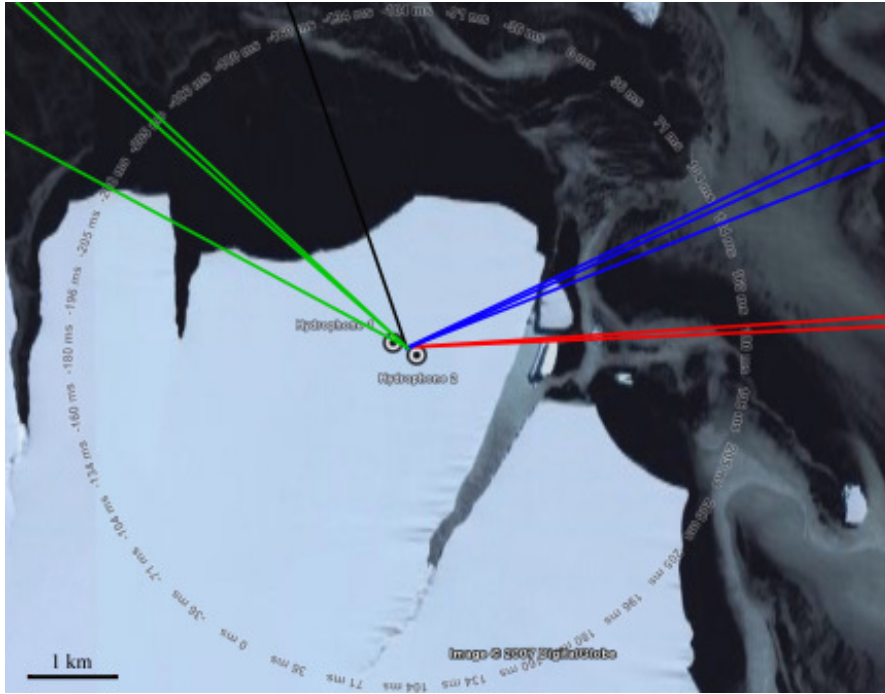


Figure 3.6A: The different directions of sound sources propose that a minimum of 3-4 Ross seals are calling during that minute of recording (n=9).

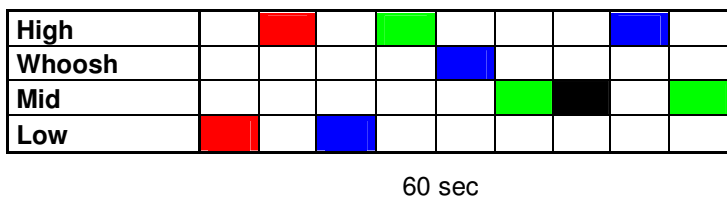


Figure 3.6B: Individual calling schema (n=9) with call types being colored according to the directions given in Fig.3.6A.

### 3. Results

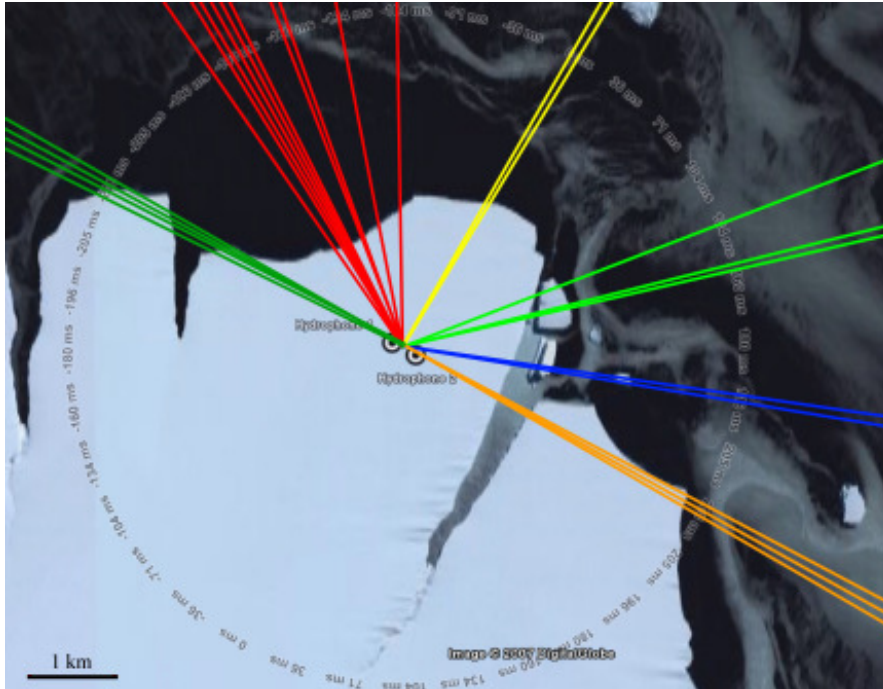
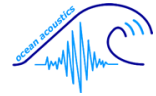


Figure 3.6C: The different directions of sound sources propose that a minimum of 6-8 Ross seals are calling during that minute of recording (n=24).

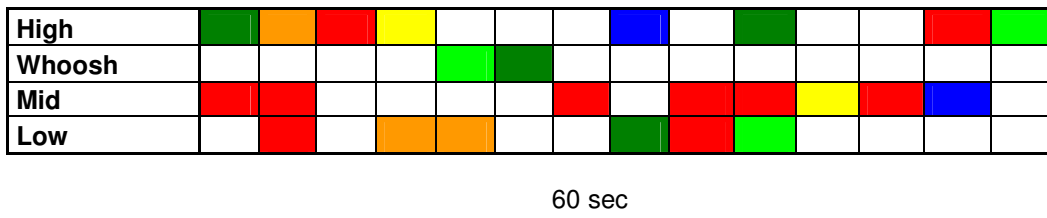


Figure 3.6D: Individual calling schema (n=24) with call types being colored according to the directions given in Fig.3.6C.

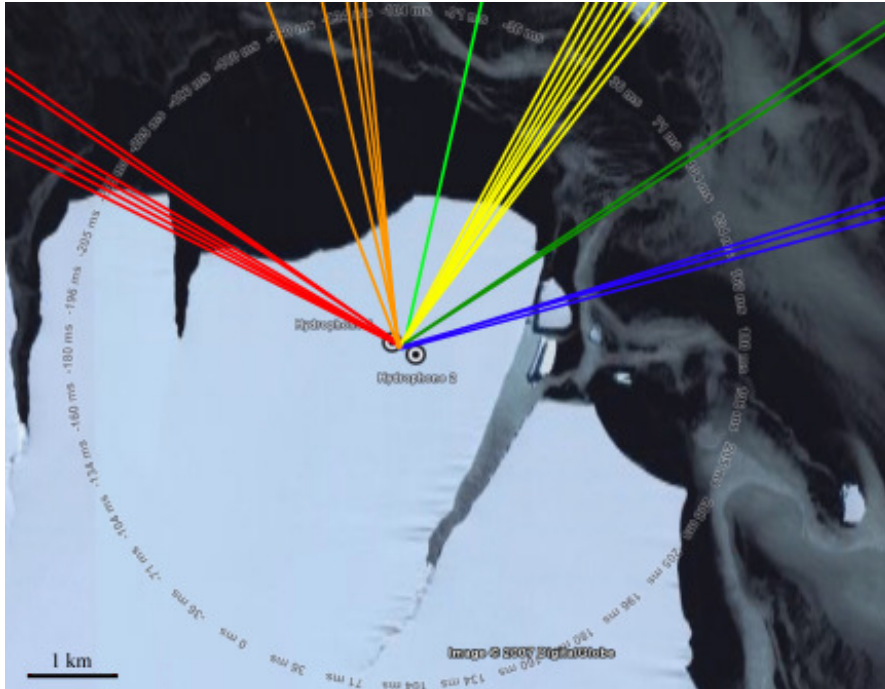
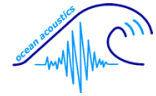


Figure 3.6E: The different directions of sound sources propose that a minimum of 5-6 Ross seals are calling during that minute of recording (n=17).

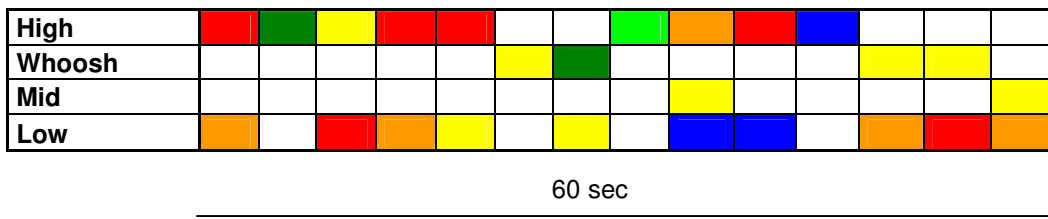


Figure 3.6F: Individual calling schema (n=17) with call types being colored according to the directions give in Fig.3.6E.

### 3. Results

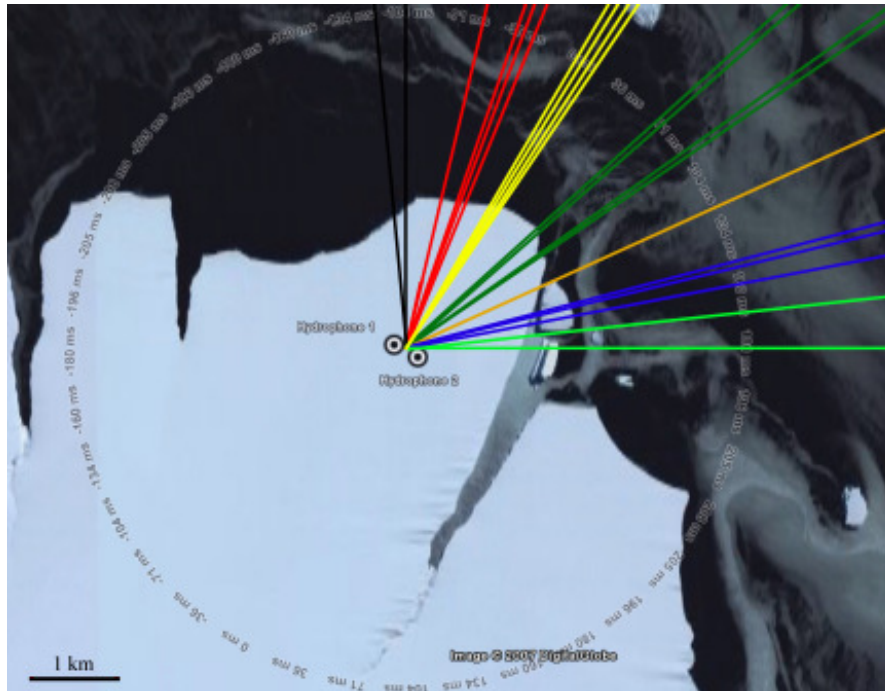
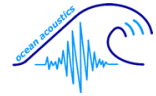


Figure 3.6G: The different directions of sound sources propose that a minimum of 4-7 Ross seals are calling during that minute of recording (n=19).

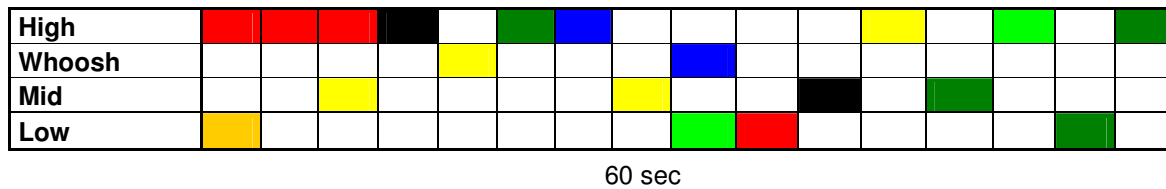
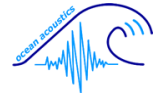


Figure 3.6H: Individual calling schema (n=19) with call types being colored according to the directions given in Fig.3.6G.



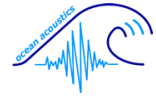


## 4. Discussion

### 4.1 Purposes for different call types

As shown in the result section of this thesis, Ross seals in the eastern Weddell Sea exhibit three siren-like calls (High, Mid, and Low) and a hissing Whoosh with a simultaneous tonal component. These calls have not been described in such detail before. Yet the purposes for these four different call types are still completely unknown, as is which animals, according to sex and age, might preferably use one or the other call type.

For other seal species it is known that different call types may serve for different purposes. For Weddell seals, it is well-documented that calls produced during mating differ from calls used in male defence of their underwater territories or from calls used for recognition between seal mothers and their pups (Thomas and Kuechle, 1982; Pahl et al., 1997). Special hunting calls seem plausible, as well as vocalizations used for orientation. The latter assumption is highly disputed. Leopard seals were found to use ultrasonic sound and harbour seals use clicking sounds similar to those used in odontocetes' echolocation. However, no active biosonar as the one used by dolphins and bats has been identified in pinnipeds. New findings support the idea that baleen whales use a not so sophisticated form of echolocation for feeding (Stimpert, 2007), and that phocids, like the Ross seal, may use sound localisation (Schusterman et al., 2000; Evans et al., 2004) to the extent known from oilbirds, swiftlets, and shrews to navigate their habitat (Griffin, 1953; Griffin and Suthers, 1970). However, seals are likely to rely on visual and tactile cues while foraging (Riedman, 1990; Schustermann et al., 2000). Ross seals are well adapted to foraging in their dark habitat under the ice, in that they have a visual system with an enlarged part of the eye behind the lens to magnify focused objects (King, 1968). They also have specialized whiskers for the tactile sense (Riedman, 1990; Thomas, 2002) and are the only mammal with a common secretory canal for microcrine and holocrine glands emptying into the tactile hair canal for an even better tactile capability in sensory perception (Ling, 1972). This visual and tactile



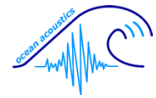
specialization might enable Ross seals to navigate deep under the ice without difficulty and without the use of other senses. Further evidence is needed to finally settle this question whether sound plays an important role for seals in orientation and navigation or not.

Even though Ross seals appear to be solitary animals, their underwater vocalizations allow for communication over long distances of several kilometres, which could be the basis for sociability or territoriality over large areas (Ray, 1981). A discussion whether mating may account for being the primary reason for Ross seal underwater vocalizations is given in chapter 4.5.

### **4.2 Inter- and intra-call specific differences**

The differentiation of the various call types is based on their different spectro-temporal content by extracting duration, minimum and maximum frequency, frequency range, peak frequency, and amplitude at peak frequency from each call. These parameters were then used to make comparisons among calls that have been identified as different call types. However, noting that calls appear to be composed of a sequence of elements (ups and downs) it seemed also worthwhile to analyse these elements individually. The resulting sweep rates were compared with those of other Ross seal call types as well. Many of the parameters mentioned above provided statistically significant differences allowing distinguishing between the various call types. In particular, the combination of minimum and maximum frequency is sufficient to reliably separate the four call types, as shown in Fig.3.2L. This concept of call identification and separation is the fundamental result of this study, and will have direct impact on the development of automated pattern recognition algorithms.

While the separation between different call types is straightforward, variability within a call type is noticeably high. Individual calls vary widely from call to call, prohibiting a clear match when a number of calls is being superposed. The combination of slight differences in call duration, sweep rates and minimum and maximum frequencies lead to a mismatch of the complete call. An explanation for the intra-call variability could be the

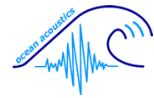


natural variance even within individuals. This variability will complicate the use of matched spectrogram techniques in automated pattern recognition algorithms. Despite the variability within the spatio-temporal content of High siren calls, each of the parameters chosen as descriptors displays a rather small variability when viewed separately (Fig.3.2C). Even associated components such as the Bowl (Tab.6.4) or the distinct edges in Mid siren calls (Tab.6.5) vary only slightly. Possibly, this is a result of the anatomy of sound production of Ross seals, which might allow certain features only. In Mid siren calls the so called low part peaks (LPP) denote another feature with low variability (Fig.2.3.8A). LPPs are the most distinct turning points of the sweeps with two LPPs per call at the same frequency. Do Ross seals obey a rule that the second peak in a Mid siren call must be as high as the first one? Apparently, since both have the same value.

### **4.3 Structures of Ross seal vocalization**

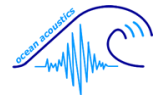
Ross seal vocalizations were described by Watkins and Ray (1984) for the first time. Compared with the current thesis, they only found high frequency calls at a frequency range of 1-4 kHz, but also mention a call at lower range, probably a Low call. Their structural descriptions and durations match with the ones presented in chapter 3, which affirms that truly Ross seals are the topic of concern.

A striking feature in High siren calls is the simultaneous occurrence of the Bowl component in about half of the measured calls. This frequency modulated tonal sound is of lower frequency than the High itself, and appears right underneath when displayed in a spectrogram (Fig.3.1). Watkins and Ray (1984) mention a “secondary sirenlike tone” with a higher frequency, indicating that their description of a call could match with the Bowl and the secondary tone would then be the High call. It is quite difficult to integrate their observations into the current results, since other methods of recording and analysis were used at that time.



Also interesting is the occurrence of some “pure” calls among the Highs. Their appearance in a spectrogram usually shows quite thick lines, sometimes with a ladder-like pattern in it. However, more than half of the Highs measured in detail showed fine thin lines instead (Fig.3.1.1.B). At first, it was thought that this could be due to background noise or the technical recording equipment. Of these Highs with thick lines, most calls own a Bowl component, which proposes that the High siren calls could be further divided into “thick Highs with Bowl” and “thin Highs without Bowl”. Whether this finding can be proven as statistically significant is beyond the scope of this study and needs to be confirmed by further analyses.

A question often asked and not yet sufficiently answered concerns the distribution of the so-called harmonics of the siren calls. The analysis showed that in Lows the overtone is a real harmonic at approximately double the frequency of the fundamental tone. Most of the Lows had such a harmonic (Fig.2.3.8B). In rare cases they even had a faint second one, again with double the frequency as the distance from the first one. The picture is not as clear in Highs and Mids. In both call types only the four lowest harmonics of greatest amplitude were measured, since the inaccuracy of detecting the borderlines for visually measuring the frequencies increased significantly for the weaker upper harmonics. At first sight, some Highs looked like two combined combs that alternate in their harmonics. Therefore it was never clear if that particular harmonic belonged to the one before or not. Already Watkins and Ray (1984) commented on sideband harmonics at a relatively constant rate that do not vary with the fundamental frequencies. The results of this thesis show that the four inter-harmonic intervals (each IHI being the distance between two harmonics in Hz, see Fig.2.3.5) vary widely. For Highs they drop from 849 Hz to 556 Hz. These decreasing values could mean that not all harmonics were noted in the appropriate order, in case they vary with the fundamental frequency. For Mids, the first three inter-harmonic intervals have almost the same value, while the fourth interval displays a higher value. This could indicate that several harmonics were left out (and were therefore not visible in the spectrogram). Interestingly, when a single call is visually analyzed, some of the harmonics seem to follow in quite regular intervals, but then the calculated fundamental tone must be much lower than the sweeps of greatest amplitude as observed in the lowest part of the call. In this case, the



fundamental frequency would not be audible, but its harmonics are. This effect also happens when, for example, a flute is being overblown in a way that only a high shriek is audible and not the tone originally intended. The shriek then consists of the harmonics of the intended but suppressed fundamental tone. Whether this actually happens in the observed Ross seal vocalizations is speculative. It could also be due to anatomical features during sound production.

If such tiny variations in their vocalization are important to Ross seals, it should play a big role whether a siren call starts with an upsweep or with a downsweep. In Lows, without exception, all start with an upsweep. In Highs, both variants occur at about the same frequency. In Mids, however, most start with an upsweep and only a minor fraction with a downsweep. Variation in Highs and Mids may partly be due to starting sweeps that could not be detected visually. This is unlikely though, since only intense calls were chosen for the measurement of acoustic features. Perhaps that variability is another feature that provides further distinction between call types, or perhaps animals of different sex or age groups prefer using one over the other, or perhaps this variability does not matter at all.

Taking Mid siren calls as an example, it was first thought that special features, such as distinct edges within the upsweep (Fig.2.3.8A), belong to an individual Ross seal. If that were the case, then estimating the number of calling seals would be easy and calling patterns could be securely assigned. It turned out, however, that all Mid calls from both seasons show these edges. Why should they have straight upsweeps in Highs and Lows, but “build in” an edge in Mids? With an almost exact duration of 100 msec these edges are too short to be detected aurally. Interestingly, in the continuous Mid call part the edges occur almost exclusively at one frequency only, which makes it look as if they are a necessity.

Some of the analyzed Mids also show a little attached “umbrella” on the right upper side at about 1.5 kHz and lasting for 300 msec (Fig.3.1.2B). This is less likely an artefact since it looks more like an actual part of the call with sometimes even parts of a sweep. However, it is not attached to the “main call”. This might be a candidate for marking an individual Ross seal with some sort of special “pronunciation skills”.



Low siren calls exhibit a tiny “dot” right in front of the call (Fig.2.3.8B). Most of the analyzed Lows showed this dot before the actual call starts. It is unknown, whether it is an artefact of resolution, background noise in the spectrogram, or an important feature of the Ross seal’s Low call. In this case, it would be useful to have recordings of Ross seal vocalizations from other locations to compare with.

Low siren calls stand out with another special feature as well. A little more than half of the Lows seem to be somewhat “washed-out” at their turning points of the sweeps. These so-called diffuse turning points (DTP, as explained in Fig.2.3.8C) could be due to either the Ross seal intentionally lowering its amplitude at those DTPs, or periodically rising background noise is partly masking the call. However, a quite high percentage of good quality calls shows this feature. The reason for this irregularity in call structure is still completely unknown.

Spectrograms of Ross seal vocalizations show the siren calls as slightly curved structures. When displayed on a logarithmic scale, the curved sweeps become an almost straight line (Fig.2.3.1B). This is quite an unusual feature, proposing that Ross seals, just like a piano, change their frequencies in whole octaves and therefore sweeps can be characterized in a rise of octaves per time.

The structures of Ross seal vocalizations, and even more their production, remain barely understood. However, this present thesis is a beginning to address some of these scientific questions.

### **4.4 Difficulties in analysing Ross seal vocalizations**

Only few publications provide substantial information on the special features of Ross seal calls (Ray, 1981; Watkins and Ray, 1984). However, no specific analysis methods existed so far and thus had to be developed and approved within the scope of this thesis.

Depending on the background noise and amplitude of the calls, it took up to 3 minutes to count the calls from a single minute-file spectrogram. Measuring and noting all features



of a High and Bowl from a chosen file could take up to 20 minutes. Theoretically, this would total more than 145 working hours for analysis alone.

One attribute that makes Ross seal calls unique in seal vocalizations, and quite difficult to measure (Watkins and Ray, 1984), is the fading-in and fading-out of their High and Mid siren calls. Even in relatively silent underwater environment, all calls start with slowly rising amplitude and end with the call “diving into” the background noise (see also chapter 4.8). Since abrupt on- and offsets increase the detectability of calls (Watkins and Schevill, 1979), Ross seals seem to lower the ability to locate each other underwater by using these “fading” siren calls. Since Ross seals are known as solitary living pinnipeds, this may not have functional relevance, as it would have otherwise in more gregarious seal species. Nevertheless, it may also be the Ross seals’ predator avoidance behaviour, since leopard seals and killer whales are abundant in the coastal pack ice at this time of the year.

### **4.5 Seasonal calling pattern**

So far, Ross seals have been recorded at PALAOA during the 2005/2006 and the 2006/2007 summer seasons. It is expected that a third complete season of recordings will be added during the upcoming months (2007/2008 summer season). Based on the fact that the first siren calls were heard in the morning of 20 December 2007, possibly already late at night of 19 December, the variability of the Ross seals’ annual arrival time at the Ekström Ice Shelf is merely  $\pm 1$  day, or even less than that! The upcoming weeks will show whether their departure time is equally set.

According to Blix and Nordøy’s (2007) interpretation of the mating behaviour, female Ross seals give birth on the pack ice in early November and drift with the ice while nursing for about a month. Females mate once the pups are weaned sometime in December, and return north again into the open ocean. During this pelagic period, female Ross seals possibly “refill their storage” in favourable hunting grounds since they had spent a substantial amount of energy while nursing their pups. After about a month’s time offshore, the females return back south deep into the pack ice again. Males and barren females, on the other hand, do not leave the pack ice of the eastern Weddell Sea

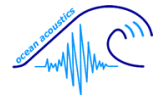


after mating but venture further south towards the ice shelf. At this time, around mid December, Ross seals become audible at PALAOA. Presumably, males and a few females arrive first, causing the slow increase in calling activity starting from mid December to the first week of January (chapter 3.4). This is followed by a sudden rise in calling activity which is noticed within four days in the second week of January, as shown in Fig.3.4. This increase might reflect the arrival of new seals – for example the females that returned to the open ocean again after mating. So far, it cannot be concluded whether it is actually the arriving females that increase the calling rate, as proposed analogously for Weddell seals (Green and Burton (1988)), or if the present males start a competitive or “welcome” calling for the females instead. Or, perhaps, both sexes call at the same rate for communication and social reasons.

Southwell (2003) states that females are further away from the coast than males. This indicates that perhaps juveniles and barren animals are responsible for the low calling rates at the beginning of the season. In this scenario, mostly males arrive after mating further north, leading to increasing calling rates, while the females would stay away from the coastline, for yet unknown reasons.

Since the mating season should be over by mid January, the need to find mating partners cannot serve as the only reason for Ross seals’ vocalization. Usually it is assumed that most seal vocalizations are associated with mating behaviour, but recent findings indicate that the animals are quite vocal prior and past the breeding season as well (Rouget et al., 2007). During that time the adults are moulting and presumably fasting, suggesting another social component causing the seals to be so acoustically active.

Another interesting aspect is the synchrony by which Ross seals either become silent or leave the area en masse within, virtually, a few hours on 30 January (as indicated in Fig.3.4). In Weddell seals, their decreasing vocal activity is correlated with the animals leaving the area, as supposed by Rouget et al. (2007). Ross seals do not live in social groups, so the notion to leave again in order to head north must be passed vocally. Perhaps this is the reason for the Ross seals’ constant calling. They stay in touch acoustically and, like in a big herd of ungulates, as soon as a few individuals start leaving and their calls become less intense, the rest follows instinctively. This way the



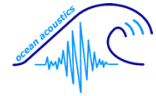
seals would ensure to keep the same rhythm for all animals for their return at approximately the same time prior to mating behaviour.

Further research should address the possibility of seasonal differences in the use of different call types, which would suggest that different sexes use separated calls for different purposes, such as underwater territory defence, competition, pup recognition, or attraction of mating partners.

### **4.6 Zeitgeber for diurnal calling rhythms**

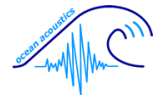
The day/night shift of Ross seal calling activity is obvious in the PALAOA recordings (chapter 3.5). At the end of January 2007, two minima of 24 calls per minute were counted in late morning and during midday, whereas there was an activity peak of 37 calls per minute around midnight (Fig.3.5B).

A plausible explanation for this apparent diurnal calling activity pattern is the frequent haul-out behaviour of Ross seals at this time of the year (Southwell, 2003). Condy (1976) already described a peak haul-out period in Ross seals which lies between 8:00 and 14:00 in the second half of January. Blix and Nordøy (2007) reported a 50% probability for Ross seals to be hauled-out through midday. This would match the times of lowest calling activity measured in this thesis. Fewer seals in the water would explain fewer underwater vocalizations. For leopard and crabeater seals it was found that the number of hauled-out animals has a significant impact on the underwater calling rate (Thomas and DeMaster, 1982). Rouget et al. (2007), however, found this diurnal vocal activity pattern for Weddell seals in the winter season as well. During most of that time, the seals do not haul-out at all, yet the diurnal pattern persisted. This would mean that haul-out behaviour alone does not account for the diurnal calling pattern. Originally, it was thought that seals haul out in order to rest after deep foraging dives. Bengtson and Stewart (1997) oppose this by reporting an aerobic metabolism during diving. Given this, it seems that seals might spend time on the ice mainly as a consequence of moulting. An alternative zeitgeber for the observed diurnal pattern could be time of the day, which is, of course, related to daylight conditions. These are measured close to PALAOA as global sun radiation at the Neumayer Station. In late January, the sun does already set



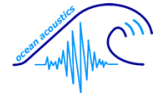
on site and thus bestows a few hours of dim light conditions around midnight, which is the peak time of Ross seal calling activity. Fig.3.5.C shows the result of a Fast Fourier Transform (FFT) of the call numbers, revealing one peak in calling activity per day. A minor peak occurs on approximately every second day, which may be an artifact due to high fluctuations of call abundance within a relatively short scanned period. This finding, along with a relatively high correlation coefficient, supports the hypothesis that daylight functions as an important zeitgeber for the Ross seals' diurnal calling rhythm (Fig.3.5D). A similar pattern was described, for example, for bearded seals by Van Parijs et al. (2001) and by Mirhaj et al. (2004) who, at the end of December 2003, showed peaks of Weddell seal calling activity shortly after midnight. During breeding season, the other Antarctic seal species exhibit clear night-time peaks in their vocalizations as well (Thomas and DeMaster, 1982; Green and Burton, 1988). A possible explanation for this nocturnal rhythm could be linked to prey availability and distribution. Many marine predators are nocturnal due to the vertical migration of their prey. This could also be true for Ross seals. In this case, their vocalizations would form an important part of their foraging and diving activities. For Weddell seals it was shown that they descend for a hunting dive in total silence but start calling again while ascending (Evans et al., 2004). Plötz et al. (2001) showed that foraging dives in Weddell seals are shallower at night – due to prey abundance – which coincides with the time of most calling activity. Referring to Ross seals, this behaviour may also indicate that the use of air flow in body cavities during sound production is restricted by higher pressure, so that vocalization in general mainly takes place in the upper water column.

Why, however, should a daylight induced diurnal pattern be stable in an environment that includes periods of continuous light and continuous darkness? Even if Ross seals move far enough north to not experience the continuous darkness during austral winter, their forage pattern would still have to be stable enough to persist during the continuous light periods of the austral summer months. It is unlikely that they would completely depend on variable cues, such as daylight, for a behaviour that is critical for survival. Ross seals have most likely an internal clock, which is merely adjusted by cues such as daylight. This way, the cue does not need to be very precise, just enough to keep the rhythm consistent.



Yet another zeitgeber, or a cue for keeping the rhythm, could be the tide. It is quite regularly, but with a fortnightly rhythm of spring tide and neap tide as extreme conditions (when the sun, moon, and earth are aligned in such a way that the tidal forces are either maximal or cancel each other out). Bornemann et al. (1998) found a significant correlation between the ultradian diving activity of Weddell seals and tidal patterns, while bearded seals display a diurnal calling pattern that does not correlate with tide (Van Parijs et al., 2001). The diurnal calling pattern of Ross seals, however, matches only parts of the tidal cycle (Fig.3.5E). On three consecutive days (28-30 January, 2007) the highest tide correlates well with the peak vocal activity. On 23-24 January, however, tidal flow and calling activity appear anti-correlated. A longer time range will have to be analyzed in order to perform statistically significant correlation analyses to find out whether this synchrony is accidental or not. Unfortunately, the CTD data was unavailable before 23 January 2007, and the Ross seal calls cease in the first week of February 2007, leaving the rather short 6-day time window, which only allows speculating on this issue. A complete set of months with both seal calls and tide measurements is expected during the upcoming austral summer season (2007/2008) which will then allow a detailed analysis.

The discussion above shows that the Ross seals' diurnal calling pattern may be influenced by a variety of factors, such as daylight, temperature, tidal currents, ice coverage, and prey availability, which are correlated among each other as well. The seals' annual life cycle, including their pelagic phase, breeding, mating, and internal clocks add additional factors. A comprehensive multivariate analysis would be required to find out the driving force(s) behind the cyclic calling pattern of Ross seals. However, this analysis was not possible in the course of this study. Instead, simple correlation coefficients and cross correlation coefficients were computed, as mentioned in chapter 2.8 and chapter 3.5. Further research is needed to shed some light on some of those aspects, and PALAOA is apt to provide the necessary database.

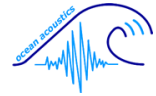


#### 4.7 Localization and distribution

Ray (1981) states that the number of calling seals always exceeds the number of animals observed on the ice. This falls in line with the notion that no Ross seals have been sighted near PALAOA at Atka Bay so far, yet their calls reveal their seasonal presence in the waters around the Ekström Ice Shelf. Variations of high frequency components and differences in intensity levels among calls can be used to relate calls to different seals (Watkins and Ray, 1984). A minimum number of vocalizing seals can be estimated by PALAOA by evaluating their directions. Unfortunately, the current PALAOA hydrophone array does not permit to localize the exact position of a sound source. Animals in close vicinity of one another cannot be clearly separated, nor can several seals along a given direction be distinguished.

However, this method provides first ideas of the minimum number of calling Ross seals (as explained in chapter 2.6.1). It could be used for acoustic censusing, as Rouget et al. (2007) proposed for Weddell seals, since visual surveys of hauled-out seals only vaguely approach real population numbers in a given area. Possibly both methods, acoustic and visual surveys combined, work best to provide the most accurate population estimates for Ross seals in Antarctica.

Having detailed information on the number of calling Ross seals, it is possible to scrutinize individual calling patterns. Determining individual calling patterns at this stage of research can only be exploratory. A single minute of recordings fails to reveal any recognizable pattern, neither in call type occurrence, nor in their frequency. However, the short examples in Fig.3.6B, Fig.3.6D, Fig.3.6F, and Fig.3.6H already suggest that several Ross seals vocalize alternating and use all of the above described call types, rather than a single seal having a monologue. Interestingly, some animals (each animal corresponding to a direction given in different colors, as described in chapter 3.6) appear to use specific calls, while others do not. Most clearly this is visible in the last example of five consecutive minutes of Fig.3.6 K where only the “red” animal produces Whooshes. This finding might be worth considering whether Whooshes are only produced by, for example, mature or territorial males. Certainly more and longer periods of

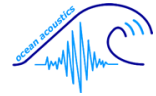


recordings must be analysed to satisfactorily answer the question if individual Ross seal vocalizations follow certain patterns. It also would be advantageous to know the exact source of calls in terms of sex and/or age of the vocally active Ross seal.

### 4.8 The ambient soundscape

While counting Ross seal calls from PALAOA spectrograms, additional comments regarding the ambient soundscape, such as ice cracking, the presence of baleen whales (with their infrasonic vocalization), killer whales (with their ultrasonic clicks), or other seals, were noted. From these comments, first speculations on acoustic interactions between Ross seals and the respective signal can be derived.

The non-biological soundscape of the Southern Ocean usually exceeds animal vocalizations in amplitude and bandwidth. The loudest recorded events were iceberg collisions, passing ships, and frequent ice break-offs from the Ekström Ice Shelf. The latter are broadband signals of high amplitude, sometimes lasting for several seconds. The Ross seals, as well as Weddell, crabeater, and leopard seals, acoustically ignored such natural sound events, meaning that they continued their vocalizations during or immediately after the event. Anthropogenic noise, such as the passing research vessel *Polarstern*, is likely to mask seal vocalizations for several days continuously. Whether this has an effect on the animals' behaviour remains to be addressed in future studies. It is, however, more likely that Ross seal respond to their surrounding biological soundscape. They could, for example, display acoustic avoidance behaviour when predators such as killer whales or leopard seals are audible. Thomas et al. (1987) suggested that Weddell seals of the Ross Sea stop vocalizing as an anti-predation strategy when killer whales or leopard seals occur. Of course, it is not possible to predict the distance between the predator and its prey from PALAOA recordings, but underwater vocalizations can be heard over long distances and if both species were recorded together, they may have heard each other as well. Because their calling rates were never affected by simultaneous killer whale sounds, Ross seals may not feel threatened by passing orcas. This very same lack of acoustic response occurred when leopard seal vocalizations were audible. Even though leopard seals are quite vocal



during the recording periods, Ross seal calling rates remained unaffected by the presence of this potential predator.

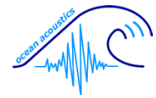
Another interesting aspect is whether Ross seals “acoustically banish” other seals by their constant vocalizations. In fact, the rather ubiquitous Weddell seal vocalizations decrease significantly as soon as Ross seals become audible. Both seal species’ vocalizations overlap by only three days in December 2006. Then, approximately six days before the last Ross seal call was detected in the first week of February 2007, Weddell seals returned to the PALAOA region or resumed vocalizing again. This behaviour has only been noted for the 2006/2007 season so far, because the full December data is missing in the year of the PALAOA setup. Hence the coming 2007/2008 season will be of most interest in this regard.

Another form of acoustic coexistence would be when one animal modulates its vocalization in a way to quasi avoid another one’s main frequency range, as is shown in killer whales and leopard seals (Mossbridge and Thomas, 1999). Further analysis is necessary to see whether leopard seals might shift their low trills (300-400 Hz) in order to avoid having their calls masked with Ross seal Low siren calls. Nevertheless, leopard seals leave the area around mid January, which is the time when Ross seals reach their peak calling rates.

It would be worthwhile to test whether Ross seals respond to underwater playback experiments. Such setups may answer the question whether Ross seals avoid predators, or if they initiate a “vocal arms race” to outcall another seal species, especially Weddell and leopard seals.

### **4.9 Limits and outlook on the use of PAM (Passive Acoustic Monitoring)**

The major problem of bioacoustics is the lack of visual validation, which complicates the interpretation of the data in its ecological and behavioural context. For example, it cannot be predicted if silence means the absence of seals or if all present animals are silent. Rouget et al. (2007) assumes that a lowering in calling rates can be taken as evidence for a decrease in seal abundance. As long as recordings of Ross seals are not combined with simultaneous behavioural observations, every conclusion about the

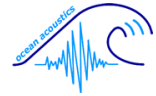


meaning of call types or occurrences will only be speculative. Acoustic recordings alone do not necessarily provide evidence for ecological questions. However, combined with other methods of observation, acoustics can be used as a powerful tool to better understand underwater behaviour of a species that spends most of its life underwater. Additional long-term acoustic monitoring of an area can provide important information on marine mammal migration patterns by detecting acoustic presence and absence of certain species. This can further be achieved by tagging individual animals combined with sonobuoys deployment arranged in arrays for complementary recordings.

In this thesis, the interpretation of the results has to be very critical. All measurements, both the characterizations of the different call types and the counting of calls for changing activity patterns, were done manually and were therefore exposed to certain subjectivity. A different observer may see the upper frequency limit at a slightly different point. However, this kind of measuring is important to begin with and for further development of automatic detection algorithms which might, one day, give more precise results on call type occurrence and seasonality in Ross seals. Until then, it is also important to measure certain acoustic parameters of their calls to allow for quality comparison among researchers all over the Antarctic (Pahl, 1997).

It must be highlighted that all of the above mentioned results refer to Ross seals of the PALAOA region at Atka Bay only! So far, it is unclear whether Ross seals in other Antarctic regions show the same calls or calling patterns. Likewise, it is not understood how these sounds are produced, what their energy levels are right in front of the vocalizing animal, how far apart they are scattered in this hostile environment, and what biological reasons they have for this non-stop “singing” in the Southern Ocean.

This study started from scratch, without prior knowledge of Ross seal occurrence or call types. Hopefully, this diploma thesis can set the foundation for future monitoring and ensuing analyses of Ross seal vocalization and its ecological implications.



## 5. References

Ackley S.F., Bengtson J.L., Boveng P., Castellini M., Daly K.L., Jacobs S., Kooyman G.L., Laake J., Quetin L., Ross R., Siniff D.B., Stewart B.S., Stirling I., Torres J., Yochem P.K. (2003) A top-down, multidisciplinary study of the structure and function of the pack-ice ecosystem in the eastern Ross Sea, Antarctica.

Polar Record 39(210): 219-230.

Bechervaise J.M. (1967) Antarctic wildlife - 11. Contrast in seals.

The Victorian Naturalist 84(2): 33-38.

Bengtson J. L., Stewart B.S. (1997) Diving patterns of a Ross seal (*Ommatophoca rossii*) near the eastern coast of the Antarctic Peninsula. Polar Biology 18(3): 214-218.

Bester M.N., Erickson A.W., Ferguson J.W.H. (1995) Seasonal change in the distribution and density of seals in the pack ice off Princess Martha Coast, Antarctica.

Antarctic Science 7(4): 357-364.

Bester M.N., Ferguson J.W.H., Jonker F.C. (2002) Population densities of pack ice seals in the Lazarev Sea, Antarctica. Antarctic Science 14(2): 123-127.

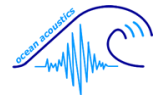
Blix A.S., Nordøy, E.S. (2007) Ross seal (*Ommatophoca rossii*) annual distribution, diving behaviour, breeding and moulting, off Queen Maud Land, Antarctica.

Polar Biology 30(11): 1449-1458.

Boebel O., Kindermann L., Klinck H., Bornemann H., Plötz J., Steinhage D., Riedel S., Burkhardt E. (2006) Acoustic Observatory Provides Real-Time Underwater Sounds from the Antarctic Ocean. EOS 87: 361-372.

Bonner W.N., Laws R.M. (1964) Seals and sealing. *in*: Antarctic Research: A Review of British Scientific Achievement in Antarctica. (Priestley R., Adie R.J., Robin G.deQ. eds.), pp. 163-190, Butterworths, London.

## 5. References



Bornemann H., Mohr E., Plötz J., Krause G. (1998) The tide as zeitgeber for Weddell seals. *Polar Biology* 20(6): 396-403.

Condy P. R. (1976) Results of the third seal survey in the King Haakon VII Sea, Antarctica. *South African Journal of Antarctic Research* 6: 2-8.

Condy P.R. (1977) Results of the fourth seal survey in the King Haakon VII Sea, Antarctica. *South African Journal of Antarctic Research* 7: 10-13.

De`ath G., Fabricius K.E. (2000) Classification and regression trees: a powerful yet simple technique for ecological data analysis. *Ecology* 81: 3178-3192.

Erickson A.W., Hofman R.J., Oehlenschlager R.J., Otis J., Kuehn D. (1971) Seal population studies in the Ross Sea. *Antarctic Journal of the United States* 6: 98-99.

Evans W.E., Thomas J.A., Davis R.W (2004) Vocalizations from Weddell Seals (*Leptonychotes weddellii*) during diving and foraging *in* Echolocation in Bats and Dolphins. pp. 541-547. The University of Chicago Press.

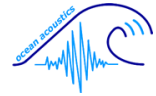
Green K., Burton H.R. (1988) Annual and diurnal variations in the underwater vocalizations of Weddell seals. *Polar Biology* 8: 161-164.

Griffin D.R. (1953) Acoustic Orientation in the Oil Bird, *Steatornis*. *Proceedings of the National Academy of Science. USA.* 39(8): 884–893.

Griffin D.R., Suthers R.A. (1970) Sensitivity of echolocation in cave swiftlets. *The Biological Bulletin* 139: 495-501.

Hall-Martin A.J. (1974) Observations on population density and species composition of seals in the King Haakon VII Sea, Antarctica. *South African Journal of Antarctic Research* 4: 34-39.

## 5. References



Ihaka R., Gentleman R. (1996) R: A language for data analysis and graphics.  
Journal of Computational and Graphical Statistics 5: 299-314.

King C. M. (1990) The Handbook of New Zealand Mammals.  
Oxford University Press.

King J. E. (1964) Swallowing modifications in the Ross seal.  
Journal of Anatomy 99: 206-207.

King J. E. (1968) Ross and other Antarctic seals. Australian Natural History 16(1): 29-32.

King J. E. (1969) Some aspects of the anatomy of the Ross Seal, *Ommatophoca rossi*  
(Pinnipedia: Phocidae).  
British Antarctic Survey Scientific Reports No.63. United Kingdom. 63: 1-54.

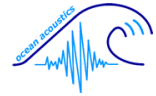
Laws R.M. (1984) "Seals" in Antarctic ecology.  
Vol. 2: 621-715. Academic Press, London.

Ling J.K. (1972) Vibrissa Follicles of the Ross Seal.  
British Antarctic Survey Bulletin 27: 19-24.

Lucas M. (1996) Antarctica – Die faszinierende Welt im ewigen Eis.  
Komet Verlag GmbH Köln.

Mirhaj M., Plötz J., Bornemann H., Kindermann L., Klinck H., Boebel O. (2004)  
Underwater calls of Weddell seals in the Weddell sea, Antarctica.  
SCAR Open Science Conference "Antarctica and the Southern Ocean in the Global  
System", 25-31 July 2004, Bremen, Germany.  
Terra Nostra, Schriften der Alfred-Wegener-Stiftung 2004/4 p 138.

## 5. References



Mossbridge J.A., Thomas J.A. (1999) An “acoustic niche” for Antarctic killer whale and Leopard seal sounds. *Marine Mammal Science* 15(4): 1351-1357.

Oritsland T. (1970) Sealing and seal research in the south west Atlantic pack ice, Sept-Oct 1964. *in: Antarctic Ecology* (Holdgate M.W. ed.) pp. 367-376. Academic Press, London.

Oritsland T. (1977) Food consumption of seals in the Antarctic pack ice. *In: Adaptations within Antarctic Ecosystems.* (Llano G.A. ed.) pp. 749-768. Smithsonian Institute, Washington, D.C.

Pahl B.C., Terhune J.M., Burton H.R. (1997) Repertoire and Geographic Variation in Underwater Vocalisations of Weddell seals (*Leptonychotes weddellii*, Pinnipedia: Phocidae) at the Vestfold Hills, Antarctica. *Australian Journal of Zoology* 45: 171-187.

Pitman R., Ensor P. (2003) Three forms of killer whales (*Orcinus orca*) in Antarctic waters. *Journal of Cetacean Research and Management* 5(2): 131-139.

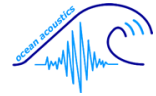
Plötz J., Bornemann H., Knust R., Schroder A., Bester M. (2001) Foraging behaviour of Weddell seals, and its ecological implications. *Polar Biology* 24: 901-908.

Ray G.C. (1981) Ross seal *Ommatophoca rossi* Gray, 1844. *in Handbook of Marine Mammals, Vol. 2* ( Ridgway S.H., Harrison R.J. eds.) pp. 237-260. Academic Press, London.

Reeves R.R., Stewart B.S., Clapham P.J., Powell J.A. (2002) *Guide to Marine Mammals of the World*, Alfred A. Knopf, New York.

Riedman M. (1990) *The Pinnipeds: Seals, Sea Lions, and Walruses.* University of California Press: Berkeley, L.A., and Oxford.

## 5. References



Robison, B.H. (2003) What drives the diel vertical migrations of Antarctic midwater fish? *Journal of the Marine Biological Association of the UK* 83(3): 639-642.

Rouget P.A., Terhune J.M., Burton H.R. (2007) Weddell Seal underwater calling rates during the winter and spring near Mawson Station, Antarctica. *Marine Mammal Science* 23(3): 508-523.

Schusterman R.J., Kastak D., Levenson D.H., Reichmuth C.J., Southall B.L. (2000) Why pinnipeds don't echolocate. *The Journal of the Acoustical Society of America* 107(4): 2256-2264.

Siniff D.B. (1991) An overview of the ecology of Antarctic seals. *American Zoologist* 31(1): 143-149.

Skinner J. D. (1984) Research on the Ross seal, *Ommatophoca rossii*, in the King Haakon VII Sea, Antarctica. *South African Journal of Science* 80: 30-31.

Skinner J.D., Westlin-Van Aarde L.M. (1989) Aspects of reproduction in female Ross seals (*Ommatophoca rossii*). *Journal of Reproduction and Fertility* 87(1): 67-72.

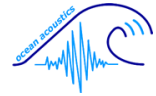
Skinner J.D., Klages N.T.W. (1994) On some aspects of the biology of the Ross seal *Ommatophoca rossii* from King Haakon VII Sea, Antarctica. *Polar Biology* 14(7): 467-472.

Southwell C. (2003) Short Note: Haul-out behaviour of two Ross seals off eastern Antarctica. *Antarctic Science* 15(2): 257-258.

Southwell C., Kerry K., Ensor P., Woehler E.J., Rogers T. (2003) The timing of pupping by pack-ice seals in East Antarctica. *Polar Biology* 26: 648-652.

Southwell C. (2005) Diving behaviour of two Ross seals off east Antarctica. *Wildlife Research* 32: 63-65.

## 5. References



Splettstoesser J.F., Gavriilo M., Field Ca., Field Co., Harrison P., Messick M., Oxford P., Todd F.S. (2000) Notes on Antarctic wildlife: Ross seals *Ommatophoca rossii* and emperor penguins *Aptenodytes forsteri*.  
New Zealand Journal of Zoology 27(2): 137-142.

Stimpert A. (2007) 'Megapclicks': acoustic click trains and buzzes produced during night-time foraging of humpback whales (*Megaptera novaeangliae*).  
Biology Letters 3(5): 467-470.

Stonehouse B. (1972) Tiere der Antarktis – Leben und Lebensräume im tiefen Süden.  
BLV Verlagsgesellschaft mbH, München.

Thom M.D., Johnson D.D.P., MacDonald D.W. (2004) The evolution and maintenance of delayed implantation in the Mustelidae (Mammalia: Carnivora).  
Evolution 58(1): 175-183.

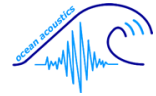
Thomas J.A., DeMaster D., Stone S., Andriashek D. (1980) Observations of a newborn Ross seal pup (*Ommatophoca rossii*) near the Antarctic peninsula.  
Canadian Journal of Zoology 58: 2156-2158.

Thomas J.A., DeMaster D.P. (1982) An acoustic technique for determining diurnal activities in leopard (*Hydrurga leptonyx*) and crabeater (*Lobodon carcinophagus*) seal.  
Canadian Journal of Zoology 60: 2028-2031.

Thomas J.A., Kuechle V.B. (1982) Quantitative analysis of Weddell seal (*Leptonychotes weddelli*) underwater vocalizations at McMurdo Sound, Antarctica.  
The Journal of the Acoustical Society of America 72(6): 1730-1738.

Thomas J.A., Ferm L.M., Kuechle V.B. (1987) Silence as an anti-predation strategy by Weddell seals. Antarctic Journal of the United States 22(5): 232-234.

## 5. References



- Thomas J. A. (2002) Ross seal, *Ommatophoca rossii*. in: Encyclopedia of Marine Mammals. (Perrin W. F., Würsig B., Thewissen J.G.M. eds), pp. 1053-1055, Academic Press, San Diego.
- Tikhomirov E.A. (1975) Biology of the ice forms of seals in the Pacific section of the Antarctic. Rap PV Reun Cons Perm Int Explor Mer 169: 409-412.  
Arctic Research 5: 31-36.
- Van Parijs S.M., Kovacs K.M., Lydersen C. (2001) Spatial and temporal distribution of vocalising male bearded seals – implications for male mating strategies. Behaviour 138: 905-922.
- Watkins W.A., Schevill W.E. (1979) Distinctive characteristics of underwater calls of the harp seal, *Phoca groenlandica*, during the breeding season. The Journal of the Acoustical Society of America 66: 983-988.
- Watkins W.A., Ray G. C. (1985) In-air and underwater sounds of the Ross seal, *Ommatophoca rossii*. The Journal of the Acoustical Society of America 77(4): 1598-1600.
- Wilson V.J. (1975) Second survey of seals in the King Haakon VII Sea, Antarctica. South African Journal of Antarctic Research 5: 31.
- Zhao L., Castellini M.A., Mau T.L., Trumble S.J. (2004) Trophic interactions of Antarctic seals as determined by stable isotope signatures. Polar Biology 27(6): 368-373.

## 6. Appendix

Table 6.1: Summary of descriptive parameters of High siren calls. Given is the mean number, the standard deviation, the standard deviation in %, the median, the minimum value, the maximum value, and the sample size (n).

High		MEAN	SD	SD in (%)	Median	MIN	MAX	n
	Call Type	H	H	H	H	H	H	50
	Subtype							50
Start with	Up/Down							50
	No. Subtype	4,84	1,22	25,17	5,00	3,00	9,00	50
	No. of ups	2,36	0,75	31,76	2,00	1,00	4,00	50
	No. of downs	2,48	0,65	26,07	2,00	2,00	5,00	50
Visible Intense Harmonics	No.	6,52	1,74	26,70	6,00	4,00	10,00	50
	1. upper limit [Hz]	1924,76	362,69	18,84	1879,50	743,00	2710,00	50
	1. lower limit [Hz]	1075,68	280,80	26,10	994,50	462,00	1914,00	50
	2. upper limit [Hz]	2470,26	458,30	18,55	2383,00	1285,00	3612,00	50
	2. lower limit [Hz]	1781,32	380,10	21,34	1695,50	874,00	2658,00	50
	3. upper limit [Hz]	2991,69	555,67	18,57	2838,00	2490,00	4521,00	48
	3. lower limit [Hz]	2361,04	453,67	19,21	2210,50	1808,00	3574,00	48
	4. upper limit [Hz]	3394,56	467,05	13,76	3320,00	2803,00	5403,00	32
	4. lower limit [Hz]	2839,06	390,75	13,76	2759,50	2367,00	4564,00	32
Inter-Harmonic Intervals [Hz]	1	849,08	210,64	24,81	884,00	232,00	1339,00	50
	2	688,94	164,40	23,86	667,00	312,00	1082,00	50
	3	630,65	167,79	26,61	597,00	391,00	1184,00	48
	4	555,50	121,87	21,94	522,00	351,00	839,00	32
	Echo							20
total	Duration [sec]	3,37	0,68	20,30	3,20	2,12	5,73	50
total	min Freq [Hz]	592,18	145,47	24,56	520,50	317,00	893,00	50
total	max Freq [Hz]	7129,38	1803,55	25,30	7297,00	3432,00	10733,00	50
total	Freq Range [Hz]	6537,20	1798,59	27,51	6706,50	2947,00	10240,00	50
	Freq Range [Oct]	3,58	0,51	14,16	3,53	2,35	4,95	50
Freq. Analysis Bandwidth [Hz]	from	802,52	163,11	20,32	817,00	421,00	1113,00	50
	to	5461,42	1618,11	29,63	4586,00	3117,00	8780,00	50
Amplitude at Peak Freq	[dB full scale]	-57,28	4,83	-8,43	-56,49	-72,42	-49,86	50
Peak Freq	at [Hz]	1585,42	226,09	14,26	1602,00	1186,00	2531,00	50

Table 6.2: Summary of descriptive parameters of High siren call elements, as described in Tab.6.1.

High Element		MEAN	SD	SD in (%)	Median	MIN	MAX	n
D	Duration [sec]	1,11	0,41	36,66	1,38	0,46	1,67	63
D	Max [Hz]	3047,44	343,98	11,29	3191,00	1855,00	3375,00	63
D	Min [Hz]	683,97	196,91	28,79	576,00	447,00	1160,00	63
D	Sweep Rate [Oct/s]	2,12	0,41	19,39	1,97	1,59	3,02	63
ed	Duration [sec]	0,31	0,13	43,35	0,28	0,15	0,79	40
ed	Max [Hz]	2312,20	385,78	16,68	2296,50	1716,00	3482,00	40
ed	Min [Hz]	1453,55	299,32	20,59	1427,50	903,00	2590,00	40
ed	Sweep Rate [Oct/s]	2,23	0,50	22,49	2,20	1,43	3,80	40
eu	Duration [sec]	0,33	0,08	23,35	0,31	0,21	0,46	10
eu	Max [Hz]	1977,00	359,69	18,19	1877,00	1560,00	2694,00	10
eu	Min [Hz]	1051,30	217,52	20,69	1022,50	817,00	1559,00	10
eu	Sweep Rate [Oct/s]	2,91	0,84	28,81	2,98	1,32	4,37	10
sd	Duration [sec]	0,67	0,21	31,82	0,68	0,32	1,03	26
sd	Max [Hz]	2831,42	581,14	20,52	2878,00	1835,00	3881,00	26
sd	Min [Hz]	1017,77	237,88	23,37	973,50	491,00	1578,00	26
sd	Sweep Rate [Oct/s]	2,28	0,33	14,32	2,25	1,79	3,19	26
su	Duration [sec]	0,43	0,14	32,38	0,48	0,16	0,70	24
su	Max [Hz]	2922,75	425,83	14,57	3111,50	1820,00	3600,00	24
su	Min [Hz]	1368,42	225,69	16,49	1356,50	842,00	1905,00	24
su	Sweep Rate [Oct/s]	2,66	0,66	25,00	2,40	1,80	4,54	24
U	Duration [sec]	0,62	0,14	21,89	0,65	0,34	0,87	79
U	Max [Hz]	2636,72	509,75	19,33	2563,00	1716,00	3482,00	79
U	Min [Hz]	773,43	281,19	36,36	797,00	470,00	1607,00	79
U	Sweep Rate [Oct/s]	3,02	0,59	19,57	3,02	2,02	4,71	79

Table 6.3: Summary of descriptive parameters of Bowl components, as described in Tab.6.1.

<b>Bowls</b>		<b>MEAN</b>	<b>SD</b>	<b>SD in (%)</b>	<b>Median</b>	<b>MIN</b>	<b>MAX</b>	<b>n</b>
Attached Elements	No.	2,00	0,31	15,39	2,00	1,00	2,00	20
	Description	interbowl	interbowl	interbowl	interbowl	interbowl	interbowl	20
	min Freq. [Hz]	371,95	72,21	19,41	362,50	270,00	567,00	20
	max Freq. [Hz]	706,90	29,12	4,12	712,00	641,00	746,00	20
	Freq.Range [Hz]	334,95	80,96	24,17	342,00	78,00	413,00	20
	Freq.Range [Oct]	0,95	0,27	28,57	0,97	0,19	1,25	20
	total Duration [sec]	2,18	0,35	15,98	2,26	1,54	2,89	20
	Gap [Hz]	-91,85	154,18	-167,86	-202,00	-241,00	214,00	20
Attached Element 1	Duration [sec]	1,03	0,44	42,41	1,01	0,44	2,11	20
	Start Freq.[Hz]	627,90	86,45	13,77	664,50	424,00	727,00	20
	End Freq.[Hz]	430,45	66,69	15,49	407,00	331,00	638,00	20
	Min [Hz]	424,40	47,67	11,23	407,00	331,00	567,00	20
	Max [Hz]	707,55	30,39	4,30	711,50	633,00	778,00	20
Sweeps	Duration [sec]	0,72	0,48	66,16	0,60	0,38	2,11	20
	2.Duration [sec]	0,33	0,22	67,93	0,29	0,11	0,63	4
	Up Rate [Oct/s]	3,50	2,19	62,38	2,97	1,53	6,54	4
	Down Rate [Oct/s]	1,30	0,45	34,83	1,32	0,09	1,95	20
Attached Element 2	Duration [sec]	0,76	0,18	24,07	0,81	0,30	1,08	18
	Start Freq.[Hz]	363,11	52,99	14,59	355,00	270,00	444,00	18
	End Freq.[Hz]	541,83	92,18	17,01	533,00	399,00	675,00	18
	Min [Hz]	360,17	50,28	13,96	355,00	270,00	444,00	18
	Max [Hz]	679,44	55,04	8,10	671,00	504,00	754,00	18
Sweeps	Duration [sec]	0,38	0,06	16,48	0,39	0,29	0,51	18
	2. Duration [sec]	0,37	0,02	5,83	0,36	0,35	0,40	5
	Up Rate [Oct/s]	2,49	0,44	17,82	2,54	1,47	3,17	18
	Down Rate [Oct/s]	2,30	0,14	6,09	2,35	2,10	2,44	5

Table 6.4: Summary of descriptive parameters of Mid siren calls, as described in Tab.6.1.

Mid		MEAN	SD	SD in (%)	Median	MIN	MAX	n
	Call Type	M	M	M	M	M	M	50
	Subtype							50
Start with	Up/Down							50
	No. Subtype	4,20	0,83	19,83	4,00	3,00	8,00	50
	No. of ups	2,08	0,44	21,37	2,00	1,00	4,00	50
	No. of downs	2,12	0,44	20,53	2,00	1,00	4,00	50
Visible Intense Harmonics	No.	5,80	1,34	23,11	6,00	3,00	9,00	50
	1. upper limit [Hz]	475,09	109,65	23,08	444,00	338,00	859,00	47
	1. lower limit [Hz]	251,34	69,93	27,82	227,00	164,00	511,00	47
	2. upper limit [Hz]	598,62	95,39	15,93	587,00	516,00	1131,00	50
	2. lower limit [Hz]	386,22	42,58	11,03	382,50	339,00	562,00	50
	3. upper limit [Hz]	760,06	99,74	13,12	733,50	678,00	1275,00	50
	3. lower limit [Hz]	568,72	63,02	11,08	553,00	514,00	851,00	50
	4. upper limit [Hz]	1394,70	146,06	10,47	1400,50	957,00	1784,00	47
	4. lower limit [Hz]	689,26	82,56	11,98	679,00	505,00	1069,00	47
Inter-Harmonic Intervals [Hz]	1	223,74	57,70	25,79	210,00	136,00	435,00	47
	2	212,40	58,85	27,71	201,50	147,00	569,00	50
	3	191,34	44,28	23,14	184,00	139,00	455,00	50
	4	705,43	137,91	19,55	719,00	323,00	1029,00	46
	Echo							38
total	Duration [sec]	3,29	0,42	12,81	3,36	2,33	4,17	50
total	min Freq [Hz]	168,42	35,45	21,05	154,00	130,00	314,00	50
total	max Freq [Hz]	2010,38	596,62	29,68	1942,00	1114,00	3745,00	50
total	Freq Range [Hz]	1841,96	599,83	32,56	1795,50	936,00	3547,00	50
	Freq Range [Oct]	3,55	0,48	13,66	3,67	2,38	4,63	50
Freq. Analysis Bandwidth [Hz]	from	312,78	38,86	12,42	307,00	228,00	392,00	50
	to	1713,06	461,08	26,92	1684,00	922,00	2894,00	50
Amplitude at Peak Freq	[dB full scale]	-44,93	13,58	-30,21	-45,67	-57,90	41,90	50
Peak Freq	at [Hz]	498,98	94,04	18,85	492,00	275,00	823,00	50
Special Features	Description	edge	edge	edge	edge	edge	edge	49
	1. Freq. [Hz]	761,13	126,41	16,61	727,00	582,00	1163,00	45
	1. Length [sec]	0,11	0,03	25,16	0,11	0,07	0,20	45
	2. Freq. [Hz]	773,76	79,98	10,34	767,00	640,00	1072,00	46
	2. Length [sec]	0,11	0,02	14,83	0,11	0,07	0,15	46
	3. Freq. [Hz]	401,09	47,95	11,95	392,00	342,00	568,00	47
	3. Length [sec]	0,11	0,03	22,29	0,12	0,05	0,16	47
Low Part Peaks [Hz]	Left Side	628,66	139,67	22,22	575,00	507,00	983,00	50
	Right Side	628,96	149,68	23,80	574,00	461,00	1091,00	47

Table 6.5: Summary of descriptive parameters of Mid siren call elements, as described in Tab.6.1.

Mid Element		MEAN	SD	SD in (%)	Median	MIN	MAX	n
D	Duration [sec]	0,91	0,25	27,66	0,99	0,20	1,22	54
D	Max [Hz]	1214,19	271,04	22,32	1136,50	752,00	2128,00	54
D	Min [Hz]	336,11	122,81	36,54	292,50	268,00	737,00	54
D	Sweep Rate [Oct/s]	2,29	1,06	46,15	1,98	1,54	8,27	54
ed	Duration [sec]	0,64	0,18	28,39	0,67	0,22	0,93	48
ed	Max [Hz]	1148,73	175,62	15,29	1140,50	664,00	1734,00	48
ed	Min [Hz]	415,15	100,49	24,21	383,50	299,00	768,00	48
ed	Sweep Rate [Oct/s]	2,42	0,38	15,73	2,36	1,40	3,40	48
eu	Duration [sec]	0,30	0,00	0,00	0,30	0,30	0,30	2
eu	Max [Hz]	667,00	155,56	23,32	667,00	557,00	777,00	2
eu	Min [Hz]	411,00	59,40	14,45	411,00	369,00	453,00	2
eu	Sweep Rate [Oct/s]	2,29	0,43	19,00	2,29	1,98	2,59	2
sd	Duration [sec]	0,67	0,35	52,36	0,68	0,35	0,97	4
sd	Max [Hz]	1197,75	689,78	57,59	860,50	838,00	2232,00	4
sd	Min [Hz]	530,50	174,02	32,80	582,00	279,00	679,00	4
sd	Sweep Rate [Oct/s]	1,59	0,17	10,84	1,59	1,43	1,77	4
su	Duration [sec]	0,67	0,14	21,17	0,70	0,24	0,94	46
su	Max [Hz]	1153,80	193,92	16,81	1125,00	758,00	1757,00	46
su	Min [Hz]	457,28	94,64	20,70	437,00	334,00	768,00	46
su	Sweep Rate [Oct/s]	2,08	0,58	27,80	1,98	1,09	5,37	46
U	Duration [sec]	0,78	0,17	21,33	0,83	0,20	0,97	56
U	Max [Hz]	1209,32	240,42	19,88	1141,00	859,00	2094,00	56
U	Min [Hz]	358,55	139,61	38,94	296,50	268,00	743,00	56
U	Sweep Rate [Oct/s]	2,40	0,42	17,36	2,31	1,47	3,72	56

Table 6.6: Summary of descriptive parameters of the Mid attachments, as described in Tab.6.1.

Mid Attachment		MEAN	SD	SD in (%)	Median	MIN	MAX	n
Attachments	Description	umbrella	umbrella	umbrella	umbrella	umbrella	umbrella	7
	Start Freq. [Hz]	1452,29	579,71	39,92	1646,00	141,00	1757,00	7
	End Freq. [Hz]	1452,29	525,59	36,19	1610,00	277,00	1800,00	7
	Freq. Range [Hz]	0,00	91,38		-26,00	-129,00	136,00	7
	Freq. Range [Oct]	0,12	0,38	315,07	-0,02	-0,12	0,97	7
	Duration [sec]	0,33	0,15	46,27	0,26	0,20	0,60	7
Attached Element 1	Duration [sec]							0
	Start Freq.[Hz]							0
	End Freq.[Hz]							0
	Min [Hz]	1310,00	515,68	39,36	1506,00	141,00	1531,00	7
	Max [Hz]	1491,29	538,27	36,09	1671,00	277,00	1800,00	7
Sweeps	Duration [sec]	0,60			0,60	0,60	0,60	1
	2.Duration [sec]							0
	Up Rate [Oct/s]	1,62			1,62	1,62	1,62	1
	Down Rate [Oct/s]							0

Table 6.7: Summary of descriptive parameters of Low siren calls, as described in Tab.6.1.

Low		MEAN	SD	SD in (%)	Median	MIN	MAX	n
	Call Type	L	L	L	L	L	L	50
	Subtype							50
Start with	Up/Down							50
	No. Subtype	3,54	0,81	22,98	4,00	2,00	5,00	50
	No. of ups	1,84	0,42	22,93	2,00	1,00	3,00	50
	No. of downs	1,70	0,46	27,23	2,00	1,00	2,00	50
Visible intense Harmonics	No.	1,08	0,27	25,33	1,00	1,00	2,00	38
	1.upper limit [Hz]	470,21	78,15	16,62	493,00	318,00	632,00	38
	1.lower limit [Hz]	256,82	41,73	16,25	264,50	184,00	361,00	38
	2.upper limit [Hz]	790,33	69,04	8,74	753,00	748,00	870,00	3
	2.lower limit [Hz]	532,67	55,82	10,48	504,00	497,00	597,00	3
Inter-Harmonic Intervals [Hz]	1	213,39	46,17	21,64	218,50	131,00	323,00	38
	2	257,67	14,57	5,66	256,00	244,00	273,00	3
	Echo							6
	Duration [sec]	2,00	0,46	22,99	2,21	0,86	2,83	50
	min Freq [Hz]	132,54	21,89	16,36	134,00	96,00	222,00	50
	max Freq [Hz]	449,14	60,85	13,55	442,00	352,00	644,00	50
	Freq Range [Hz]	316,60	60,87	19,23	304,00	207,00	502,00	50
	Freq Range [Oct]	1,77	0,26	14,63	1,81	0,95	2,30	50
	Start Freq [Hz]	234,22	36,72	15,68	235,00	136,00	306,00	50
	Freq 1.Peak [Hz]	439,24	51,72	11,78	437,50	352,00	547,00	50
	Freq 1.Low [Hz]	131,20	21,54	16,42	132,50	96,00	222,00	44
	Freq 2.Peak [Hz]	407,56	72,47	17,78	407,00	273,00	644,00	41
	End Freq [Hz]	221,08	58,43	26,43	210,50	114,00	424,00	50
Freq.Analysis Bandwidth [Hz]	from	148,66	22,11	14,87	149,00	105,00	205,00	50
	to	500,42	142,85	28,55	448,00	345,00	904,00	50
Amplitude at Peak Freq	[dB full scale]	-45,68	4,23	-9,25	-45,96	-60,11	-39,49	50
Peak Freq	at [Hz]	225,84	49,82	22,06	224,50	138,00	325,00	50
Special Features	Description	dot in front	35					
	Freq. [Hz]	218,54	26,57	12,16	220,00	166,00	286,00	35
	Distance [sec]	0,07	0,03	43,04	0,06	0,02	0,12	35
Diffuse turning points (DTP)	Peaks	1,17	0,38	32,79	1,00	1,00	2,00	29
	Lows	1,00	0,00	0,00	1,00	1,00	1,00	17

Table 6.8: Summary of descriptive parameters of Low siren call elements, as described in Tab.6.1.

Low Element		MEAN	SD	SD in (%)	Median	MIN	MAX	n
D	Duration [sec]	0,63	0,08	12,57	0,65	0,42	0,77	43
D	Max [Hz]	449,40	43,78	9,74	447,00	372,00	536,00	43
D	Min [Hz]	129,81	15,22	11,72	130,00	105,00	161,00	43
D	Sweep Rate [Oct/s]	2,89	0,43	14,68	2,82	2,23	4,18	43
ed	Duration [sec]	0,41	0,18	43,44	0,38	0,14	0,89	42
ed	Max [Hz]	427,02	69,26	16,22	415,00	321,00	681,00	42
ed	Min [Hz]	184,29	34,08	18,49	185,50	118,00	260,00	42
ed	Sweep Rate [Oct/s]	3,37	1,53	45,44	3,14	1,39	8,22	42
eu	Duration [sec]	0,82	0,45	54,58	0,78	0,09	1,30	6
eu	Max [Hz]	328,83	70,39	21,40	339,50	222,00	423,00	6
eu	Min [Hz]	128,83	14,58	11,32	121,00	117,00	149,00	6
eu	Sweep Rate [Oct/s]	2,43	1,99	81,65	1,82	1,11	6,39	6
su	Duration [sec]	0,48	0,16	34,22	0,49	0,17	0,97	50
su	Max [Hz]	441,90	43,62	9,87	440,50	355,00	526,00	50
su	Min [Hz]	220,72	33,47	15,17	217,00	153,00	295,00	50
su	Sweep Rate [Oct/s]	2,29	0,65	28,19	2,15	1,22	4,03	50
U	Duration [sec]	0,79	0,06	7,79	0,80	0,65	0,92	36
U	Max [Hz]	424,78	69,49	16,36	408,50	309,00	656,00	36
U	Min [Hz]	132,47	16,55	12,49	136,00	105,00	166,00	36
U	Sweep Rate [Oct/s]	2,13	0,33	15,39	2,17	1,30	2,83	36

Table 6.9: Summary of descriptive parameters of the Whoosh Broadband Component, as described in Tab.6.1.

Whoosh Broadband Component		MEAN	SD	SD in (%)	Median	MIN	MAX	n
	Call Type	WBC	WBC	WBC	WBC	WBC	WBC	50
	WTC present	1,00	0,00	0,00	1,00	1,00	1,00	50
WBC total	Duration [sec]	2,51	0,30	11,82	2,52	1,44	3,02	50
total	Freq Range [Hz]	9557,28	1324,30	13,86	9535,00	4636,00	12288,00	50
	Freq Range [Oct]	2,93	0,23	7,77	2,95	2,07	3,35	50
	Start/Max Freq. [Hz]	10996,54	1305,36	11,87	10951,00	6081,00	13777,00	50
	End/Min Freq. [Hz]	1439,26	104,70	7,27	1430,00	1251,00	1764,00	50
Peak Frequency [Hz]	at mid part [Hz]	2296,00	168,98	7,36	2300,00	1900,00	2600,00	50
	1sec. left of mid part [Hz]	5892,00	840,76	14,27	5800,00	4000,00	8100,00	50
Frequency [Hz] at	1.visible band	1710,00	111,12	6,50	1700,00	1500,00	1900,00	50
	2.visible band	1942,00	175,07	9,01	1900,00	1700,00	2400,00	50
	3.visible band	2192,00	243,98	11,13	2200,00	1800,00	3100,00	50

Table 6.10: Summary of descriptive parameters of the Whoosh Tonal Component, as described in Tab.6.1.

Whoosh Tonal Component		MEAN	SD	SD in (%)	Median	MIN	MAX	n
	Call Type	WTC	WTC	WTC	WTC	WTC	WTC	WTC
WTC total	Duration [sec]	2,33	0,44	18,74	2,33	1,35	3,36	50
total	Freq Range [Hz]	129,84	21,53	16,58	131,50	73,00	188,00	50
	Freq Range [Oct]	0,31	0,05	16,24	0,31	0,17	0,45	50
	Start Freq. [Hz]	574,18	11,42	1,99	577,50	541,00	592,00	50
	End Freq. [Hz]	591,50	47,31	8,00	582,00	534,00	873,00	50
Upsweep	Min [Hz]	548,42	11,07	2,02	551,00	511,00	568,00	50
	Max [Hz]	678,26	16,95	2,50	677,50	635,00	715,00	50
	Duration [sec]	0,54	0,14	25,64	0,54	0,20	0,87	50
	Up Rate [Oct/s]	0,60	0,17	27,48	0,57	0,37	1,39	50
Freq. Analysis Bandwidth [Hz]	from	550,60	8,87	1,61	553,00	524,00	568,00	50
	to	661,62	18,59	2,81	659,00	635,00	729,00	50
Amplitude at Peak Freq	[dB full scale]	-50,66	4,87	-9,62	-50,97	-61,45	-41,13	50
Peak Freq	at [Hz]	605,64	30,80	5,09	612,00	556,00	667,00	50
Gap	Min [Hz]	656,98	18,33	2,79	654,00	621,00	732,00	50
	Max [Hz]	1540,16	85,53	5,55	1540,50	1377,00	1767,00	50
	Gap [Hz]	883,18	91,81	10,40	893,50	645,00	1117,00	50

Fig.6.1-Fig.6.12 show scatterplots of two parameters of all four call types plotted against each other to reveal if any variable has an effect on the others. Only the pairings that result in a more or less good distinction between the calls types are shown here. The remaining plots were viewed but did not contain any valuable information. For each parameter n=50 for each call type.

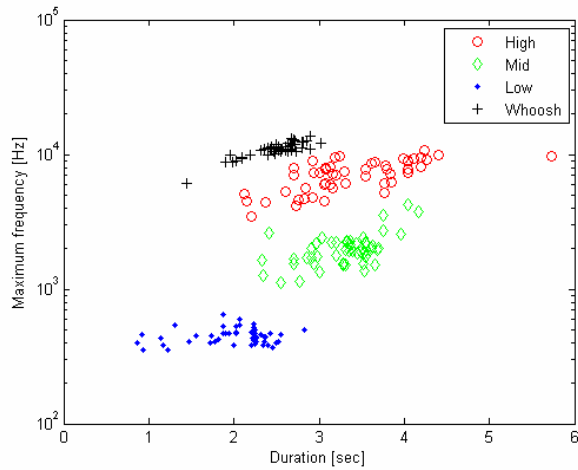


Figure 6.1: The duration in seconds plotted against the maximum frequency in Hz. The different call types are plotted in different colours (Highs in red circles, Mids in green diamonds, Lows in blue dots, and Whooshes in black crosses). For the parameters  $n=50$  respectively. The calls can be distinguished by duration against maximum frequency as well, but the clusters do not appear as clear as in Fig.3.2K. Again, the Whooshes mark the highest frequency, followed by Highs, Mids, and Lows.

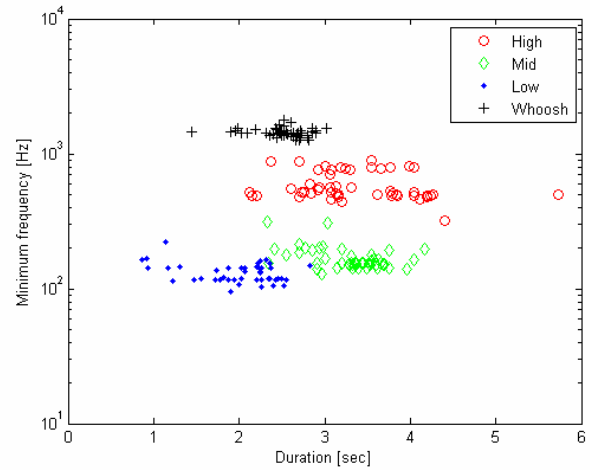


Figure 6.2: The duration in seconds plotted against the minimum frequency in Hz. Description as given in Fig.6.1. Lows and Mids seem to mix more in minimum frequencies than they did with the parameters mentioned previously in Fig.3.2K and Fig.6.1.

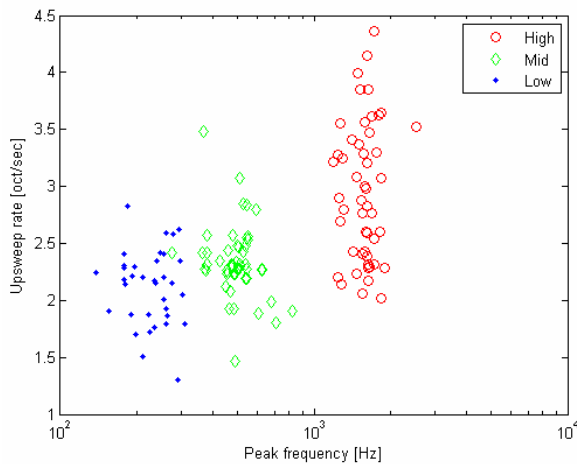


Figure 6.3: The peak frequency in Hz plotted against the upsweep rate in octaves per second. Description as given in Fig.6.1. The peak frequencies of the Highs stand out clearly from the ones of Mids and Lows, which are close to mix in the lower part of the spectrum.

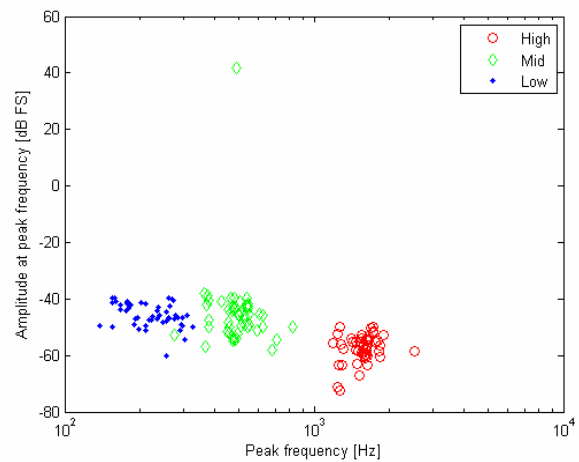


Figure 6.4: The peak frequency in Hz plotted against the amplitude in dB FS. Description as given in Fig.6.1. Again, the Highs stand out with far higher peak frequencies but almost equal amplitudes to the Mids and Lows.

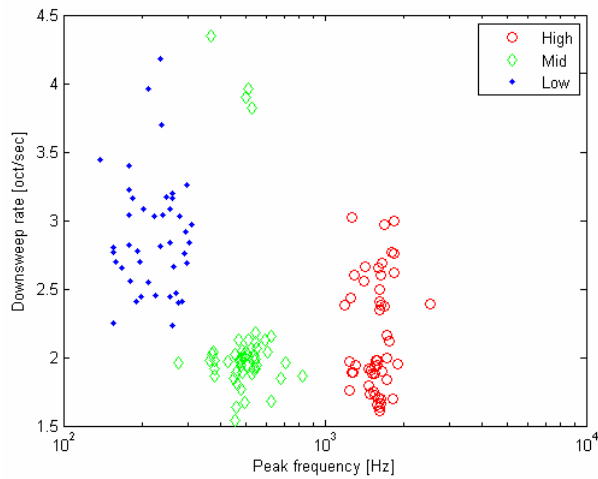


Figure 6.5: The peak frequency in Hz plotted against the downsweep rate in octaves per second. Description as given in Fig.6.1. The downsweep rates are broadly scattered, especially for the Lows and Highs, but not so much in the Mids, which seem to have a bimodal distribution.

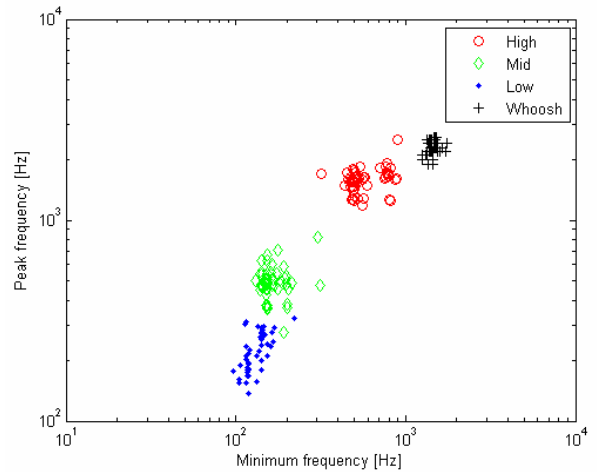


Figure 6.6: The minimum frequency in Hz plotted against the peak frequency in Hz. Description as given in Fig.6.1. This plot approaches the appearance of Fig.3.2K with the distinct call types describing a nice curve from lowest minimum frequency and peak frequency in Lows up to highest of both in Whooshes.

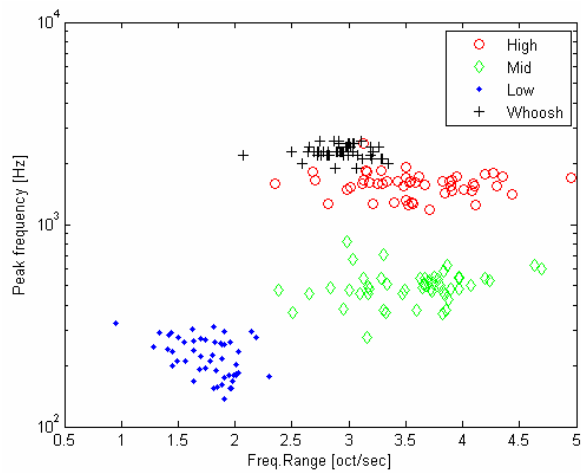


Figure 6.7: The frequency range in octaves per second plotted against the peak frequency in Hz. Description as given in Fig.6.1. The frequency range is quite scattered for the different call types, but the peak frequency has the same typical sequence with Whooshes at the high end, followed by Highs and Mids, and Lows at the lowest end.

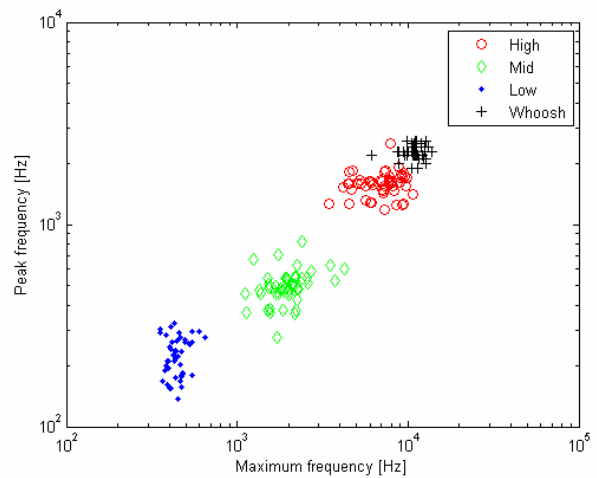


Figure 6.8: The maximum frequency in Hz plotted against the peak frequency in Hz. Description as given in Fig.6.1. The maximum frequency of all call types is perfectly correlated with the peak frequency, describing an almost straight line with the Lows at the bottom part and the Whooshes at the upper part.

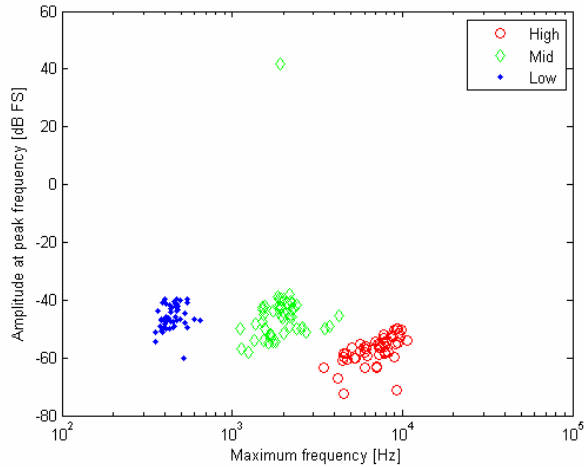


Figure 6.9: Here the maximum frequency in Hz plotted against the amplitude at peak frequency in dB FS. Description as given in Fig.6.1. The maximum frequencies separate the three siren calls quite nicely with their amplitude varying only slightly.

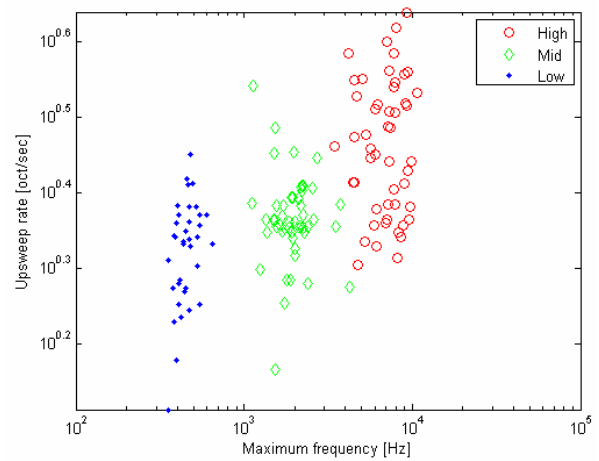


Figure 6.10: The maximum frequency in Hz plotted against the upsweep rate in octaves per second. Description as given in Fig.6.1. The upsweep rates vary greatly within calls while the maximum frequency shows the familiar pattern of Highs lying higher than Mids and these, again, higher than Lows.

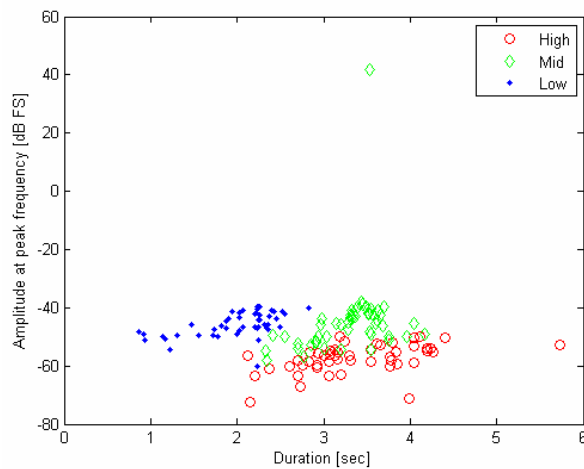


Figure 6.11: The duration in seconds plotted against the amplitude at peak frequency in dB FS. Description as given in Fig.6.1. The amplitudes do not clearly separate Highs and Mids from each other, especially since their duration seems to be quite the same. Only Lows can be marked separately since their duration is lower almost by half than the duration of the other two siren call types.

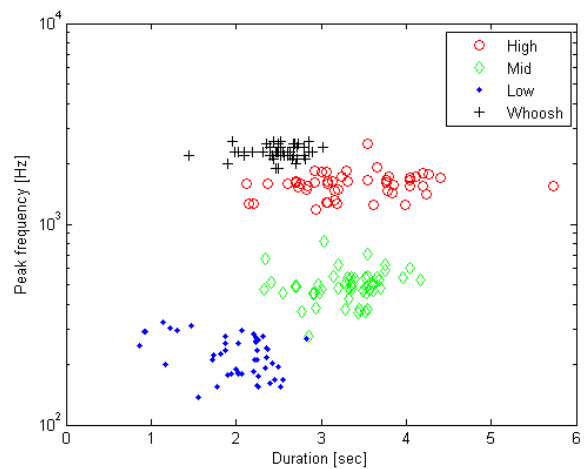
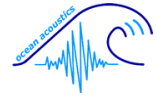


Figure 6.12: The duration in seconds plotted against the peak frequency in Hz. Description as given in Fig.6.1. Peak frequency can be used to distinguish the four call types from each other, however, not as nicely as maximum frequency, as shown in Fig.6.1. Again, the Whooshs lie above Highs, followed by Mids, and Lows.



## 7. Acknowledgements

The title picture was kindly provided by Ruben Fijn, IMARES, who found this Ross seal on an ice floe some way from RV Polarstern in 2006.

First of all, I would like to thank my AWI Ocean Acoustics group for their great support in basically every stage of this work. My supervisor Prof. Dr. Peter Lemke made my stay in Bremerhaven possible. Dr. Lars Kindermann supervised me daily with his expertise and experience and helped me whenever Excel had no solution or Matlab struck on me. He also provided me with some of his great photographs taken in Antarctica. Holger Klinck always had useful practical input, lots of PALAOA data and pictures, and the question if I was done yet. The quasi unlimited knowledge of Dr. Horst Bornemann saved me from spending my nights at the library, helped me with my statistics, and we also had some very fruitful discussions not only about Ross seals. Dr. Joachim Plötz was very patient in answering all my biological questions and kindly provided me with photos and video material about Antarctic seals. Dr. Olaf Boebel covered all questions concerning oceanography, provided me with data on ice coverage in Atka Bay, and helped me giving this thesis a more realistic shape. My colleague Ilse van Opzeeland always had an open ear for my concerns resulting in very helpful discussions, provided me with important data on seal occurrence and classification trees, and encouraged me to follow my way. Without Dr. Elke Burkhardt my literature search would have taken ages, and she often came up with interesting facts and background knowledge to consider. Our short-time guest Harold Figueroa from Cornell University patiently helped me to overcome computational frustrations and afterwards cleared my brain not only with awesome talks. Our HiWi Cornelia Kreiss shared my situation with encouraging words. I wish her good luck with her thesis as well! And Dr. Gerd König-Langlo kindly provided me with the recent meteorological raw-data of the Neumayer Station.

Without my supervisors at the University of Munich, Dr. Lutz Wiegrebe and Prof. Dr. Gerd Schuller, who helped me whenever needed via long-distance analysis, this external thesis at the AWI would not have been possible.

## 7. Acknowledgements



And, of course, this work would not have been possible without the support, the good advice and the needed distraction of my beloved ones, especially my mom and dad, and my friends all over the world, who never got tired in finding encouraging words whenever I had the feeling to be lost in science. Thank you very much, Amanda and Kristina, for proof reading my English texts!

Hiermit versichere ich, dass ich die vorliegende Arbeit selbstständig verfasst und nur die angegebenen Hilfsmittel und Quellen verwendet habe.

Anna-Maria Seibert

München, den 27.12.2007